Characterising the behavioural and neural deficits of face recognition in developmental prosopagnosia

Gabriela Ivanova Epihova

Doctor of Philosophy

University of York

Psychology

January 2023

Abstract

Developmental prosopagnosia (DP) is a neurodevelopmental condition in which there is an impairment in the ability to recognise face identities. The aim of this thesis was to explore the behavioural and neural deficits that characterise DP. Chapter 2 examined a current debate about the extent to which DP is face-specific or also affects the recognition of other objects. We asked whether objects that were perceived as faces (pareidolia) would also be affected in DP. Recognition of pareidolic objects was impaired in DP, but only if the objects had similar image properties to faces. This suggests that the underlying deficit in DP may reflect a disruption to processing image properties typically found in face images. In Chapters 3 and 4, we demonstrated that the deficit in DP extends to faces from different races and faces from different species. These findings suggest that the deficit in DP encompasses a range of configural and morphological structures. Chapters 5 and 6 explored the neural correlates of DP. Chapter 5 explored the identity recognition deficits in DP through investigating the neural signatures elicited by individual faces. We show that in contrast to neurotypical controls, DPs do not evidence identity discrimination at the neural level. Chapter 5 further showed that DP is marked by alterations in the overall functional connectivity organization. Finally, Chapter 6 showed that, although global structural connectivity is not affected in DP, there were local reductions in connectivity within the temporal lobe. Taken together, the results from this thesis provide new insights into our understanding of the behavioural and neural mechanisms that underlie the deficits evident in DP.

List of Contents

List of Tables

List of Figures

Acknowledgements

I would like to express my gratitude to my academic supervisor, Professor Tim Andrews, for his continued guidance and advice. His indispensable support, encouragement and lessons on figure aesthetics have been instrumental in my academic development. I am grateful to my TAP members, Dr. Angela de Bruin and Dr. Philip Quinlan who provided me with academic advice. Special thanks to Dr. David Watson and Dr. Holly Brown for their technical expertise and code!

My academic journey would not be possible without the support of my husband, Dimitar. For inspiring me to love and peruse science, for the long discussions and scientific arguments, for all the late-night R tutorials, and for never letting me believe that I have exhausted all possible analyses - I am forever grateful. I would also like to thank my parents for their support, nurturing my curiosity from a young age and always finding a way to help me succeed.

I am grateful to all participants who invested their time, effort, and curiosity in our experiments. Without you, none of the experiments in this thesis would have been possible. Finally, I would like to express my gratitude to the ESRC – thank you for allowing me to realise my dreams.

Author's Declaration

I declare that this thesis is a presentation of original work, carried out under the supervision of Professor Tim Andrews, and I am the sole author. This work has not previously been presented for an award at this, or any other, University. All sources are acknowledged as References.

The empirical work presented in Chapter 2 and Chapter 3 of this thesis has been published in the following peer-reviewed journals:

Epihova, G., Cook, R., & Andrews, T. J. (2022). Recognition of pareidolic objects in developmental prosopagnosic and neurotypical individuals. Cortex, 153, 21-31.

Epihova, G., Cook, R., & Andrews, T. J. (2023). Recognition of animal faces is impaired in developmental prosopagnosia. Cognition, 237, 105477.

Results from Chapter 2 have been presented at the following conference:

Epihova, G., Cook, R., & Andrews, T. J. (2022). Recognition of pareidolic objects in developmental prosopagnosic and neurotypical individuals, The European Conference on Visual Perception (ECVP), Nijmegen, Netherlands, 2022

Chapter 1

Literature review: The behavioural and neural correlates of developmental prosopagnosia

1.1. Developmental prosopagnosia

Prosopagnosia is a deficit in face identity recognition with a prevalence in the general population of approximately 2% (Hecaen & Angelergues, 1962). Prosopagnosia is divided into two general subtypes – *acquired prosopagnosia* (*AP*) and *developmental prosopagnosia* (*DP*) (Cook & Biotti, 2016). AP is a condition which results from brain damage such as concussion and stroke. In contrast, DP is a neurodevelopmental disorder, characterised by deficits in face identity recognition, despite intact low-level vision and no history of brain damage (Cook & Biotti, 2016; Duchaine & Nakayama, 2006; Susilo & Duchaine, 2013). DP individuals struggle to identify people by their faces and often resort to recognition based on non-facial features, including voice, hairstyle, clothes, and gate (Fine, 2012). As face recognition is a biologically and socially fundamental ability, DP could lead to a number of negative psychosocial consequences for the individuals suffering with the disorder such as social anxiety, feelings of embarrassment, guilt and feeling of failure (Yardley, McDermott, Pisarski, Duchaine, & Nakayama, 2008; Davis et al., 2011). Research efforts into DP have benefited our understanding of the aetiology of this disorder as well as elucidating the cognitive and neural frameworks of face recognition.

1.2. Mnemonic and apperceptive accounts of development prosopagnosia

By definition, DP is characterised by impaired face memory. However, there is an on-going debate about the extent to which DP can be described as an independent deficit in the perception or memory of faces. Mnemonic accounts suggest that the deficits observed in DPs can be explained by the inability to retrieve memory representations of different faces in the absence of face perception impairments. There are a few reports supporting the idea that DP is a condition characterised by face memory deficits with intact face perception abilities. Dalrymple, Garrido, & Duchaine, (2014) found that less than half of their DP participants displayed impairments in face perception. Another report showed the same pattern - 4 out of 6 DPs showed normal performance with face perception (McKone et al., 2011). However, both studies used a single measure to test face perception - Dartmouth Face Perception Test (DFPT) and Cambridge Face Perception Test (CFPT), respectively, thus it is possible that there was insufficient power to capture finer perceptual impairments.

Other studies have demonstrated an impairment in both memory and perceptual face tasks in DP, in line with an apperceptive account of the disorder. According to this account, DP might result from deficits in perceiving and encoding face features, resulting in consequent deficits in retrieval. One study tested DPs on a delayed match-to-samples task with varying retention intervals, thus manipulating memory demands (Biotti, Gray, & Cook, 2019). In support of the apperceptive account, there was no effect of memory demands on face recognition deficits in DPs. Moreover, an extension of the apperceptive hypothesis is that DP will not only have deficits in identity perception, but also with perception of subtle cues in discriminating facial gender, age and emotion. Reports have found mixed results. Some demonstrate no age and gender discrimination deficits in DPs (Chatterjee & Nakayama, 2012).

However, a study using more sensitive measures of signal detection theory showed that DPs have deficits in facial gender perception (Marsh, Biotti, Cook, & Gray, 2019). Taking into consideration the high heterogeneity of DP (Stollhoff, Jost, Elze, & Kennerknecht, 2011), it is possible that the condition is divided into an apperceptive and mnemonic sub-types. Biotti & Cook (2016) divided DP participants into two sub-groups based on their scores on the Cambridge Face Perception Test (CFPT): apperceptive (scores <2SD on the CFPT) and non-apperceptive. The authors found that only the apperceptive DPs showed deficits in emotion discrimination compared to controls.

Another possibility that can account for the mixed results concerns how DP is classified and validated. DP is not currently listed in the Diagnostic and Statistical Manual of Mental Disorders (DSM-5) and no formal diagnostic criteria exist. The most common approach for diagnosis involves completion of a combination of self-report questionnaires and face memory tasks such as the Cambridge Face Memory Task (CFMT) and the Famous Faces Task (FFT). Based on the scores of these tests, individuals who perform 2SD below the control mean are usually classified as DPs. This diagnostic procedure has clear implications for the estimated prevalence of DP in the population – classifying anyone scoring 2SD below the mean on a given test as a DP will result in ~2% estimate for the condition. Based on the diagnostic procedure it is also possible that there is an overrepresentation of mnemonic impairment in the selected DP samples as the screening tests selectively test for face memory deficits.

1.3. Developmental prosopagnosia: a domain-specific or domain-general disorder?

The degree to which deficits in DP are face-specific or involve more general processing mechanisms has been the subject of a longstanding debate and carries important theoretical implications for how the visual system is organised. Domain-specific accounts have proposed that face recognition engages a domain-specific mechanism, dissociated from mechanisms responsible for recognition of other object classes. In support of this some individuals with DP have face-specific deficits and preserved object recognition abilities (Duchaine, Yovel, Butterworth, & Nakayama, 2006; Duchaine & Nakayama, 2006). For instance, DPs perform comparable to controls on a wide range of objects such as guns, horses, glasses, bicycles (Barton, Albonico, Susilo, Duchaine, & Corrow, 2019), shoes (Stollhoff et al., 2011), seashells (Esins, Schultz, Stemper, & Bülthoff, 2014) and flowers (Song, Zhu, Li, Wang, & Liu, 2015). Further, one study tested a large number of DP participants (*n = 40*) and found a selective deficit with face matching and preserved matching abilities for biological (hands) and non-biological (houses) objects (Bate, Bennetts, Tree, Adams, & Murray, 2019). Other reports have also found no recognition deficits with other animate and biological classes of objects (butterflies and hands, respectively) (Shah, Gaule, Gaigg, Bird, & Cook, 2015). Furthermore, some have suggested that DP might be characterised by a deficit in experience-dependent learning of novel objects. To address this, Fry, Wilmer, Xie, Verfaellie, & DeGutis, (2020) tested 30 DPs with a novel object memory task (NOMT) – a task with matching structure and demands to the CFMT. There were no differences in accuracy and reaction time on the NOMT between the DP and control participants, indicating a lack of object recognition deficit for novel objects in DP.

Although many researchers have asserted that individuals with prosopagnosia have exclusive face-selective deficits, the results of many other studies favour a more domain-general explanation and have reported an impairment for other visual categories. For example, Biotti, Gray, & Cook, (2017) found that relative to control participants, individuals with DP exhibit impaired body matching accuracy. Deficits in car recognition abilities have also been reported, relative to matched controls (Gray, Biotti, & Cook, 2019), although see (Esins, Schultz, Stemper, Kennerknecht, & Bülthoff, 2016). In a large meta-analysis investigating the comorbidity of prosopagnosia and object agnosia, Geskin & Behrmann, (2018) examined 238 individuals with prosopagnosia and found that only 19.7% of DP had a selective problem with faces, while 80.3% of DPs demonstrated an association between prosopagnosia and object agnosia. However, this number is likely overestimated as a large number of studies were excluded from the meta-analysis for lacking reaction time data and studies varied greatly in their diagnostic methods of DP. Moreover, some studies tested participants with multiple object recognition tests. As such, the chance for scoring low on one of the tests and therefore being inaccurately classified as having object agnosia is increased. Indeed, Garrido, Duchaine, & DeGutis, (2018) pointed out that using the criteria implemented by Geskin & Behrmann (2018), 50% of their control sample will be misclassified as having object agnosia.

One explanation for the co-occurrence of face and object deficits in DPs is provided by the independent disorders hypothesis (IDH) (Gray & Cook, 2018). The IDH states that face and object recognition deficits are independent neurodevelopmental conditions that co-occur more commonly in DPs, similarly to the higher rate of co-occurrence between DP and Autism Spectrum Disorder (ASD). Indeed, DP is a condition with considerable heterogeneity (Rosenthal & Avidan, 2018). Reports have consistently demonstrated that even in the absence

of a reduced performance with object recognition on a group level, some DP individuals exhibit object deficits (Barton et al., 2019). Conversely, Gray et al., (2019) found that although on a group level individuals with DP were impaired with cars, there was a large heterogeneity among the sample, with several DPs achieving scores comparable with the top-performing control participants. Indeed, there are cases with pure face deficits in the absence of any object deficits and vice versa (Duchaine et al., 2006; Germine, Cashdollar, Düzel, & Duchaine, 2011). According to the IDH, the probable mechanisms of shared face and object deficits might stem from a shared developmental atypicality and common genetic and environmental factors. Consistent with this, one study investigating 10 genetically related family members with prosopagnosia reported that all of them were also impaired on recognition of cars and guns (Duchaine, Germine, & Nakayama, 2007).

A consistent problem with investigating the association between DP and object agnosia is the lack of theoretical justification for choosing a particular object category when probing the recognition deficits in DPs. This makes it difficult to draw comparisons between studies and conclusions about any shared attributes among the objects that DPs have deficits with. The artificial division of visual stimuli into faces and objects does not reflect the underlying complexity and diversity of physical and semantic properties of different objects.

Variability in any cognitive measure is likely an emergent property of multiple structural or functional neural processes. As such, neural patterns of activity for different objects might provide an insight into the behavioural recognition mechanism, and specifically, the association (or lack of) between different objects as well as faces and objects. Neural patterns of activity in the ventral temporal cortex have been shown to differentiate between sub-categories within a domain (Margalit et al., 2020), animate and inanimate objects

(Kriegeskorte et al., 2008), real-world object's size (Konkle & Oliva, 2012) and semantic relatedness of objects (Wen, Shi, Chen, & Liu, 2018). However, these parameters are not orthogonal to objects' low-level visual properties, which presents a bias in assessing their independent contribution to neural representations. For example, inanimate objects (e.g. a cow-shaped mug) that visually resemble an animate object elicit a similar neural pattern of response to that of the animate object (e.g. cow) (Bracci et al., 2019).

Furthermore, face recognition impairment is the hallmark symptom of DP. However, faces themselves are a heterogeneous category, including other-race, other-species and cartoon faces. The extent to which DP affects recognition of non-white, non-human faces is currently not well understood. Only one study has investigated the recognition of other-race faces in DP, whereas recognition of animal faces in DP has not been explored at all. Cenac et al., (2019) demonstrated that DPs were impaired at recognising both own-race and other-race faces, and this impairment was proportional for own- and other-race faces.

1.4. Neural correlates of face recognition

Neuroimaging studies have demonstrated a strong selectivity for recognition of object categories in higher-order areas of the visual system. Category-selective areas have been observed in the inferior temporal (IT) cortex in the ventral visual stream. Faces selectively activate areas in the IT cortex – the fusiform face area (FFA), the occipital face area (OFA) and the superior temporal sulcus (STS) (Kanwisher, 2010). These selective activations for faces are robust and have reliably been replicated over the past 20 years. Figure 1.1 shows the results from a large-scale meta-analysis of published functional magnetic resonance imaging (fMRI)

studies (*n* = 896) demonstrating that face images evoke preferential activation in stereotypical locations within the IT cortex - the FFA OFA, STS.

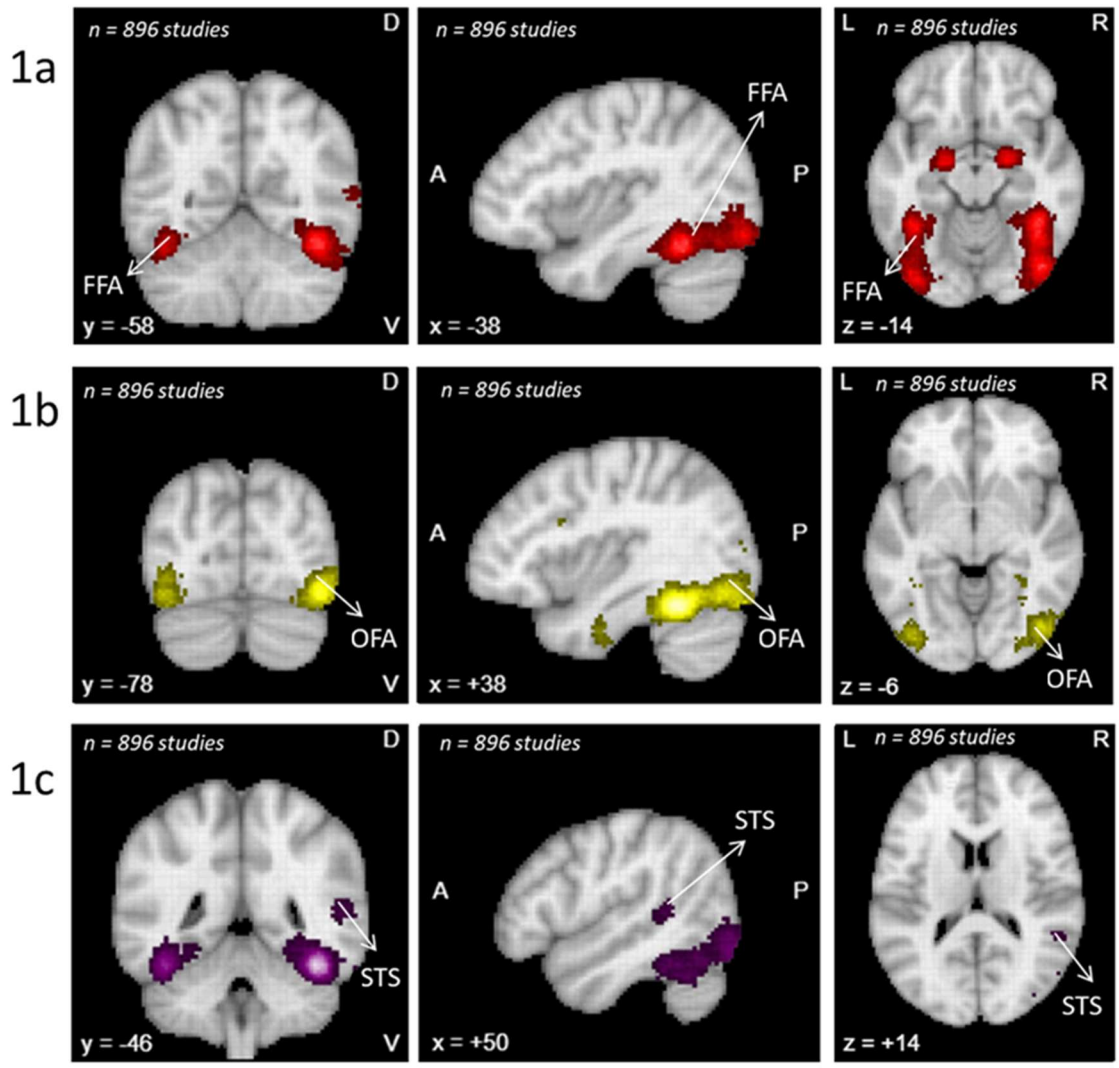

Figure 1.1. Locations of core face selective regions. The figure was created by the author of this thesis using data from a large-scale automated meta-analysis of functional neuroimaging data. Face selectivity maps identified by mapping voxels preferentially related to the term *"face"* (*n*=896 studies) are shown in the 1a) fusiform face area, 1b) occipital face area, 1c) superior temporal sulcus. The evoked activity was identified using association test maps, showing voxels that are reported more often in articles containing the term *face* in their abstract than articles that do not. Maps are corrected with FDR = 0.01, threshold = 5. For detailed explanation of the methodology, please see Yarkoni, Poldrack, Nichols, Van Essen, & Wager, (2011). A list of all the studies contributing to the meta-analysis can be found in the NeuroSynth database at neurosynth.org

1.5. A framework for the special status of faces based on organizational principles of low-level properties

The domain-specificity of neural selectivity has several limitations. Firstly, it only accounts for the neural correlates of a limited number of categories. There are numerous categories of objects, which fail to produce activity clustered in a specific area and many regions within IT cortex do not exhibit selectivity to any preferred category. Further, the domain-specific hypothesis does not explain how the brain reorganizes information from image-based representations in early visual areas to categorical representations in higher visual areas. Higher-level semantic information about images such as their category is discontinuous in nature, and it is unclear how it can serve as an organization principle of the IT.

One biologically plausible hypothesis for the emergence of face-selective clusters is the diagnostic featural coding hypothesis, which is based on low-level properties as the organizing principle of object representation. According to this hypothesis, the IT cortex contains subareas selective for combinations of low-level visual features which characterise particular object categories (Andrews, Watson, Rice, & Hartley, 2015; Bracci, Ritchie, & Beeck, 2017). Indeed, the stereotypic locations of high order object areas correspond with eccentricity biases - objects which require fine detail processing such as faces and text are associated with central-biased representations, while objects which require large-scale integration processing such as scenes exhibit a bias towards peripheral visual fields (Malach, Levy, & Hasson, 2002). IT neurons also exhibit shape selectivity by integrating highly specific information about the orientations and positions of contour fragments (Brincat & Connor, 2004). Similarly, Rice, Watson, Hartley, & Andrews, (2014) reported a correlation between neural patterns of response in IT and low-level visual features of objects in humans. The

influence of low-level properties on representations is also evident within the FFA. In the FFA variations in low-level features of faces correlated with patterns of neural response (Rice et al., 2014). The FFA also displays a geometric pattern-specific response and preferentially responds to curvilinear patterns with more high-contrast elements in the upper part of the image (Caldara et al., 2006). Activation of the FFA when viewing concentric patterns is stronger compared to viewing radial or parallel patterns (Wilkinson et al., 2000). Moreover, the FFA activation in response to concentric geometry was approximately half the amount of FFA activation in response to faces, suggesting that processing image structure is a major component of face perception.

Importantly, the model fits well with the reported lack of correlation between face and other object classes in behavioural tasks, as distinct processing mechanisms might be expected for any class of images that have high intra-class and low inter-class similarity in their low-level properties. Faces are one such image class with high inter-category similarity of low-level properties and low between-category similarity. To illustrate this point, we carried out a non-metric multidimensional scaling analysis of the low-level properties of different image exemplars from 9 categories (Figure 1.2).

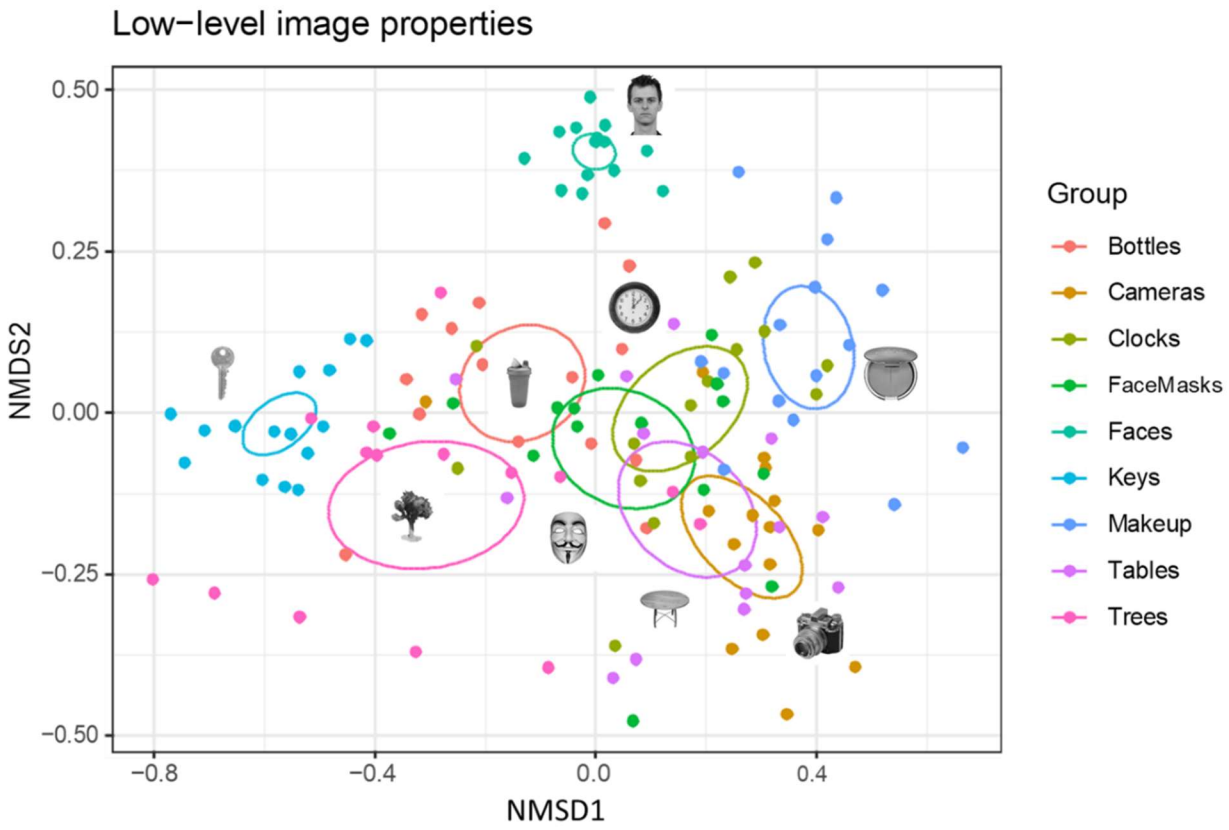

Figure 1.2. A non-metric multidimensional scaling (NMDS) analysis of low-level visual properties of 9 object categories. Each dot represent an image. Each dot's position is determined by its' low-level properties - 2048 values, calculated using the GIST descriptor (Torralba & Oliva, 2001). Ellipses represent standard error (SE).

As illustrated, faces form a distinct cluster, clearly separated from other categories, with the highest within-cluster similarity in low-level properties. Therefore, based on low-level properties, it is not surprising that face recognition is consistently found to be dissociated from recognition of other object categories. Interestingly, different objects categories show heterogeneity in low-level properties among them, illustrating that object categories do not form a uniform cluster and their heterogeneity in physical properties should be considered in object recognition research.

A clear prediction of the diagnostic featural coding hypothesis is that there will be an association between abilities to discriminate faces and abilities to discriminate exemplars of within-object classes sharing similar low-level properties to faces. A further extension of this

prediction is that DPs will also have deficits in recognition of objects with sufficient similarity in low-level properties to faces. To the best of the author's knowledge, there are no prior studies in the literature that measured low-level properties of images and assessed their contribution to face and object recognition abilities in neither DP, nor neurotypical groups.

1.6. Measuring low-level properties with the GIST descriptor

Throughout this thesis low-level properties of images were measured using the GIST descriptor (Torralba & Oliva, 2001). The GIST descriptor is an image analysis tool that captures the spectral and spatial properties of an image. For any input image, the GIST descriptor convolves the image with 32 Gabor filters at 4 spatial scales, across 8 orientations, producing 32 feature maps at each location of the image. The number of locations in the image is defined by the user but is typically 16 (the image is divided into 4x4 grid). The 16 locations each have 32 feature maps, resulting in a 16x32=512 numbers to describe the low-level image properties of an image (GIST descriptor). Put simply, the GIST descriptor summarises the spatial scales and orientations across different parts of an image with the goal to provide a description (the gist) of that image. Figure 1.3 illustrates the GIST descriptor output for a few images used in experiments within the thesis.

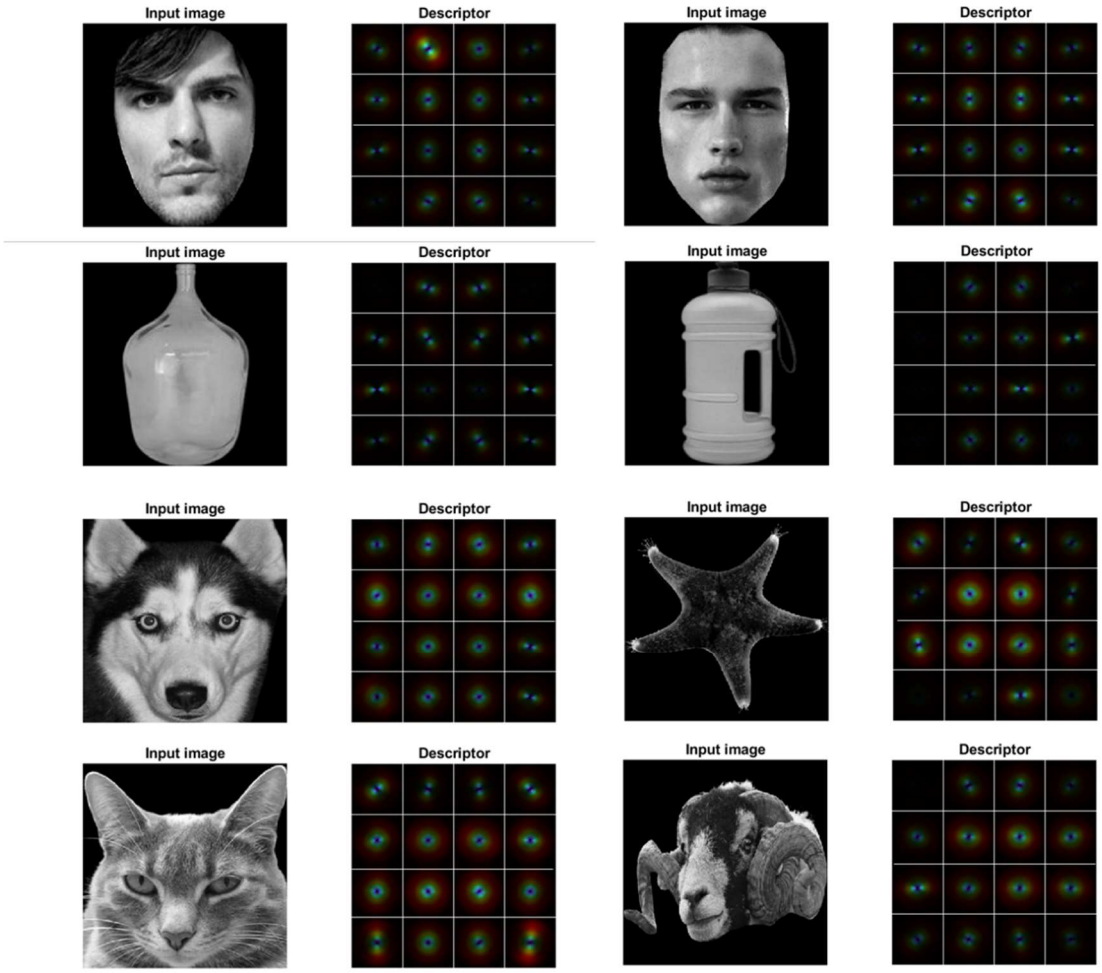

Figure 1.3. Average energy after applying Gabor filters in each location. From each location 32 GIST features (4 scales and 8 orientations) are extracted and visualized in polar coordinates.

The GIST descriptor was initially proposed in scene perception (Torralba & Oliva, 2001) with the aim to develop a low dimensional representation of the scene. The authors propose a set of perceptual dimensions (naturalness, openness, roughness, expansion, ruggedness) that represent the dominant spatial structure of a scene. They show that these dimensions can be reliably estimated using the GIST descriptor. Since then, The GIST descriptor, as a model of low-level image properties, has been successfully utilised beyond scene perception. For example, similarity in low-level properties of objects such as bottles, chairs, houses and, shoes, measured with the GIST descriptor can explain similarity in neural patterns to these

object categories (Rice et al., 2014). More importantly, the GIST descriptor has successfully captured variations in patterns of neural response to face identities (Rice et al., 2014). Although the GIST descriptor was built to capture low-level properties, it is important to note that the model can be subject to the same biases in low-level properties that it so well measures. For example, in a typical face matching task where the goal is to state whether two face identities match, difference in image background should not influence the decision. However, GIST does not have "high-level" cognition, and thus no way of distinguishing meaningful objects (the ones important for the matching task) from their background. It simply calculates the low-level properties of the whole image, treating the 16 locations as equally important. Figure 1.4 illustrates this point by visualizing the average energy across the 16 locations of the same face identity with different backgrounds. Similarly, as illustrated on Figure 1.3. different image categories will naturally have different shapes. When these images are superimposed on a background, the pattern of background (space not covered by stimuli) will be more similar between some categories and can influence the similarity estimates. Therefore, care should be taken to standardise backgrounds when using the GIST descriptor and interpreting the similarity estimates.

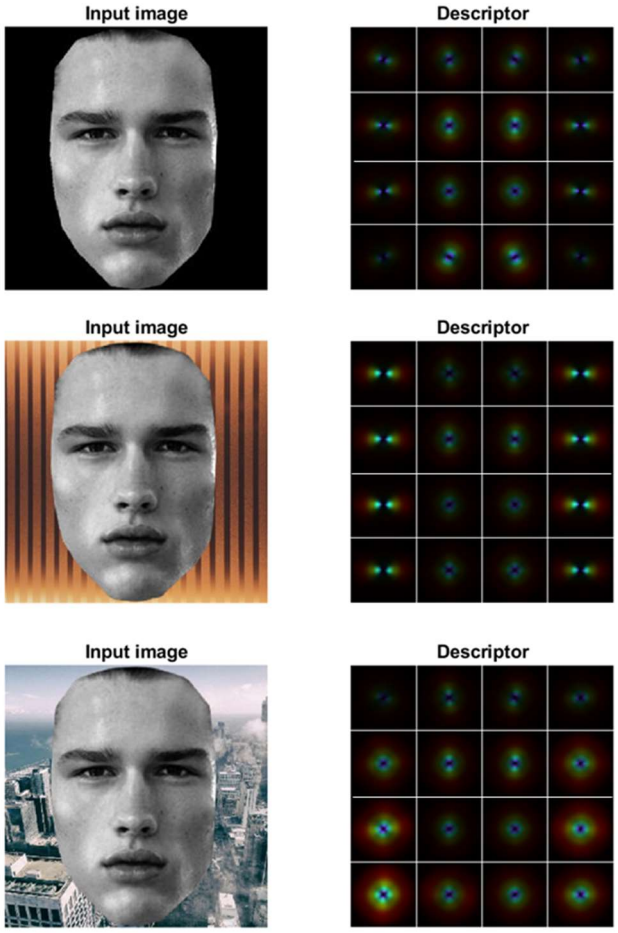

Figure 1.4. Average energy after applying Gabor filters in each location for the same face identity with different backgrounds.

1.7. Neural correlates of face recognition deficits in developmental prosopagnosia

The underlying neural mechanisms responsible for developmental prosopagnosia are still a subject of debate. The face-specificity observed in regions of the IT cortex of neurotypical individuals has focused research efforts to these face-specific areas as probable candidates of the neural correlates of DP. While some studies link deficits in DP to lower selectivity in the face-selective regions (Hadjikhani & De Gelder, 2002; Furl, Garrido, Dolan, Driver, & Duchaine, 2011; Jiahui, Yang, & Duchaine, 2018), others suggest that activation in the core face regions in DP is comparable to that of controls (Avidan, Hasson, Malach, & Behrmann, 2005; Hasson, Avidan, Deouell, Bentin, & Malach, 2003; Rivolta et al., 2014). Core

face-selective areas are identified by showing higher activity for faces compared to non-face objects, suggesting that they are involved in face recognition on a categorical level, rather than recognition of individual face identities. However, individuals with DP do not have any difficulties with recognising that a face is a face but are impaired with distinguishing different face identities. Face recognition on a categorical level and identity recognition need not necessarily be co-localized. Some areas may not exhibit face selectivity, yet still play a role in processing features important for face identity recognition (Anzellotti & Caramazza, 2014). While the core face network is specialised for face perception, the need to associate face images with person-specific knowledge necessary for identity recognition requires the neural network to increasingly integrate signals beyond the core face network. The anterior temporal cortex has been implicated as the neural correlate of recognising individual face identities. Activity in the anterior temporal cortex is sensitive to previously familiar faces (Gobbini & Haxby, 2007; Sugiura et al., 2001; Gorno-Tempini et al., 1998; Leveroni et al., 2000; Gorno-Tempini & Price, 2001; Collins & Olson, 2014) but also supports fine-grained perceptual discrimination in previously unfamiliar face identities (Kriegeskorte et al., 2007; Anzellotti et al., 2014; Yang et al., 2016) and is proposed to bridge high-level visual perception with memory (Collins et al., 2016). Specifically, neuropsychological lesion studies show that the left anterior temporal lobe is involved in associating verbal and semantic knowledge with faces, whereas the right anterior temporal lobe is involved in the visual representation and sense of familiarity (Gainotti, 2007). Further support for the importance of the anterior temporal lobe in identities recognition comes from findings demonstrating that deficits in connectivity with the anterior temporal lobe are linked to deficits in face recognition ability in DP and neurotypical populations (Rosenthal et al., 2017; Levakov et al., 2022).

Further, the interpretation of face selectivity is limited by univariate analyses. Univariate analyses compare BOLD responses on a voxel-by-voxel basis, with statistically significant voxels indicating stimulus-specific neural activity. In contrast multi-voxel pattern analysis (MVPA) allows for detecting differences between conditions with higher sensitivity. The pattern of activity of individual voxels is jointly analysed, capturing activation in voxels that might have been below threshold or have shown similar activation magnitude in a univariate analysis (Figure 1.3). For instance, when object representations are probed with MVPA, reliable distinct patterns of response emerge for many object categories (Haxby et al., 2001), compared to univariate analyses which show region-specific activation only for a very limited number of categories (faces, places, and bodies). One of the methodological strengths of MVPA is that it can treat each stimulus as its own condition and allows for investigation of the subtle differences in the overlap between the neural representation patterns of different face identities and as such is better equipped to probe the deficits in face identity recognition in DP.

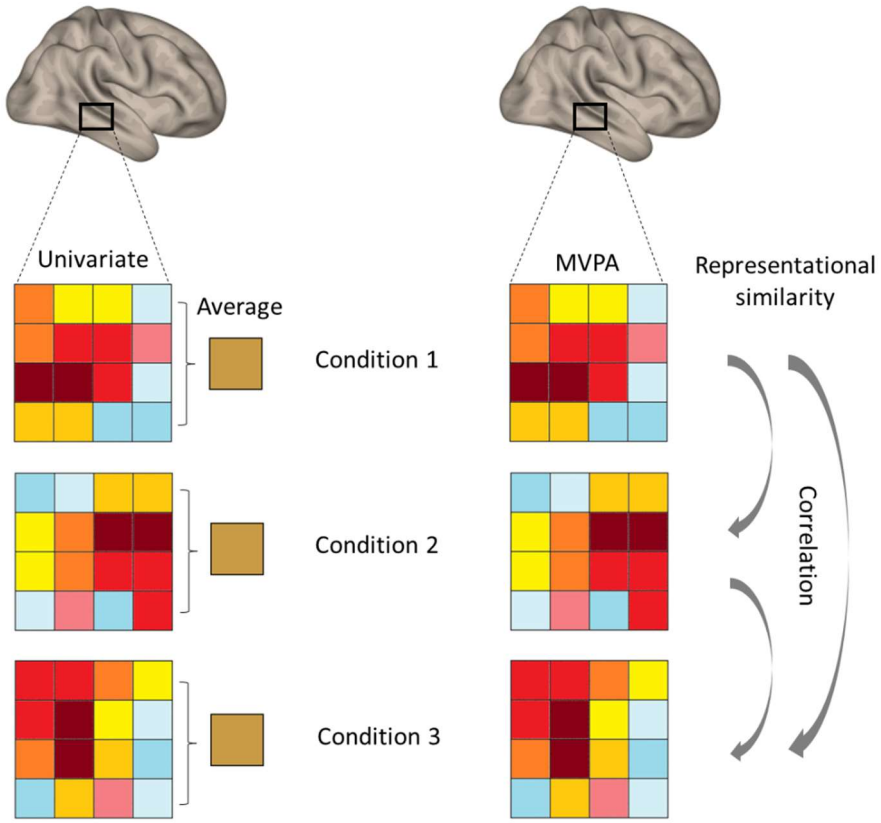

Figure 1.5. Schematic representation of univariate analysis (left) and MVPA (right). The same voxel-based activity can lead to different interpretations depending on the method used. Univariate analysis shows the same average activity across the 3 conditions, whereas MVPA shows differences in the pattern similarity between the conditions.

An alternative proposal has suggested that face-selective regions exhibit typical brain activity, however aberrant connectivity between them can account for the deficits in face recognition in DPs (Behrmann & Plaut, 2013). Connectivity can be structural and functional. Structural connectivity refers to the physical (white matter) connections between regions, while functional connectivity is measured by the correlation between regions' timeseries and thus reflects the level of neural synchronization. Disruptions in functional connectivity have been implicated in face recognition abilities (Levakov et al., 2022). Specifically, Rosenthal et al., (2017) demonstrated reduced functional connectivity between posterior face-selective regions and the anterior temporal cortex in DP. It is possible that to some extent the functional reductions in connectivity are constrained by reductions in structural connectivity.

Structurally, two white matter tracts have been implicated in face and object recognition. The inferior longitudinal fasciculus (ILF) - a long range, multi-layered white matter tract with bidirectional projections between the extrastriate cortex of the occipital lobe and the ventral anterior temporal lobe. One of the four major branches of the ILF is the fusiform branch, which connects the fusiform gyrus to the anterior temporal regions, thus linking the "core" with the "extended" face network (Latini et al., 2017). The second fibre tract integral for face and object processing is the inferior fronto-occipital fasciculus (IFOF), linking the occipiral and frontal lobes. Both ILF and IFOF have cortical terminations in posterior occipito-temporal areas such as the lateral-occipital cortex and the fusiform gurus (Herbet et al., 2018). Alterations of ILF's and IFOF's connectivity have been implicated in visual agnosia and prosopagnosia. Thomas et al., (2009) showed that DP individuals evidence reduced structural integrity of the ILF and IFOF in both hemispheres, despite showing BOLD activation in the core face areas comparable to controls. Importantly, higher structural integrity of both tracts was associated with fewer errors on a face recognition task. Moreover, structural integrity in the vicinity of face-selective regions, rather than the entire tract, might better account for the behavioural face recognition difficulties in DPs (Gomez et al., 2015; Song et al., 2015).

1.8. Thesis objectives

The overreaching objective of this thesis is to advance our understanding of DP by investigating the behavioural recognition profile and neural correlates of DP. The first aim of the thesis was to characterise the extent to which face, and object processing engage shared mechanisms and investigate the organizational principles behind the concurrent deficits in face and object recognition in DP. Specifically, Chapter 2 addressed the hypothesis that

similarity in low-level image properties will modulate the association between recognition abilities for faces and objects. Across 2 Experiments, we investigated the extent of association between recognition abilities of neurotypical adults as well as the recognition deficits in DP for faces and face-like objects varying in their low-level similarity to faces. Taken together, Chapter 2 will address the overreaching theoretical question of the extent to which face recognition is a specialised ability (domain specific) or engages a shared perceptual mechanism (domain-general).

Although face recognition is well-studied, a comprehensive mapping of the course of its development, and the role of perceptual experience to its development, is still missing. Behavioural results suggest that the specialisation for human face recognition is a gradual experience-dependent process not fully present at birth (Pascalis et al., 2002; Pascalis et al., 2005). Face recognition impairments are a hallmark symptom of DP, however, it is currently unclear whether recognition deficits emerge as a function of perceptual experience. Chapters 3 and 4 directly address whether DPs' recognition abilities will be influenced by the level of experience with different types of faces, or a general face deficit, independent of experience. Specifically, Chapter 3 addressed the hypothesis that face deficits in DP will extend to faces from other races. Similar in its conception, Chapter 4 addressed the hypothesis that DPs' face deficits will extend to animal faces. Together, Chapters 3 and 4 investigated the overreaching question of whether DPs have a general, experience-independent, deficit in the recognition of faces that encompasses a range of configural and morphological structures.

Lastly, despite the increased number of recent investigations, a comprehensive account of the neural correlates of DP is still missing. A final aim of the thesis was to explore how the brain may give rise to deficits in face recognition by focusing on measures relevant

to the behavioural deficits and developmental course in DP. As DP is a condition affecting the recognition of individual face identities, rather than faces as a category, Chapter 5 explored the neural correlates in DP by probing the neural signatures elicited by individual faces. Moreover, current theories of the neural basis of DP focus on the face processing network in the temporal lobe. While this core face network is specialised for face perception, the need to associate face images with person-specific knowledge necessary for recognition, requires the neural architecture to increasingly integrate signals across the whole brain. To this end, Chapters 5 and 6 used data-driven analyses to explore whether a disruption to global connectivity could explain the deficits in face recognition evident in DP.

Taken together, the overreaching aim of this thesis is to understand the behvaioural and neural mechanisms of typical and atypical face recognition abilities in DP. Chapters 2, 3, and 4 directly address whether face recognition in DP is a specific or shared impairment, and the extent to which this impairment is dependent on visual experience. Chapters 5 and 6 explore the significance of functional and structural integration of information across the whole brain in supporting face recognition abilities.

Chapter 2

Recognition of pareidolic objects in developmental prosopagnosic and neurotypical individuals

2.1. Abstract

Developmental prosopagnosia (DP) is a neurodevelopmental disorder associated with difficulties in the perception and recognition of faces. However, the extent to which DP affects non-face object is an ongoing debate. In this study, we asked whether pareidolic objects (which give rise to the perception of a face) are also affected in DP. First, we compared performance in DPs (*n*=30) and controls (*n*=27) on a recognition task with faces, pareidolic objects and non-pareidolic objects (bottles). The pareidolic objects had either similar or dissimilar image statistics to faces. Consistent with our understanding of DP, we found that the pattern of recognition across items between DPs and controls was lowest for faces. Interestingly, there was also a low correlation between DPs and controls for pareidolic-similar objects that was similar to faces. In contrast, there were higher correlations between DPs and controls for pareidolic-dissimilar objects and bottles, which were both significantly different to faces. These findings suggest that the deficit in DP involves processing image properties that are common to faces. Next, using an individual differences approach across a large group of neurotypical adults (*n*=94), we found that face recognition covaried with the recognition of pareidolic-similar objects, but not with pareidolic-dissimilar objects or non-pareidolic objects. Together, these findings support the idea that a representation based on image properties plays an important role in the perception and recognition of objects and faces and that the deficit in the perception of some object categories in DP could be explained by their

similarity to the image properties found in faces.

2.2 Introduction

The extent to which the underlying cognitive processes involved in face and object recognition are specific for each category (domain-specific) or shared between categories (domain-general) is an ongoing debate in psychology and neuroscience (Kanwisher, 2010; Behrmann & Plaut, 2014). Support for a domain-specific organization has been demonstrated in neuropsychological disorders, such as prosopagnosia in which lesions to the temporal lobe can result in severe deficits in face recognition but leave object recognition relatively intact (McNeil & Warrington, 1993). Conversely, other lesions are reported to affect non-face object processing, but leave face perception intact (Moscovitch et al., 1997). Further support for domain specificity is found in fMRI studies that have shown discrete regions in the temporal lobe respond selectively to faces (Kanwisher et al., 1997), whereas other regions are selective for different categories of non-face objects (Downing, Jiang, Shuman, & Kanwisher, 2001; Epstein & Kanwisher, 1998).

Other evidence supports a domain-general neural organization of the visual brain. In cases of acquired prosopagnosia, individuals develop typical face recognition ability, but subsequently experience face recognition difficulties following a brain injury (Renzi De, Faglioni, Grossi, & Nichelli, 1991; McNeil & Warrington, 1993). However, there is now growing evidence that these individuals also acquire deficits in the recognition of non-face objects (Behrmann & Plaut, 2013;Behrmann & Plaut, 2014). There are also individuals in the general population who experience lifelong face recognition difficulties without any history of brain injury (Duchaine & Nakayama, 2006). This condition is often referred to as developmental prosopagnosia (DP), to reflect the fact that the disorder is lifelong in duration. The degree to

which deficits in DP are face-specific or involve more general processing mechanisms has been the subject of debate (Behrmann & Plaut, 2013; Susilo & Duchaine, 2013). Some behavioural studies suggest that individuals with DP have preserved object recognition abilities (Duchaine, Yovel, Butterworth & Nakayama, 2006; Duchaine & Nakayama, 2006; Bate, Bennetts, Tree, Adams & Murray, 2019; Garrido, Duchaine & DeGutis, 2018), whereas other studies report deficits in object recognition (Behrmann, Avidan, Marotta & Kimchi, 2005; Biotti, Gray & Cook, 2017; Gray, Biotti & Cook, 2019;Geskin & Behrmann, 2018).

Further support for a domain-general neural organization can also be found in neuroimaging studies. For example, fMRI studies using multivariate analysis methods (in which the pattern, rather than the magnitude, of response is compared) show that overlapping patterns of response across the entire ventral temporal cortex may be important for the discrimination of different object categories (Haxby et al., 2001; Rice, Watson, Hartley & Andrews, 2014; Harris, Rice, Young & Andrews, 2015). The potential importance of the pattern is demonstrated by the fact that the ability to discriminate particular object categories is still evident when the most category-selective regions are removed from the analysis (Haxby et al., 2001b). For example, the pattern can still discriminate faces when the most face-selective regions are removed from the analysis. These findings suggest a distributed domain-general representation could underlie the perception of faces and non-face objects in ventral temporal cortex.

A key problem in understanding whether prosopagnosia is a domain-general disorder is that there has not been a clear theoretical rationale for which objects to test (Bate, Bennetts, Tree, et al., 2019). This has led to the use of a diverse range of object categories. As objects vary widely in both their visual and semantic properties (Rice et al., 2014; Coggan et

al., 2019), it is difficult to compare results across different studies and this may account for some of the discrepancies in the literature. It also makes it difficult to draw wider conclusions about the perceptual or cognitive origins of the disorder.

The aim of this study is to determine whether objects with similar visual or semantic properties are affected in the DP. To test this prediction, we used an old/new recognition paradigm using objects that give rise to the perception of faces (pareidolia). Pareidolic objects not only give rise to the perception of a face, but they also elicit face-like patterns of neural response (Wardle, Taubert, Teichmann & Baker, 2020; Taubert, Wardle & Ungerleider, 2020; Decramer et al., 2021) and can engage higher-level semantic properties, such as gender, age, and emotional expression (Wardle, Paranjape, Taubert & Baker, 2022). To determine the importance of visual and semantic properties, we selected pareidolic images that had either similar or dissimilar image statistics to faces. In Experiment 1, we compared the representational pattern similarity and performance on the recognition memory tasks for each condition with DPs and control participants. If semantic properties are important, we would expect the recognition of pareidolic objects to depend on perceived facial appearance. However, if image properties are important, we would only expect recognition to be affected for the pareidolic images with similar image statistics to faces. In Experiment 2, we used an individual differences approach with a larger analysis of neurotypical participants. We compared individual differences in performance on the face recognition task with performance with pareidolic objects. If image properties are important, we would only expect covariation in performance between faces and pareidolic images with similar image statistics to faces. On the other hand, if semantic properties are important, we would expect covariation between faces and all pareidolic images.

2.3. Methods

2.3.1. Participants

We report how we determined our sample size, all data exclusions (if any), all inclusion/exclusion criteria, whether inclusion/exclusion criteria were established prior to data analysis, all manipulations, and all measures in the study. Sample size was determined based on similar group studies investigating object recognition in DP (Biotti et al., 2017; Malaspina, Albonico, Toneatto & Daini, 2017; Bate et al., 2019). In Experiment 1, there were 30 participants with DP (M_{age} = 41.17, SD_{age} = 11.04, 21 females) and 27 control participants (M_{age} = 36.93, SD_{age} = 11.31, 16 females). There was no significant difference in age [t(55) = 1.43, p = 0.158, two-tailed] or gender [X^2 (1) = 0.72, p = 0.396, two-sided] between the two groups. All participants were over 18 years-old, had normal or corrected-to-normal vision and had no history of neurological conditions, schizophrenia or Autism Spectrum Disorder. All participants provided written informed consent and were fully debriefed after the experimental procedure. In Experiment 2, 95 participants (M_{age} = 19.05, SD_{age} = 0.98, 81 females) were recruited via an opportunity sample. One participant was excluded from the study for reporting face recognition difficulties (PI20 score > 65). All participants were over 18 years-old, had normal or corrected-to-normal vision and had no history of psychiatric or neurological conditions. All participants provided written informed consent and were fully debriefed after the experimental procedure. All experiments presented were approved by the Psychology Research Ethics Committee at the University of York.

2.3.2. Diagnostic Tests

DP participants were recruited through www.troublewithfaces.org. Diagnostic evidence for the presence of DP was collected using the PI20 questionnaire - a 20-item self-report measure

of face recognition abilities - https://www.troublewithfaces.org/pi20_printable.pdf (Shah, Gaule, Sowden, et al., 2015) and the Cambridge Face Memory Test (CFMT) – an objective measure of face recognition (Duchaine & Nakayama, 2006). CFMT consists of a learning stage where a target face is presented from 3 viewpoints for 2 seconds per viewpoint and 500ms. ISI. There were 3 types of test stages: 1) identical stage – target is presented the same as in the learning stage among 2 distractors; 2) novel stage – target is presented in a different viewpoint from the learning stage among 2 distractors; 3) noise stage – target is presented in a different viewpoint from the learning stage among 2 distractors and visual noise is added to all images. To be classified with DP, a participant had to score both > 65 on the PI20 and < 65% on the CFMT (Supplementary Table 1). The use of convergent diagnostic evidence from self-report and objective computer-based measure of face recognition ability is thought to provide reliable identification of DP; for example, less than 2% of the population score > 65 on the PI20 and < 65% on the CFMT (Gray et al., 2017).

2.3.3. Additional tests

In order to assess face perception and car recognition abilities participants who were classified into controls and DPs based on their pre-screening scores completed the Cambridge Face Perception Test (CFPT) (Duchaine, Germine & Nakayama, 2007), assessing the ability to perceive similarity between faces. Each trial required participants to arrange 6 faces morphed to different degrees according to their perceived similarity to a target face. Half of the trials were comprised of upright faces and half of inverted faces. Participants had 60 seconds to complete each trial. Performance was calculated as a deviation from the correct ordering of images across the upright and inverted trials (higher scores indicate more deviation and lower

performance). All participants completed the Models Face Matching Test (MFMT) (Dowsett & Burton, 2015) assessing unfamiliar face matching abilities. The MFMT entails seeing 90 pairs of face images and assessing whether the 2 faces within a pair are the same or different identity. Half of the pairs contained faces of the same identity and the other half had faces with different identities. Participants also completed the Cambridge Car Memory Test (CCMT) (Dennett et al., 2012) – a well-validated test for car recognition abilities with the same task structure and demands as CFMT. As expected, there were significant differences in performance between DPs and Controls for tests of upright face processing (Table 1). Participants with DP showed significant differences from controls on the PI20, $t(55) = 16.8$, $p < 0.0001$, CFMT, $t(55) = 12.55$, $p < 0.0001$, MFMT, $t(55) = 4.66$, $p < 0.0001$, CFPT Upright , $t(55) = 5.94$, $p < 0.001$. However, there were no significant differences on the control tests: CFPT Inverted, $t(55) = 1.49$, $p = 0.143$; CCMT, $t(55) = 1.55$, $p = 0.127$.

Table 2.1. Group comparisons results on diagnostic and additional tests. Mean scores (± 1 SE) on the Twenty-Item Prosopagnosia Index (PI20), Cambridge Face Memory Test (CFMT), Models Face Matching Test (MFMT), Cambridge Face Perception Test (CFPT) – Upright and Inverted, and Cambridge Car Memory Test (CCMT) for control (*n = 27*) and DP (*n = 30*) participants • reverse scored. ***p<0.001, *n.s.* not significant.

Test	**Controls (*n=27*)**	**DPs (*n=30)***	**Significance**	**Effect size (Cohen's *d*)**
PI20 •	39.6 ± 1.9	77.2 ± 1.2	***	4.40
CFMT %	83.8 ± 2.0	54.0 ± 1.4	***	3.30
MFMT %	72.9 ± 1.3	64.0 ± 1.4	***	1.24
CFPT Upright •	29.5 ± 1.8	47.9 ± 2.5	***	1.59
CFPT Inverted •	64.0 ± 2.6	69.1 ± 2.2	*n.s.*	0.39
CCMT %	70.2 ± 2.4	65.6 ± 1.8	*n.s.*	0.41

2.3.4. Old/New Recognition Task

The old/new recognition test consisted of 4 conditions: 1) faces, 2) pareidolic objects with similar visual properties to faces, 3) pareidolic objects with dissimilar visual properties to faces, and 4) non-pareidolic objects (bottles). Face images were from young-adult, male, Caucasians and were taken from the MFMT (Dowsett & Burton, 2015). Images of pareidolic objects and bottles were taken from a variety of freely available Internet sources. Our rationale for choosing bottles as a control condition was threefold: (1) a category with exemplars that were similar to each other; (2) a category with dissimilar image properties to faces; (3) a category in which the neural response to bottles is dissimilar to faces (Coggan et al., 2016). All images were presented in gray-scale and had a resolution of 256x256 pixels.

A GIST descriptor was used to determine the image similarity of pareidolic images to faces (Torralba & Oliva, 2001). The GIST descriptor is an image analysis tool that captures the spectral and spatial properties of an image. Each image is spatially divided into 16 (4x4) locations. The GIST descriptor calculates low-level properties by convolving the image with 32 Gabor filters at 4 spatial scales, each with 8 orientations, producing 32 feature maps for each of the 16 spatial locations. This produces a total of 512 values describing the low-level properties of each image.

First, we measured the GIST for all 60 face images to generate an average GIST descriptor for faces. Next, we measured the GIST of 120 pareidolic images and correlated the resulting vector with the average face vector. Based on the correlation values, the 20 pareidolic images with highest correlations to the 20 face targets were selected as targets for the face-like similar condition. The 20 pareidolic images with the lowest correlations to the 20 target faces were selected as targets for the face-like dissimilar condition. We compared

the low-level properties of bottles with the average face vector. Figure 2.1 illustrates example images of each condition and their correlation with the average GIST descriptor of faces. A one-way ANOVA indicated that there were significant differences in the similarity with faces across the different conditions ($F(3,76) = 739.4$, $p < 0.001$). *Post-hoc* multiple comparisons (FDR-corrected) showed that pareidolic-similar images had a higher correlation with faces ($M = 0.58$, $SD = 0.07$) compared to the pareidolic-dissimilar images ($M = 0.08$, $SD = 0.06$), $t(76) = 26.75$, $p < 0.001$) and bottles ($M = 0.29$, $SD = 0.07$, $t(76) = 15.25$, $p < 0.001$).

To select the distractors, we ran a cluster analysis of the pareidolic objects, which produced a matrix of similarity of each image to all other images. Based on the cluster analysis we chose the PS and PD distractor images from the clusters that contained the PS and PD targets. This allowed us to ensure that both targets and distractors in each condition had similar image properties. We also calculated low-level similarity of all 60 PS (targets and distractors) and 60 PD images to the face targets. Together, PS targets and distractors were the most face-like based on their image properties. PD targets and distractors were the least face-like based on their image properties. An independent t-test showed that low-level similarity to faces was significantly higher for the pareidolic-similar ($M = 0.41$, $SD = 0.15$) compared to pareidolic-dissimilar condition ($M = 0.26$, $SD = 0.15$), $t(118) = 5.82$, $p < 0.0001$).

To determine whether the observed low-level similarity of PS and PD images to faces generalises to a more diverse set of images, we calculated low-level similarity to faces from two other face databases (Supp Fig.1): Radboud face database (Langner et al., 2010) and the London face dataset (DeBruine et al., 2017). This analysis shows that PS images ($M = 0.43$, $SD = 0.08$) were significantly more similar to faces from the Radboud database than the PD images ($M = 0.08$, $SD = 0.15$), $t(38) = 9.28$, $p < 0.0001$. Similarly, PS images ($M = 0.31$, $SD =$

0.13) were more similar to faces from the London dataset compared to the PD images (M = 0.05, SD = 0.14), t(38) = 5.89, p < 0.0001).

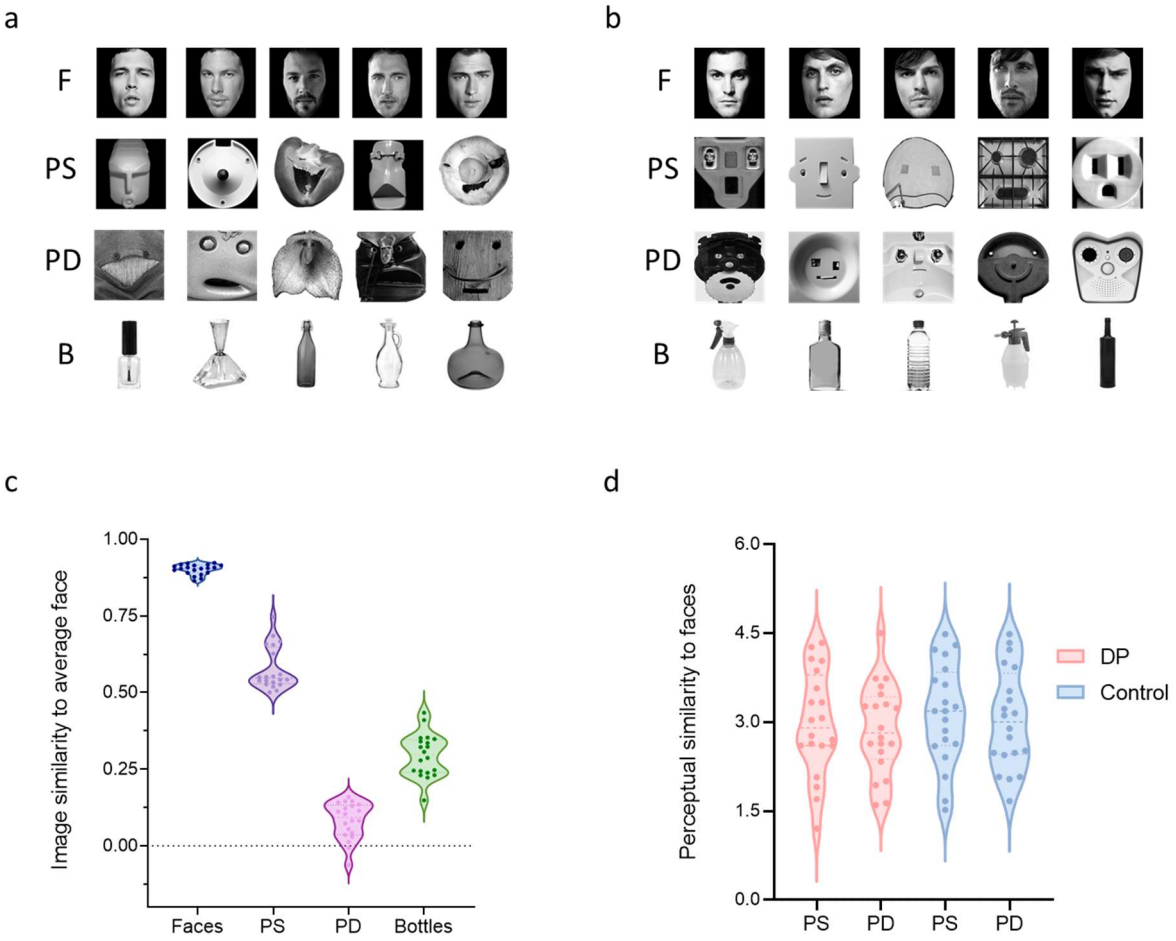

Figure 2.1. Example target (a) and distractor (b) images from F) Faces, PS) Pareidolic-Similar, PD) Pareidolic Dissimilar and B) Bottles conditions. (c) Similarity in low-level properties (Pearson's *r*) between the images from each condition and the average face descriptor. (d) Mean face resemblance rating for PS and PD targets in DP and Control participants.

The old/new recognition task involved a learning phase and a test phase. In the learning phase of each condition participants were presented with 20 target images for 2 sec each with a 1 sec inter-stimulus-interval. Participants were instructed to remember the

images. During the recognition phase the 20 target images were presented along with 40 distractor images. The recognition phase followed immediately after the learning phase for each condition. Conditions were counterbalanced and the order of image presentation in the recognition phase within each condition was randomised. Distractor images in each condition were from the same category as the target images. Participants were instructed to indicate by a button press whether the image was old or new. Images stayed on screen until participants made a response.

2.4. Results

2.4.1. Experiment 1

First, we performed an item analysis to determine whether there were differences in the way DPs and control participants represent images from the different conditions. To do this, we calculated the average accuracy for each item in the recognition task across all participants in either the DP or the control group, thus constructing a multi-item discriminability pattern for each task (Fig. 2.2). The mean and the range for each condition are shown in Table 2 and Supp Fig 1. The internal reliabilities are shown in Supp. Table 2. These are similar for the PS and PD conditions. We then correlated the average item values across the two groups for each condition. Correlations were then compared statistically using Fisher' *z*. A power analysis revealed that to detect an estimated correlation of $r = 0.54$, the required sample size is 24, (alpha = .05 and power = 0.80). Thus, the number of items ($n = 60$) used in the current analysis is sufficient for this analysis. We carried out a further sensitivity power analysis to determine whether the number of items is sufficient for comparing correlations. The power analysis revealed that to detect an effect size of 0.60 (power = 0.80), 47 items are required, critical *z*

score = ±1.96. However, for detecting a medium effect size of 0.3, 178 items are required. This suggests that the current analysis had limited sensitivity to detect small or medium effect sizes.

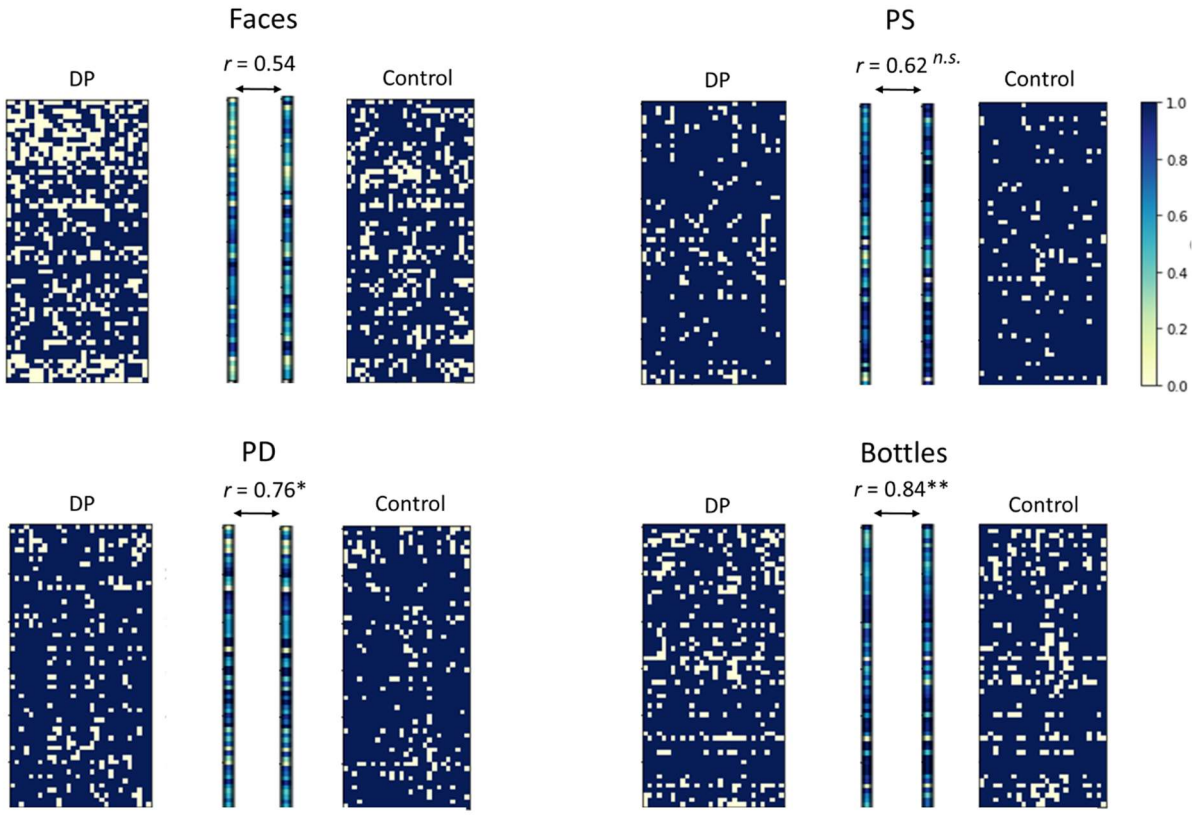

Figure 2.2. Correlations of multi-item patterns between DPs and controls for each recognition task. Each matrix shows participants on the x-axis and trials on the y-axis. Blue cells show correct responses and white cells show incorrect responses. The average values for each participant group were calculated for each trial and the corresponding item analysis correlated between DP and controls. The correlation between DPs and controls for faces was not significantly different to that of pareidolic similar (PS) but was significantly different to pareidolic dissimilar (PD) and Bottles. Significance values reflect whether each correlation is significantly different from the correlation value for faces ***p<0.001, **p<0.01, *p<0.05, *n.s.* p>0.05.

The multi-item pattern for faces showed the lowest correlation between DP and control participants. This is consistent with a general deficit in face perception in DPs. The correlation

between DPs and control participants was significantly higher for bottles (z = -3.29, p = 0.001) and for pareidolic-dissimilar objects (z = -2.09, p = 0.036) compared to faces. However, there was no significant difference between DPs and controls for pareidolic-similar objects compared to faces (z = -0.65, p = 0.519). The correlation between DPs and controls for pareidolic-similar objects was, however, significantly lower than for bottles (z = -2.65, p = 0.008). There was no significant difference between bottles and pareidolic-dissimilar objects (z = -1.20, p = 0.229). These findings suggest a difference in the way DPs represent faces and objects with similar image properties to faces compared to objects with dissimilar image properties to faces.

To determine whether these results could be explained by perceptual similarity to faces, participants rated the 20 pareidolic-similar and 20 pareidolic-dissimilar targets for their resemblance to faces on a 5-point scale (1: very low resemblance to faces to 5: very high resemblance to faces) at the end of the testing session. A 2-way mixed ANOVA with Group (DPs and Controls) as the between-subject factor and Image (PS, PD) as the within-subject factor. There was a significant main effect of Group ($F(1, 38) = 9.80$, $p = 0.003$). However, there was no effect of Image ($F(1, 38) = 0.16$, $p = 0.694$) or any interaction between Group and Image, $F(1, 38) = 0.01$, $p = 0.921$. *Post-hoc* multiple comparisons (FDR-corrected) revealed that DP participants (M = 2.98, SD = 0.88) reported lower face-like ratings for PS images compared to controls (M = 3.14, SD = 0.85, $t(38) = 2.23$, $p = 0.032$, Cohen's $d = 0.18$). PD images were also rated lower by DP (M = 2.88, SD = 0.76) than control (M = 3.04, SD = 0.84) participants ($t(38) = 2.20$, $p = 0.034$, Cohen's $d = 0.20$). This shows that the difference between pareidolic-similar and pareidolic-dissimilar objects did not reflect a difference in face likeness.

As a further test of whether perceptual similarity might explain the pattern of data, we reanalysed the data with the 20 'most face-like' (M = 3.68, SD = 0.44) and 20 'least face-like' (M = 2.34, SD = 0.45) pareidolic images, irrespective of the image properties. The correlation between the multi-item patterns of DPs and controls for the 20 most face-like images was $r(18) = 0.71$, $p < 0.0001$ and for least face-like images, $r(18) = 0.66$, $p = 0.002$. In order to compare these values to the correlations with faces, PS, PD and bottles from Experiment 1, we repeated the analysis with the 20 target images from the original conditions. The correlation between control and DP participants (restricted to the 20 target images) were as follows: faces ($r = 0.51$, $p = 0.021$), PS ($r(18) = 0.48$, $p = 0.032$), PD ($r(18) = 0.79$, $p < 0.0001$ and bottles ($r(18) = 0.66$, $p = 0.002$). Consistent with the original analysis, when pareidolic images are separated based on low-level properties, the correlation for faces ($r = 0.51$) is similar to PS ($r = 0.48$), but is different from PD ($r = 0.79$), (Supp Table 3). However, when the pareidolic images are separated based on perceived similarity to faces, the 'most face-like' and 'least face-like' conditions are higher (showing more similarity between DPs and Controls) and more similar to each other.

Next, we compared recognition accuracy for DP and control participants in the old/new recognition task. Item scores were entered into a 2 (group: DP and Control) x 4 (condition: face, pareidolic-similar, pareidolic-dissimilar and bottle images) repeated measures ANOVA. There were significant main effects of group ($F(1, 236) = 33.26$, $p < 0.0001$, $\eta p^2 = 0.12$) and condition ($F(3, 236) = 34.05$, $p < 0.0001$, $\eta p^2 = 0.30$). The interaction between group and condition was also significant ($F(3, 236) = 7.06$, $p < 0.001$, $\eta p^2 = 0.08$). To explore the interaction in more detail, we performed *post-hoc* comparisons (FDR-corrected) between DPs and controls for all tasks (Table 2). We also explored the strength of the evidence for the alternative hypothesis using Bayesian t-tests. Specifically, we tested the strength of evidence

for differences (the alternative hypothesis stating that DPs and Controls will differ) using BF_{10}. As the Bayes factor (BF_{10}) increasingly deviates from 1, (which indicates equal support for the null and the alternative hypotheses), more support is gained for the alternative hypothesis. BF_{10} between 1 and 3 is considered to be weak support, BF_{10} between 3 and 10 is considered moderate, and BF_{10} greater than 10 is considered strong evidence in support of the alternative hypothesis. We found a significant difference between DPs (M = 0.68, SD = 0.18) and controls (M= 0.77, SD = 0.14) on the face condition, ($t(236) = 6.79$, $p < 0.0001$), $BF_{10} = 10.99$). There was also a significant difference in accuracy between DPs (M = 0.90, SD = 0.08) and controls (M = 0.93, SD = 0.07) on the pareidolic-similar condition ($t(236) = 2.27$, $p = 0.049$), BF_{10} =1.35. However, there were no significant differences between DP (M = 0.87, SD = 0.10) and control participants (M = 0.89, SD = 0.10) on the pareidolic-dissimilar ($t(236) = 1.51$, $p = 0.178$, BF_{10} = 0.34) and the bottles, ($M_{DP} = 0.83$, $SD_{DP} = 0.15$, $M_C = 0.84$, $SD_C = 0.14$, $t(236) = 0.97$, $p = 0.331$, $BF_{10} = 0.22$).

We also analysed the heterogeneity of performance in the DP group across the 4 conditions (Suppl. Fig. 3). We found that the number of DPs who performed 1SD below the mean of the control group was 13 (43.3%) in the face task, 9 (30%) for the PS task, 6 (20%) for the PD task and only 4 (13.3%) for bottle task. This pattern of results mirrors that of the multi-item analysis. However, a Chi-square test indicated that there was no significant difference between the number of DPs who were impaired with PS objects (9) and the number of DPs impaired with PD objects (6), X^2 (1, N = 30) = 0.89, p = 0.371.

Table 2.2. Group comparisons results on the old/new recognition tasks**.** Mean (± 1SEM) recognition accuracy for the old/new recognition tasks in Control (*n=27*) and DP participants (*n=30*). ****p*<0.001, ***p*<0.01, **p*<0.05, *n.s.* p>0.05.

	Controls	DPs	Significance	Effect size (Cohen's *d*)
Faces	0.77 ± 0.02	0.68 ± 0.02	***	0.56
PS	0.93 ± 0.01	0.90 ± 0.01	*	0.40
PD	0.89 ± 0.01	0.87 ± 0.01	*n.s.*	0.20
Bottles	0.84 ± 0.02	0.83 ± 0.02	*n.s.*	0.07

We calculated reaction time (RT) for all correct trials. There was a significant interaction between group and task ($F(3, 220) = 2.73$, $p = 0.045$). *Post-hoc* multiple comparisons (FDR-corrected) showed that RT was significantly higher for faces in the DP group ($M = 2.31$, $SD = 0.69$, $BF_{10} = 25.26$) compared to Controls ($M = 1.74$, $SD = 0.55$) ($t(220) = 4.62$, $p < 0.0001$). However, there was no difference between DPs and controls for pareidolic-similar ($M_{DP} = 1.41$, $SD_{DP} = 0.39$; $M_C = 1.28$, $SD_C = 0.31$, $t(220) = 1.04$, $p = 0.299$, $BF_{10} = 0.58$), pareidolic-dissimilar ($M_{DP} = 1.58$, $SD_{DP} = 0.47$; $M_C = 1.37$, $SD_C = 0.34$,$t(220) = 1.70$, $p = 0.091$, $BF_{10} = 1.19$), or bottles ($M_{DP} = 1.46$, $SD_{DP} = 0.45$; $M_C = 1.29$, $SD_C = 0.35$, $t(220) = 1.34$, $p = 0.182$, $BF_{10} = 0.70$).

Finally, we analysed the data using an individual differences approach. We calculated the correlation between individual performance with faces with performance on the other conditions. For controls, accuracy scores for faces were significantly correlated with PS, ($r_s = 0.53$, $p = 0.005$, $BF_{10} = 8.96$), but not with PD ($r_s = 0.31$, $p = 0.115$, $BF_{10} = 0.69$) or bottles ($r_s = 0.37$, $p = 0.057$, $BF_{10} = 1.29$). For DPs, there was no significant correlation between performance with faces and PS ($r_s = 0.03$, $p = 0.883$, $BF_{10} = 0.47$), PD ($r_s = 0.25$, $p = 0.192$, $BF_{10} = 0.35$) or bottles, ($r_s = -0.26$, $p = 0.158$, $BF_{10} = 0.67$). This shows similar individual variation between faces and PS in controls, but not in DPs. To ensure that the lack of correlation

between DPs is not caused by lower variability of scores we correlated individual differences between bottles and PS and PD. In Controls, performance with bottles did not correlate with PS, (r_s = 0.30, p = 0.126), but correlated with PD (r_s = 0.76, p < 0.001). In DPs performance with bottles significantly correlated with PS, (r_s = 0.56, p = 0.001), and PD (r_s = 0.39, p = 0.031), suggesting that the previously reported lack of correlation between faces and PS in DPs reflects that DPs are not sensitive to the low-level properties common to faces.

2.4.2. Experiment 2

Experiment 2 used an individual differences approach to compare performance on tasks of face and object processing in a large group of neurotypical adults. First, we compared performance on the standard diagnostic tests used in Experiment 1 (scores on tests in which lower scores indicate better performance were reverse-coded). Fig 2.3a shows the individual variation in all the tests: CFMT (M = 80.0, SD = 12.9), CFPT Upright (M = 31.9, SD = 13.1), and Inverted (M = 62.9, SD = 14.7), MFMT (M = 70.4, SD = 8.9) and CCMT (M = 66.2, SD = 11.5).

Figure 2.3c shows a correlation matrix across all the diagnostic tests. We found that the CFMT had the highest correlation with the other tests of upright face perception, namely the CFPT upright (r_s (92) = 0.50, p < 0.0001, BF_{10} = 31705.2) and the MFMT (r_s (92) = 0.56, p < 0.0001, BF_{10} = 382025.1). The CFMT was also correlated with the CFPT inverted (r_s (92) = 0.26, p = 0.011, BF_{10} = 0.88). The MFMT correlated positively with both CFPT upright (r_s (92) = 0.34, p = 0.001, BF_{10} = 27.9) and inverted conditions (r_s (92) = 0.34, p = 0.0009, BF_{10} = 29.1). Finally, there was a significant positive correlation between the upright and inverted CFMT (r_s (92) = 0.46, p < 0.0001, BF_{10} = 57853.1). In contrast, the CCMT was not correlated with any of the

tests at p < 0.05. These findings show that the significant inter-individual variation across participants covaries with tasks involving upright faces.

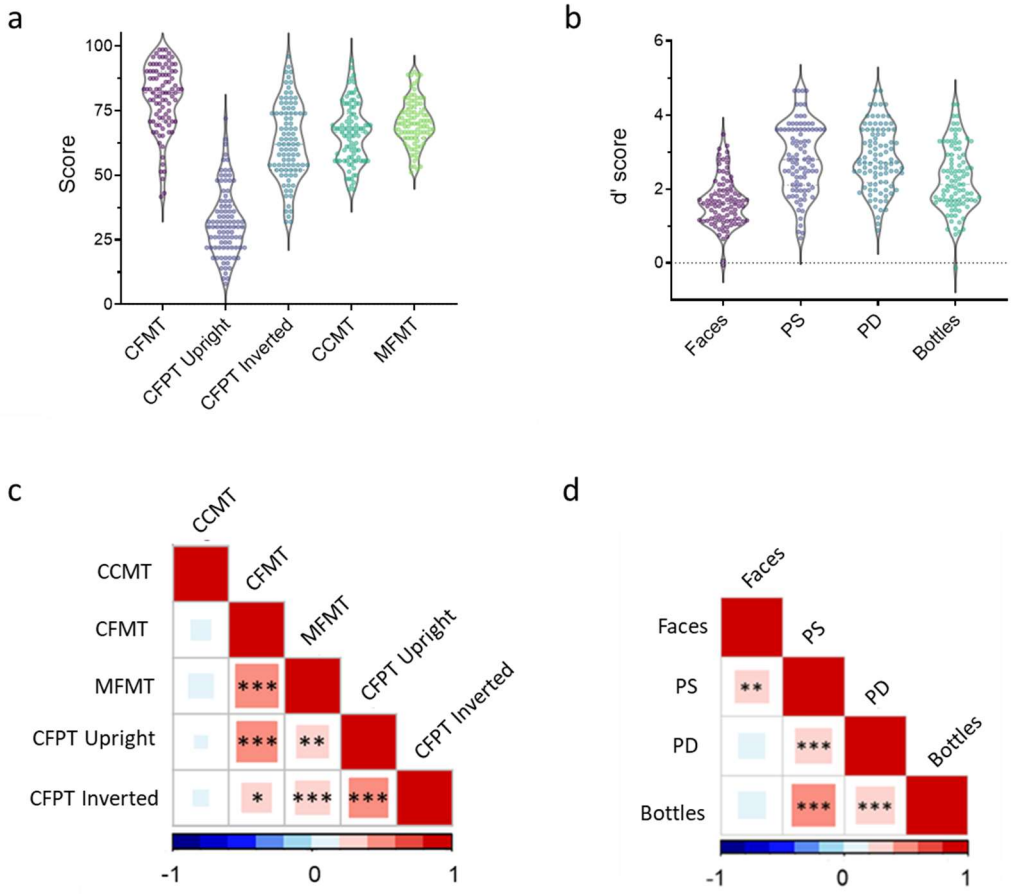

Figure 2.3. (a) Individual variation of scores on the diagnostic tests. (b) Individual variation of d' scores on the 4 conditions of the old/new recognition paradigm. (c) Correlation matrix between the diagnostic tests. (d) Correlation matrix between the *d*' values for Faces, PS, PD and Bottles conditions in the old/new recognition task ***p<0.001, **p<0.01, *p<0.05

Performance for each participant on the old/new recognition tasks was calculated with *d'*, by using the hit rate (correctly recognising an image as a target) and false alarm rates (incorrectly mistaking an image for a target). In cases where hit rate was 1 and/or false alarm rate was 0, *d'* was calculated by decreasing the hit rate to 0.99 and increasing the false alarm to 0.01. Fig. 2.3b shows there was significant individual variation in the *d'* scores on the face

(M = 1.65, SD = 0.66), pareidolic-similar (M = 2.83, SD = 0.94), pareidolic-dissimilar (M = 2.83, SD = 0.85) and bottles conditions (M = 2.27, SD = 0.88). Although there was significant variation in performance across the 4 conditions, $F(3, 279) = 63.26$, $p < 0.0001$, there was no significant difference in overall performance between the critical PS and PD conditions ($t(93) = 0.01$, $p = 0.990$, FDR-corrected).

Next, we compared individual variation on the recognition tasks (Fig. 2.3d). There was a significant positive correlation between recognition accuracy on the face condition and the pareidolic-similar condition ($r_s(92) = 0.30$, $p = 0.004$, $BF_{10} = 6.91$). In contrast, there was no correlation between performance on the face condition and pareidolic-dissimilar ($r_s(92) = 0.18$, $p = 0.081$, $BF_{10} = 2.16$) or bottle ($r_s(92) = 0.20$, $p = 0.054$, $BF_{10} = 1.39$) conditions. Recognition of pareidolic-similar and pareidolic-dissimilar objects was positively correlated ($r_s(92) = 0.34$, $p < 0.001$, $BF_{10} = 50.2$) and recognition performance with bottles was correlated positively with both pareidolic-similar objects ($r_s(92) = 0.49$, $p < 0.001$, $BF_{10} = 93179.7$), and PD objects, ($r_s(92) = 0.39$, $p < 0.001$, $BF_{10} = 231.6$).

2.5. Discussion

The aim of the study was to investigate the extent to which individuals with developmental prosopagnosia also exhibit impaired recognition of objects. Although some studies suggest that individuals with DP have preserved object recognition abilities (Bate, Bennetts, Tree, Adams & Murray, 2019; Garrido, Duchaine & DeGutis, 2018), there is now growing evidence that individuals with DP have deficits in the recognition of some non-face objects (Geskin & Behrmann, 2018). A key issue that has not been resolved is why some objects appear to be affected whereas others are not. In this study, we asked whether objects with similar visual

or semantic properties to faces are more likely to be affected in DP. To do this, we used the phenomenon of face pareidolia, in which inanimate objects give rise to the perception of faces (Liu et al., 2014; Wardle et al., 2020; Decramer et al., 2021; Omer et al., 2019; Alais et al., 2021; Keys et al., 2021; Wardle, Paranjape, Taubert & Baker, 2022).

We compared pareidolic objects with similar image properties to faces to pareidolic objects with dissimilar image properties to faces. In Experiment 1, we used an item-wise correlation analysis to determine the pattern of performance for DP and match-control participants. For each recognition condition, we first measured the mean accuracy for each item across all individuals within a group (DPs and neurotypical controls). The accuracy across the different items gives rise to the multi-item pattern. We measured the similarity of these multi-item patterns in DPs and controls for each condition. We found that the similarity between DPs and controls was significantly lower for faces compared to the control non-pareidolic object condition (bottles). This demonstrates a clear difference in the way that faces and non-face objects are represented in DPs and is consistent with a recent study using a similar item-wise correlation method (Xue et al., 2020). The key novel finding in this study is that the similarity in the multi-item pattern between DPs and controls was also lower for pareidolic objects with similar image properties to faces. In contrast, the similarity in the item analysis was greater for pareidolic objects with dissimilar image properties and with bottles. This suggests that these objects are perceived more similarly in DPs and controls. Importantly, the ranges and reliability for PS and PD scores were comparable.

A possible alternative explanation of the data could be that the pareidolic objects with more similar image properties were also perceived to be more ‘face-like’. To address this issue, we measured the perceived ‘face-likeness’ of pareidolic objects with similar and

dissimilar image properties to faces. We found that both pareidolic similar and pareidolic dissimilar objects were perceived to have a similar face-likeness. This allows us to differentiate between low-level and high-level properties in the main analysis of the data. We also reanalysed the data by separating the pareidolic images into the 'most face-like' and 'least face-like'. We found that the item-wise correlation was similar in these two conditions and was higher than for faces. Together, this suggests that the deficit in DP is better explained by the visual properties of the images.

We also found that DPs were impaired in the recognition of faces and pareidolic objects that had similar image statistics to faces. However, there was no difference in performance between DPs and controls for pareidolic objects that had dissimilar low-level image properties or non-pareidolic objects (bottles). The group difference in recognition accuracy for pareidolic similar objects was significant, but it was smaller compared to faces. There was also no difference in response time. There are two reasons for why there might be a smaller effect on overall recognition with pareidolic similar objects between DPs and controls. The first is that, although the image properties are similar, they are not identical to faces. This is consistent with previous studies have also shown that neural response to pareidolic objects is similar, but not identical to faces (Liu et al., 2014; Wardle et al., 2020; Decramer et al., 2021; Omer et al., 2019; Alais et al., 2021; Keys et al., 2021). Another reason for the smaller difference in pareidolic similar objects might be the higher accuracy for the pareidolic objects in the old/new recognition task, which may have masked the effect of group.

In Experiment 2, we tested a large group of neurotypical adults on the recognition tasks. One hypothesis about the deficit in DP is that it reflects the lower end of the normal

distribution of face processing abilities (Barton & Corrow, 2016). With this theoretical perspective, we used an individual differences approach to ask whether recognition performance on faces could be predicted by recognition performance on other objects. Although some studies have found correlations between face and object tasks (Zhao et al., 2016; Malaspina et al., 2017; Biotti et al., 2017), other studies have failed to report significant covariation between faces and non-face objects (Bate, Bennetts, Tree, et al., 2019). Here, we report that performance on the face recognition task was only correlated with performance on the pareidolic-similar object task. There was no correlation between faces and pareidolic-dissimilar objects or bottles. We performed a similar individual differences analysis on the data in Experiment 1, albeit with a smaller sample size. Consistent with the findings from Experiment 2, we found the highest correlation between faces and PS in control participants. Interestingly, there was no correlation between faces and PS in DPs. This was not caused by less variability of scores in DPs as the correlation between bottles and PS was significant. Hence, the lack of correlation between faces and PS in DPs likely results from lack of a unified mechanism for faces and PS recognition. While, low-level properties are driving the covariation of performance in Controls, this is not the case for DPs. Together these findings suggest that variation in previous studies comparing the perception of faces and objects may reflect variance in the image statistics. Again, this suggests that performance on these recognition tasks is linked to the representation of the image properties.

One interesting result we observed from the additional tasks is that there was no group difference between DPs and controls for inverted faces (CFPT Inverted task) in Experiment 1 and this task showed the weakest correlations with other face tasks in Experiment 2. This fits with a previous study that found a reduced face inversion effect in DPs that reflected poorer performance on upright faces compared to controls (Klargaard, Starrfelt

& Gerlach, 2018). Most studies using inverted faces suggest that the difference in performance is explained by an absence of configural or holistic processing in inverted faces (Carey & Diamond, 1977). However, when faces are inverted, their low-level properties do not match those of upright faces. The role of low-level properties might be an alternative framework for future studies when trying to explain face and object inversion effects.

The importance of image statistics in the recognition of faces and objects shown across the two experiments raises important questions about the underlying neural representations of complex objects. Although the ventral visual pathway is directly involved in the perception and recognition of objects (Milner & Goodale, 1995; Haxby et al., 1991), the extent to which the neural representation of objects in this region reflects low-level or high-level properties remains unresolved. Patterns of response in higher-visual areas of the ventral visual pathway have been linked to higher-level properties of objects, such as category (Connolly et al., 2012; Haxby et al., 2001), animacy (Kriegeskorte et al., 2008a), semantics (Naselaris et al., 2009) and real-world size (Konkle & Oliva, 2012b). However, it remains unclear how these representations emerge from the image-based representations found in early visual areas. One possibility is that the patterns of response in high-level visual areas reflect an underlying representation that is based on more fundamental properties of the stimulus (Andrews, Watson, Rice, & Hartley, 2015). Recent studies have shown that differences in image properties of objects can explain a significant amount of the variance in high-level regions of visual cortex (Coggan et al., 2019; Rice et al., 2014; Watson, Hartley & Andrews, 2014; Sormaz, Watson, Smith, Young & Andrews, 2016). For example, category-selective patterns of response are still evident when images have been scrambled in a way that preserves some of their visual properties, but removes their semantic properties (Coggan, Baker, & Andrews, 2016; Coggan, Liu, Baker & Andrews, 2016; Long, Yu & Konkle,

2018; Watson, Hartley & Andrews, 2017). Similarly, objects from different categories but with similar image properties give rise to similar patterns of response (Coggan et al., 2019). The behavioural findings in this study using pareidolic objects provide strong converging evidence for the importance of image properties in the representation and recognition of objects and provide insights into the way that domain-general processing might occur (Behrmann & Plaut, 2013; Andrews, Watson, Rice & Hartley, 2015).

In conclusion, we show that faces and pareidolic objects with similar image properties to faces are significantly affected in individuals with DP. However, we did not find any effects for pareidolic objects that did not have similar image properties to faces. This difference between pareidolic objects could not be explained by how face-like they were perceived. These results provide new insights into object recognition deficits in DP. Further evidence for the role of image properties is shown by the covariation between faces and pareidolic objects with similar image properties in the neurotypical population. Together, our results support the idea of an underlying domain-general representation in visual cortex that is based on the image statistics of objects.

2.6. Data accessibility

Experimental stimuli, code and anonymised data are publicly available at https://osf.io/c7esz/ Legal copyright restrictions prevent public archiving of the additional tests used in this study, which can be obtained from the copyright holders in the cited references (see 'Additional tests').

Chapter 3

Different mechanisms explain face recognition deficits in developmental prosopagnosia and the other-race effect

3.1. Abstract

Individuals with developmental prosopagnosia (DP) are impaired in their ability to recognise faces when compared to neurotypical controls. Neurotypical controls, on the other hand, are impaired in the recognition of other-race faces compared to own-race faces – a phenomenon known as the other-race effect (ORE). However, it is not clear whether these deficits in face recognition reflect a common mechanism. In this study, we compared recognition for own-race and other-race faces in DPs and Controls. Participants completed matching tasks with own-race (White) and other-race faces (Black and Asian). DPs were impaired with both own-race and other-race faces, however, the impairment was larger for own-race faces. We used an individual differences approach to assess whether performance for own- and other race faces will co-vary within the same individuals. At the individual level performance of controls on own-race faces strongly predicted performance on other-race faces, suggesting that faces from different races engage a common cognitive mechanism. However, DPs performance with own-race faces did not predict their performance with other-race faces, suggesting a lack of a shared processing mechanism across all faces. Together, these results suggest different processes may underpin the deficits in face recognition found in DP and the ORE.

3.2. Introduction

Developmental prosopagnosia (DP) a neurodevelopmental disorder, characterised by deficits in face identity recognition, despite normal low-level vision and no history of brain damage (Cook & Biotti, 2016; Duchaine & Nakayama, 2006; Susilo & Duchaine, 2013). Tests reveal that these individuals perform significantly below average on a range of common tests of face perception, matching and recognition (Biotti et al., 2019; Duchaine et al., 2007; Duchaine & Nakayama, 2006).

The Other-Race Effect (ORE) is another deficit in face recognition in which neurotypical controls show better recognition with own-race faces compared to other race faces. The ORE is a well-established phenomenon in which individuals show better recognition with own-race faces, relative to other race faces (Malpass & Kravitz, 1969). The ORE is a well-replicated effect across different ethnic groups (Bothwell et al., 1989; Walker & Tanaka, 2003) and is present in humans as early as 4 months old (Chien et al., 2016). The ORE is typically demonstrated with memory tasks, however, the effect is present in perceptual and matching tasks as well (Wang et al., 2022; Bate et al., 2019; Megreya et al., 2011; Robertson et al., 2020), suggesting that the ORE might emerge at the encoding level of face processing. An influential explanation of the ORE is the perceptual expertise hypothesis (Goldstein & Chance, 1985; Rhodes et al., 1989). According to it, the ORE reflects increased sensitivity to differences in own race faces as a function of visual experience. Importantly, the theory predicts that despite lower recognition of own- compared to other- race faces, performance across different faces will depend on a shared mechanism and will co-vary. There is growing evidence in support of this. Despite lower accuracy for other-race faces, face matching and sorting of own races co-varied with that of other-race faces (Wang et al., 2022; Kokje et al., 2018), suggesting that own and

other-race faces recruit the same processing mechanism. Super recognisers are a group of individuals who display superior performance in face identity recognition but show an ORE comparable to controls (Bate, Bennetts, Hasshim, et al., 2019) and their performance on matching own-race faces also predicts their other-race matching abilities (Robertson et al., 2020).

Although DP and the ORE both involve a deficit in face recognition, it is not clear whether the underlying mechanism is similar in both. One reason for this is that the tests used to define DP typically involve own-race faces. Only two studies have investigated the interaction of other-race face processing and DP. The first study demonstrated that DPs were impaired at recognising both own-race and other-race faces, and this impairment was proportional for own- and other-race faces (Cenac et al., 2019). However, this study did not demonstrate an ORE in either controls or DPs, and the authors did not make conclusions about the magnitude of ORE within the DP sample. The second study investigated face memory abilities in white DPs and white and asian controls (Esins et al., 2014). As expected, DPs were worse on recognition of white faces compared to neurotypical white participants. Interestingly, white DPs also performed worse than asian control participants, suggesting that DP and the ORE result from different processing impairments. Nevertheless, the study did not investigate recognition of different races in DP.

The study had two aims. First, to determine whether the perceptual impairments in DP, typically shown using own-race faces, extend to other-races. To test this, we used own-race (White) and other-race (Asian and Black) identity matching tasks to assess the discrimination abilities of DPs relative to neurotypical individuals. We also used an item analysis to explore whether there are qualitative differences between DPs and Controls in the patterns of

performance across items for own-race and other-race faces. The second aim of the study was to determine the extent to which processing other-race faces engages the same mechanisms of own-race faces in neurotypical and DP participants. To do this, we used an individual differences approach to assess whether performance for own- and other race faces will co-vary within the same individuals.

3.3. Methods

3.3.1. Participants

29 White participants with DP (M_{age} = 43.10, SD_{age} = 12.70, 24 females) and 26 White control participants (M_{age} = 40.00, SD_{age} = 13.08, 18 females) completed the experiment online via Pavlovia - https://pavlovia.org. Some of the DP and control participants recruited for the current study have already participated in the experiment from Chapter 2. We performed a power analysis based on the effect size found in our experiment from Chapter 2 (Epihova et al., 2022), using the same own-race perceptual task as in the current study (Models Face Matching Test). Based on an effect size of 1.24 (Cohen's d) with an alpha = 0.05 and power = 0.80, the projected sample size needed was a minimum of 12 participants per group. The groups did not differ significantly in age, t(53) = 0.89, p = 0.377 or gender, X^2 (1) = 1.39, p = 0.238. All participants were over 18 years-old, had normal or corrected-to-normal vision and had no history of psychiatric or neurological conditions (schizophrenia, Autism Spectrum Disorder). All participants had grown up and were currently living in Western European countries. All participants provided written informed consent before participation. The study was approved by the Psychology Research Ethics Committee at the University of York. Participants were given a £5 Amazon voucher for participating in the experiment.

3.3.2. Diagnostic Tests

DP participants were recruited through www.troublewithfaces.org. Diagnostic evidence for the presence of DP was collected using the PI20 questionnaire - a 20-item self-report measure of face recognition abilities - https://www.troublewithfaces.org/pi20_printable.pdf (Shah, Gaule, Sowden, Bird, & Cook, 2015) and the Cambridge Face Memory Test (CFMT) – an objective measure of face recognition (Duchaine & Nakayama, 2006). CFMT consists of a learning stage where a target face is presented from 3 viewpoints for 2 seconds per viewpoint and 500ms. ISI. There were 3 types of test stages: 1) identical stage – target is presented the same as in the learning stage among 2 distractors; 2) novel stage – target is presented in a different viewpoint from the learning stage among 2 distractors; 3) noise stage – target is presented in a different viewpoint from the learning stage among 2 distractors and visual noise is added to all images. To be classified with DP, a participant had to score above the established cut-off on the PI20 (> 65) and < 65% on the CFMT to ensure their score falls at least 2 standard deviations below the typical mean on the CFMT (Table 1). The average DP scores on the diagnostic tests were: PI20 (M = 77.86, SD = 5.99), CFMT: (M = 53.69, SD = 8.79). The use of convergent diagnostic evidence from self-report and objective computer-based measure of face recognition ability provides reliable identification of DP (Gray et al., 2017; Tsantani et al., 2021). Where a participant has completed the PI20 and CFMT as part of the selection criteria for a previous experiment, the score from their first attempt was taken to avoid practice effects.

Table 3.1. Demographic information and individual scores on the diagnostic tests used to validate developmental prosopagnosia (PI20 questionnaire and Cambridge Face Memory Test (CFMT)). Comparison data (N = 54) for the PI20 and CFMT were taken from Biotti et al., 2019.

Participant	Age	Gender	Hand	PI20	CFMT %
DP1	57	F	R	72	62.5
DP2	21	F	R	84	34.72
DP3	33	F	L	76	56.94
DP4	29	F	R	84	45.83
DP5	54	F	R	74	58.33
DP6	59	M	R	84	43.05
DP7	25	F	R	83	59.72
DP8	50	F	R	84	54.17
DP9	51	F	L	79	55.55
DP10	40	F	R	82	62.5
DP11	52	F	L	75	41.67
DP12	33	M	R	67	48.61
DP13	57	F	R	78	34.72
DP14	52	M	R	84	51.39
DP15	22	F	R	77	59.72
DP16	19	M	R	75	51.39
DP17	63	F	R	75	45.83
DP18	41	F	R	75	48.61
DP19	43	F	R	68	56.94
DP20	49	F	R	75	61.11
DP21	42	F	R	73	63.89
DP22	48	F	R	86	62.5
DP23	23	F	R	86	41.66
DP24	45	F	R	79	62.5
DP25	60	F	L	68	61.11
DP26	48	F	R	79	52.78
DP27	39	F	R	84	63.89
DP28	46	F	R	67	63.89
DP29	49	M	R	85	51.39
DP Mean	**43.10**			**77.86**	**53.69**
DP SD	**12.70**			**5.99**	**8.79**
Comparison Mean	**39.2**			**38.0**	**85.0**
Comparison SD	**13.4**			**9.1**	**8.9**

3.3.3. Face Matching Tasks

Participants completed 3 face matching tasks – Asian, Black, and White male face matching tasks. Each matching task had 90 trials, where a pair of face images were presented together on each trial (Fig. 3.1). Half of the trials contained face pairs with the same identity and the other half had face pairs with a different identity. Participants were instructed to press a key to indicate the pair of faces are from the same identity and a different key to indicate if the pair had a different identity. Response times was recorded for all trials. The order of tasks was counterbalanced across all participants. Images were taken from the Models Face Matching Task (MFMT) (Dowsett & Burton, 2015). Images for the Asian and Black face matching tasks were taken from Wang et al., (2022). We used Signal detection theory (SDT) to measure performance. We calculated *d'* - a measure of discriminability from hit rate (correct match of same identity pair) and false alarm rates (incorrect match of different identity pair).

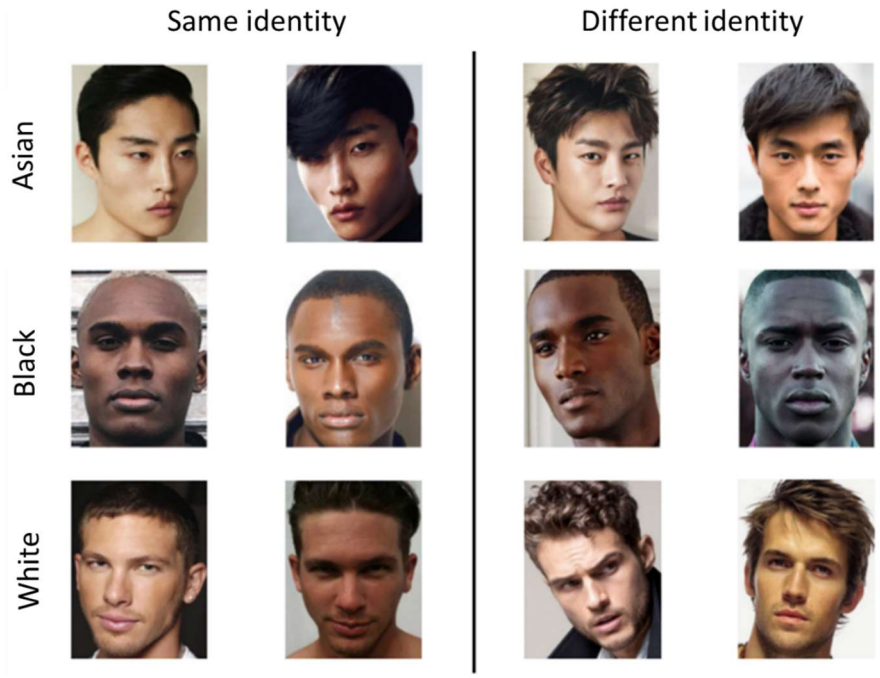

Figure 3.1. Example images from the Asian, Black and White face matching tasks showing Same identity (left) and Different identity (right) face pairs.

3.4. Results

First, we asked whether DPs are impaired with other-race faces and whether the magnitude of the impairment was similar to that of Controls. Discriminability (*d*') scores for DP and control participants were compared for white, black and asian tasks. A 2 (Group: Control, DP) by 3 (Race: White, Black, Asian) ANOVA showed a significant main effect of Group, $F(1, 159) = 26.89$, $p < 0.001$, Race, $F(2, 159) = 48.91$, $p < 0.001$ and a significant interaction, $F(2, 159) = 3.66$, $p = 0.028$. *Post-hoc* multiple (FDR-corrected) showed that DPs scored significantly lower than controls on both White, $t(159) = 4.97$, $p < 0.001$ and Black faces, $t(159) = 2.82$, $p = 0.008$. There was no significant difference between Controls and DPs in performance with Asian faces, $t(159) = 1.17$, $p = 0.243$. *Post-hoc* multiple comparisons (FDR-corrected) showed that Controls scored significantly higher on white faces (M = 1.52) compared to black faces (M = 1.21), $t(159) = 2.30$, $p = 0.023$. Controls also had significantly higher *d'* on white compared to asian faces (M = 0.41), $t(159) = 8.28$, $p < 0.001$ and on black than on asian faces $t(159) = 5.98$, $p < 0.0001$. In DPs there wasn't any significant difference in performance between white (M =0.87) and black faces (M = 0.84), $t(106) = 0.20$, $p= 0.842$ (Figure 3.2a). DPs were significantly better at matching white faces compared to asian (M = 0.26), $t(159) = 4.82$, $p < 0.001$ and black compared to asian faces, $t(106) = 4.62$, $p < 0.001$.

Next, we further examined response time (RT) of correct responses (Fig. 3.2b). Responses longer than 2 minutes per pair were removed, which resulted in the removal of 2 responses. RTs were entered in a 2 (Group: Control, DP) x 3 (Race: White, Black, Asian) ANOVA. There was no effect of Group, $F(1, 159) = 0.51$, $p = 0.478$, but there was a significant main effect of Race, $F(2, 159) = 3.15$, $p = 0.045$. The interaction between Group and Race was not significant, $F(2, 159) = 0.01$, $p = 0.988$. *Post-hoc* multiple comparisons (FDR-corrected)

indicated that RT was not significantly different between any 2 tasks in Control and in DP participants at $p < 0.05$.

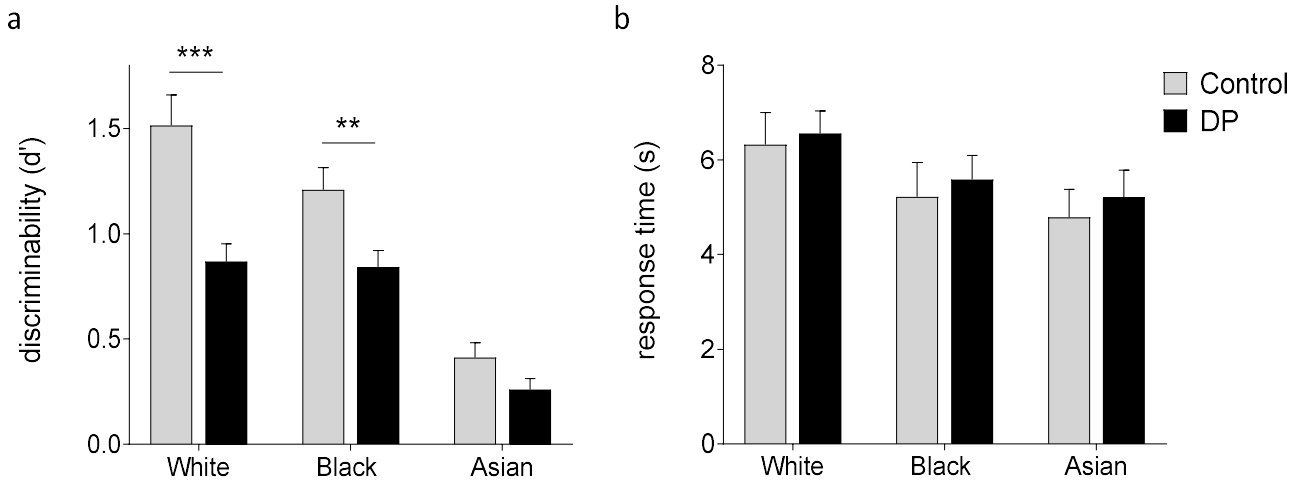

Figure 3.2. a) Mean *d'* score and b) mean RT data for Control and DP participants for White, Black and Asian face matching tasks. Error bars represent ± 1 SEM.

Next, we investigated the pattern of response on the different face matching tasks for controls and DPs. For each image pair we computed the average % correct answers for controls and DPs. We then correlated the values to determine the similarity between controls and DPs (Fig. 3.3). Although we found significant correlations for each face matching task (White: $r(88) = 0.74$, $p < 0.001$; Black: $r(88) = 0.88$, $p < 0.001$; Asian: $r(88) = 0.81$, $p < 0.001$), there were differences in the magnitude of the correlations. We determined whether these correlations were significantly different using Fisher's *z*. The similarity of patterns for White faces was significantly lower than for Black faces ($z = -2.81$, $p = 0.005$) but not for Asian faces

(z = -1.16, p = 0.244). There was no difference between Black faces and Asian faces (z = 1.64, p = 0.101).

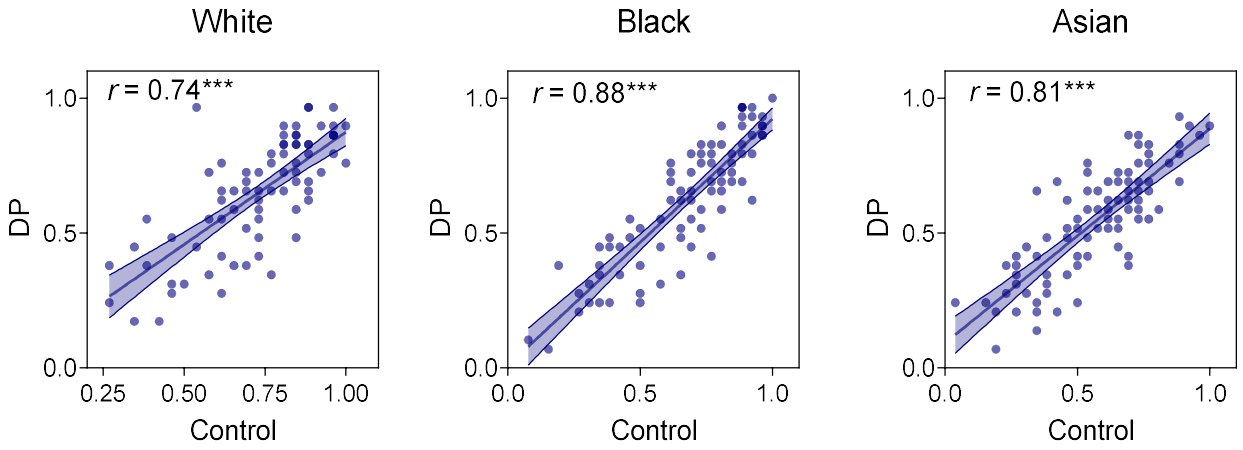

Figure 3.3. Correlations between the multi-item patterns of Control and DP participants for White, Black and Asian faces. Blue shaded region represent 95% confidence intervals.

Next, we compared individual variation on both tasks to determine if performance on own-race faces can predict performance with other-race faces (Fig. 3.4). There was a significant correlation among control participants between White and Black faces (r(24) = 0.77, p < 0.001) and between White and Asian faces (r(24) = 0.57, p = 0.002). There was also a correlation between Black and Asian faces (r(24) = 0.59, p = 0.001). In contrast, DPs showed no significant correlations between White and Black faces (r(27) = 0.25, p = 0.188), White and Asian faces (r(27) = 0.28, p = 0.141) or Black and Asian faces (r(27) = -0.04, p = 0.828).

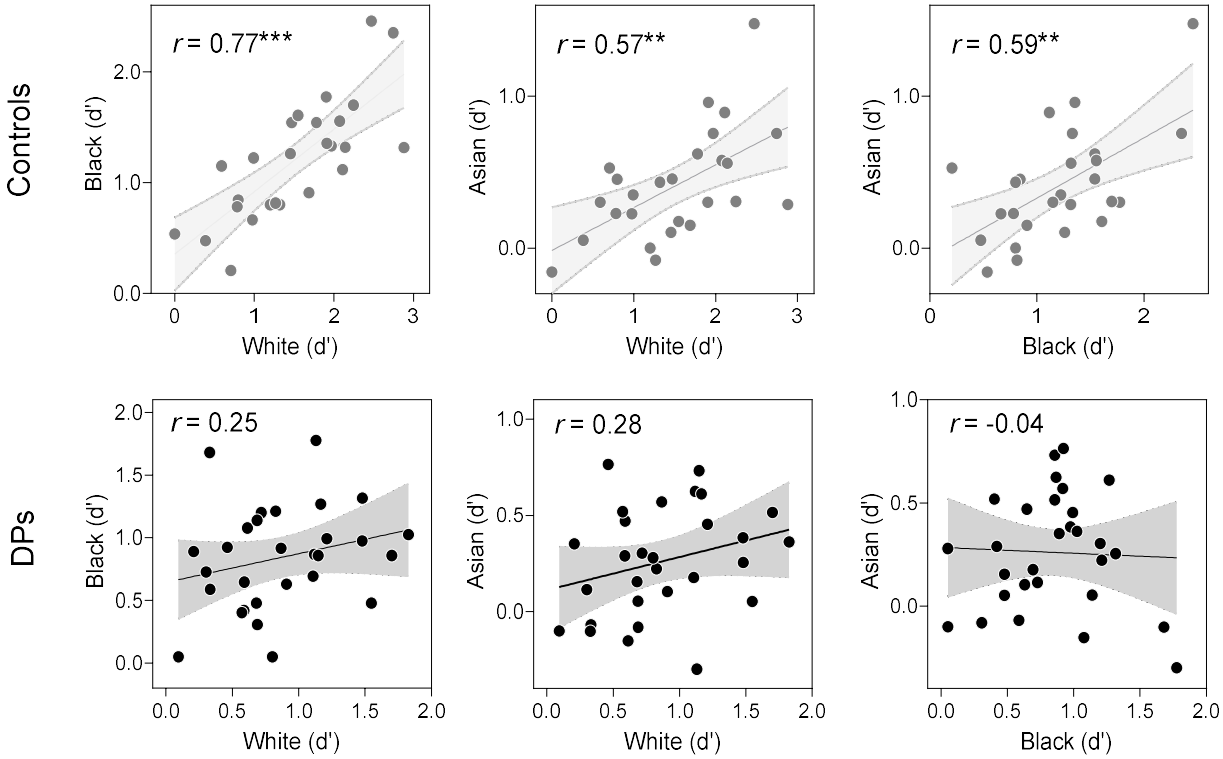

Figure 3.4. Correlation (Pearson's r) in *d'* scores between White, Black and Asian faces for control and DP participants. ***p<0.001, **p<0.01, *n.s.* p > 0.05

3.5. Discussion

The first aim of the study was to determine whether the perceptual impairments in DP, typically shown using own-race faces, extent to other-races. To address this, we tested face matching abilities of white control and DP participants with own-race (White) and other race (Asian, Black) faces. Overall, we found that DPs performed worse on both own- and other-race faces relative to controls, but the magnitude of impairment was lower for other-race faces. The performance with Black faces was significantly lower in DPs, and a similar trend was observed with Asian faces, but the difference did not reach significance. This suggests that the face identity recognition deficits in DP extend to other-race faces. These

results are consistent with recent findings demonstrating impairment in both own and other-race faces in DPs relative to controls (Cenac et al., 2019). However, the authors found a proportional impairment for White and Black faces. One explanation for this discrepancy might be the different difficulty between own-races and other-race tasks in Cenac et al., (2019). The authors used other-race faces with higher variability then own-race faces, thus making the other-race task easier. As a result, no ORE was observed in Controls or DPs. In fact, the data illustrates a reverse trend – higher performance with other-race relative to own-race faces. It is possible that the easier other-race tasks have amplified the magnitude of impairment to match that for own-race faces. When the difficulty between own-race and other-race (Asian) tasks was equal, the magnitude of impairment for own-race faces was bigger than for other-race faces.

A more general issue in ORE studies is determining whether the effect is driven by a genuine ORE or differences in the difficulty of the stimulus sets that are used for own-race and other-race tasks other-race faces being more difficult than own-race faces). Wang et al., (2022) developed the tasks used in the current study and used them in a cross-over design where the Asian, Black, and White face matching tasks were performed by Asian and White participants. This cross-over design is critical in studies of the ORE in order to show a cross-over interaction and rule out the possibility of the potential confound of task difficulty. The Asian face matching task was more difficult which was reflected by the fact that Asian participants did not demonstrate superior performance for it compared to other-race tasks. However, performance of Asian participants on the Black and White tasks was similar, suggesting that they their difficulty is comparable. These results suggests that in the current study the better performance of Controls with White (own-race) faces compared to Black faces cannot be explained by task difficulty, but reflects a genuine ORE.

We used an item-wise correlation analysis to determine the pattern of performance for DP and match-control participants. For each matching task, we first measured the mean accuracy for each pair of faces across all individuals within a group. The accuracy across the different pairs gives rise to the multi-item pattern. We measured the similarity of the multi-item patterns in DPs and controls for each task. Overall, we found that the multi-item patterns of DPs and Controls were significantly similar– that is, pairs that were found to be difficult for controls were also difficult for DPs, whereas pairs that were easier for controls were also easier for DPs. However, the similarity between DPs and controls was significantly lower for White faces compared to Black faces. This demonstrates a difference in the way that White and Black faces are represented, suggesting that the most prominent differences in face representations between the two groups was for own-race faces. These results show that DPs' disproportionate quantitative difference in impairment for White faces was associated with the highest qualitative difference in the pattern of performance.

Our results support the idea that DP and ORE are associated with different face processing deficits (Esins et al., 2014; Cenac et al., 2019). Despite clear evidence for an ORE in controls, at the individual level performance of controls on own-race faces strongly predicted performance on other-race faces, suggesting that faces from different races engage a common cognitive mechanism. This is consistent with previous reports, showing a shared cognitive mechanism for own- and other-race faces in neurotypical individuals and super recognisers (Wang et al., 2022; Bate & Bennetts, 2015; Robertson et al., 2020; Kokje, Bindemann, & Megreya, 2018). However, DPs performance with own-race faces did not predict their performance with other-race faces, suggesting a lack of, or less tuned shared processing mechanism across all faces. Successful recognition entails judging similarity between faces. In typically developed individuals such principles will be updated as a function

of visual experience, to optimally processes variance between individual faces. This can be illustrated by the face-space framework, which postulates that similarity between faces is encoded as a mean relative vector in a multi-dimensional space (Valentine, 1991). Due to the highest experience with own-race faces, these principles will be optimally tuned for processing variance within own-race faces, and less so for other-race faces, resulting in the ORE. The lack of correlation between performance with own- and other-race faces in DPs might stem from less tuned principles which guide similarity judgements affecting faces from all races. Indeed, DPs have been demonstrated to show atypical mechanisms of face identity coding in a multi-dimensional faces space (Palermo et al., 2011). This is consistent with the lack of correlation we report between own- and other-race faces in DP, as the impairment in coding face-identity properties is irrespective of race in DPs. Nevertheless, previous reports have demonstrated that DPs have some coarse face-space that subserves overt recognition of some faces (Nishimura et al., 2010). This is in line with our results as DPs scored above chance on both own- and other-race face tasks. This suggests that although face identity coding might be impaired, DPs have retained some residual properties based on which face identity is judged above chance.

In conclusion, we show that DPs were impaired with both own- and other-race faces, but the impairment was larger for own-race faces. An item analysis showed there was lower similarity in the patterns of recognition for White faces compared to Black faces. These results suggest that the highest quantitative and qualitative differences between DPs and Controls were observed for own-race faces. Further, performance on own-race faces co-varied with performance on other-race faces in controls, but not in DPs. Together, these findings suggest that DP, and reduced visual experience with other-race faces differentially influence the ORE.

3.6. Data accessibility

Anonymised data from this study is publicly available at https://osf.io/2esw5/

Chapter 4

Recognition of animal faces is impaired in developmental prosopagnosia

4.1. Abstract

Developmental prosopagnosia (DP) is a neurodevelopmental disorder associated with difficulties in the recognition of human faces. However, it is unclear whether the recognition of non-human faces is also affected in DP. To address this question, we compared recognition performance in DPs and controls with human and animal faces. We found that DPs showed deficits in the recognition of both human and animal faces compared to neurotypical controls. However, differences in the response to human and animal faces in DPs suggest somewhat different processing strategies may underlie these deficits. In contrast to human and animal faces, we found no deficit in the recognition of animate or inanimate objects in DPs. Using an individual-level approach, we demonstrate that in 60% of cases in which face recognition is impaired, there is a concurrent deficit with animal faces. Together, these results show that DPs have a general deficit in the recognition of faces.

4.2. Introduction

Prosopagnosia is the inability to recognise faces despite normal visual processing. In cases of acquired prosopagnosia (AP), individuals develop normal face recognition, but following brain damage to the occipito-temporal cortex, experience difficulty in recognising faces (Barton, 2008; de Renzi et al., 1991). Developmental prosopagnosia (DP), on the other hand, reflects deficits in face recognition in the absence of any observable brain injury (Cook & Biotti, 2016;

Duchaine & Nakayama, 2006; Susilo & Duchaine, 2013). Tests reveal that these individuals perform significantly below average on a range of common tests of face perception and recognition (Biotti et al., 2019; Duchaine et al., 2007; Duchaine & Nakayama, 2006). However, the extent to which prosopagnosia selectively affects the perception of human faces remains contentious (Geskin & Behrmann, 2018).

It is unclear whether the deficit in prosopagnosia also affects animal faces, as standard tests for prosopagnosia only use human faces (Duchaine & Nakayama, 2006; Shah, Gaule, Sowden, et al., 2015). There are a few case studies of individuals with AP who report impairments in the ability to discriminate different categories of animal faces and also in the ability to recognize individuals within the same species (Bornstein et al., 1969; Landis et al., 1986; Toftness, 2019). However, there are other cases of AP, in which the ability to recognise animal faces remains intact (Landis et al., 1986; McNeil and Warrington, 1993). For example, patient WJ was a sheep farmer, who acquired prosopagnosia after a stroke, but was still able to differentiate between different sheep (McNeil & Warrington, 1993). These studies provide mixed evidence for impaired animal face recognition in AP. However, to our knowledge, there have been no systematic investigations of animal face recognition in DP.

Neurophysiological and neuroimaging studies provide some support for the idea that similar neural processes underpin the perception and recognition of both human and animal faces. For example, face-selective regions such as the FFA show similar preferential activity for human and animal faces compared to images of bodies and objects (Kanwisher et al., 1999; Tong et al., 2000). Other studies have investigated the pattern of response in the inferior temporal lobe and found similar patterns of response to human and animal faces that is distinct from non-face objects (Kriegeskorte et al., 2008). Evidence for the association of

human and animal faces also comes from single neuron activity in humans. Face-selective neurons in humans are more responsive to animal faces compared to other object categories (Decramer et al., 2021). Single neuron studies in monkeys have also shown that most face cells respond in a similar way to monkey and human faces (Perrett et al., 1992).

In contrast to these neuroimaging and neurophysiological studies, developmental work suggests that the mechanisms underlying the perception of human and animal faces may be somewhat different. Although young human infants show similar sensitivity to human and monkey faces, they gradually become tuned to human faces throughout infancy reflecting the perceptual experience of the individual (Pascalis et al., 2002; Pascalis et al., 2005). For example, it has been reported that 6-month-old infants are able to discriminate between monkey faces, in a way that 9-month-olds and adults cannot (Pascalis et al., 2005). Moreover, exposure to monkey faces in early infancy is thought to attenuate this 'perceptual narrowing' (Pascalis et al., 2002).

Previous studies have, therefore, provided conflicting evidence in support of the idea that the recognition of human and animal faces might engage similar processing mechanisms. To address this question, we investigated human and animal face recognition in DP. Despite the important theoretical implications of this question, this has not been directly investigated in DP. Using an old/new recognition paradigm, we compared performance with human, cat, dog, monkey, and sheep faces in DPs and neurotypical controls. We also compared performance with animate (starfish) and inanimate (bottle) object categories that do not have faces.

4.3. Methods

4.3.1. Participants

Thirty-seven DPs (7 males, M_{age} = 36.92, SD_{age} = 6.61) and 27 Controls (10 males, M_{age} = 31.78, SD_{age} = 13.27) participated in the experiment. Some of the DP and control participants recruited for the current study have already participated in the experiment from Chapter 2 and Chapter 3. There have been no previous studies of animal face recognition. However, we performed a power analysis using the data from Biotti, Gray & Cook (2017) because the authors used the same diagnostic tests to identify DP and investigated the recognition deficit of a biological class of stimuli (bodies). Based on an effect size of 0.89 (Cohen's d) with an alpha = 0.05 and power = 0.80, the projected sample size needed was a minimum of 21 participants per group. The groups did not differ significantly in age ($t(62) = 1.53$, $p = 0.131$), or in gender (X^2 (1) = 1.62, p = 0.105). All participants were over 18 years-old, had normal or corrected-to-normal vision and had no history of neurological conditions, schizophrenia or Autism Spectrum Disorder. All participants provided written informed consent and were fully debriefed after the experimental procedure. The experiment was approved by the Psychology Research Ethics Committee at the University of York.

4.3.2. Diagnostic Tests

DP participants were recruited through www.troublewithfaces.org. Diagnostic evidence for the presence of DP was collected using the PI20 questionnaire – a 20-item self-report measure of face recognition abilities (Shah, Gaule, Sowden, et al., 2015), and the Cambridge Face Memory Test (CFMT) – an objective measure of face recognition (Duchaine & Nakayama, 2006). To be classified with DP, a participant had to score above the established cut-off on

the PI20 (> 65) and < 65 % on the CFMT, to ensure their score falls at least 2 standard deviations below the typical mean on the CFMT (Table 1). The average DP scores on the diagnostic tests were: PI20 (M = 79.11, SD = 6.61), CFMT: (M = 50.69, SD = 8.49). The use of convergent diagnostic evidence from self-report and objective computer-based measure of face recognition ability provides reliable identification of DP (Gray et al., 2017; Tsantani et al., 2021). Where a participant has completed the PI20 and CFMT as part of the selection criteria in a previous experiment, the score from their first attempt was taken to avoid practice effects.

Table 4.1. Demographic information and individual scores on the diagnostic tests used to validate developmental prosopagnosia, namely the PI20 questionnaire (PI20) and Cambridge Face Memory Test (CFMT).

DP	Gender	Hand	Age	PI20	CFMT	zPI20	zCFMT
DP1	F	R	21	84	34.72	5.05	-5.65
DP2	F	R	28	80	41.67	4.62	-4.87
DP3	F	R	49	86	44.45	5.27	-4.56
DP4	F	R	56	80	55.58	4.62	-3.31
DP5	F	R	53	77	63.89	4.29	-2.37
DP6	M	R	59	70	41.67	3.52	-4.87
DP7	F	R	57	78	34.72	4.40	-5.65
DP8	F	R	48	79	52.78	4.51	-3.62
DP9	F	L	52	75	41.67	4.07	-4.87
DP10	F	R	43	68	56.94	3.30	-3.15
DP11	F	R	26	81	51.38	4.73	-3.78
DP12	F	R	45	84	51.39	5.05	-3.78
DP13	M	R	45	77	56.94	4.29	-3.15
DP14	F	R	47	87	44.44	5.38	-4.56
DP15	F	R	41	69	59.72	3.41	-2.84

DP16	F	R	22	69	52.77	3.41	-3.62
DP17	F	R	55	74	58.33	3.96	-3.00
DP18	F	R	26	83	59.72	4.95	-2.84
DP19	F	R	44	88	48.61	5.49	-4.09
DP20	M	R	25	89	43.05	5.60	-4.71
DP21	F	L	34	76	56.94	4.18	-3.15
DP22	F	R	31	80	52.78	4.62	-3.62
DP23	F	R	52	84	54.17	5.05	-3.46
DP24	F	R	59	72	62.5	3.74	-2.53
DP25	M	R	20	90	26.39	5.71	-6.59
DP26	M	R	20	82	47.22	4.84	-4.24
DP27	F	L	32	89	47.22	5.60	-4.24
DP28	F	R	25	74	45.83	3.96	-4.40
DP29	M	R	20	83	48.61	4.95	-4.09
DP30	F	R	42	88	47.22	5.49	-4.24
DP31	F	L	24	73	54.17	3.85	-3.46
DP32	F	R	36	73	58.33	3.85	-3.00
DP33	F	R	36	70	63	3.52	-2.47
DP34	F	R	26	77	61.11	4.29	-2.68
DP35	F	L	22	88	54.17	5.49	-3.46
DP36	M	R	20	80	50	4.62	-3.93
DP37	F	R	25	70	51.39	3.52	-3.78
DPs Mean			**36.92**	**79.11**	**50.69**		
DPs SD			**13.29**	**6.61**	**8.49**		
Comparison Mean			**39.2**	**38.0**	**85.0**		
Comparison SD			**13.4**	**9.1**	**8.9**		

Nb. Comparison data (N = 54) for the PI20 and CFMT were taken from Biotti et al., 2019.

4.3.3. Old/New Recognition Task

The old/new recognition test used 7 object categories: 1) human face, 2) cat face 3) dog face 4) monkey face, 5) sheep face, 6) starfish and 7) bottles. Figure 4.1a shows example images from all conditions. Face images were from young-adult, male, Caucasians and were taken from the MFMT (Dowsett & Burton, 2015). Monkey faces were obtained from the PrimFace databse (https://visiome.neuroinf.jp/primface/). Dog faces were obtained from the Flickr-dog dataset (Moreira et al., 2017). All other images were obtained from a variety of freely available Internet sources. Animal face categories were selected based on the availability of sufficient number of front-view, clear images. Additionally, sheep faces were included as previous work has reported an acquired case of prosopagnosia following stroke in a sheep farmer (WJ) who retained the ability to recognise sheep. As such, we wanted to specifically test sheep face recognition in our DP sample. Starfish were chosen based on the rationale that they belong to the category of animals but do not have a face, whereas bottles were chosen as an object condition to which DPs have previously demonstrated normal recognition performance (Epihova et al., 2022). All images were presented in gray-scale and had a resolution of 400x400 pixels.

A GIST descriptor was used to determine the image similarity of pareidolic images to faces (Torralba & Oliva, 2001). Each image was spatially divided into 64 (8x8) locations. The GIST descriptor calculates low-level properties by convolving the image with 32 Gabor filters at 4 spatial scales, each with 8 orientations, producing 32 feature maps for each of the 64 spatial locations. This produces a total of 2048 values describing the low-level properties of each image. Next, we correlated the 2048 numbers between any pair of images to derive their index of similarity (higher correlation indicates higher similarity) with respect to their low-level image properties. To investigate how the animal faces compare with human faces

with respect to their low-level properties, the average similarity of cats, dogs, monkeys, and sheep to each of the 30 human faces was calculated. Sheep (r = 0.31) and monkeys (r = 0.31) had the highest similarity to human faces followed by dog faces (r = 0.22) and cats were least similar (r = 0.01).

The old/new recognition task involved a learning phase and a recognition phase (Figure 4.1b). In the learning phase each trial began with the presentation of fixation cross (500 ms) followed by a presentation of a target image (3000 ms). A total of 10 target images were presented in each condition. Participants were instructed to remember the images prior to being testing for recognition. In the recognition phase the 10 target images were presented along with 20 foil images from the same category as the target images. Conditions were counterbalanced and the order of image presentation in the recognition phase within each condition was randomised. Participants were instructed to indicate by a button press whether the image was old or new. Images stayed on screen until participants made a response.

We used Signal detection theory (SDT) to measure performance in the old/new recognition task. First, we calculated *d*' - a measure of sensitivity, incorporating information from hit rate (correctly recognising an image as a target) and false alarm rates (incorrectly mistaking an image for a target). In cases where hit rate was 1 and/or false alarm rate was 0, *d'* was calculated by decreasing the hit rate to 0.99 and increasing the false alarm to 0.01. A d' score of 0 indicates the observer cannot distinguish between a signal and background noise (chance performance).

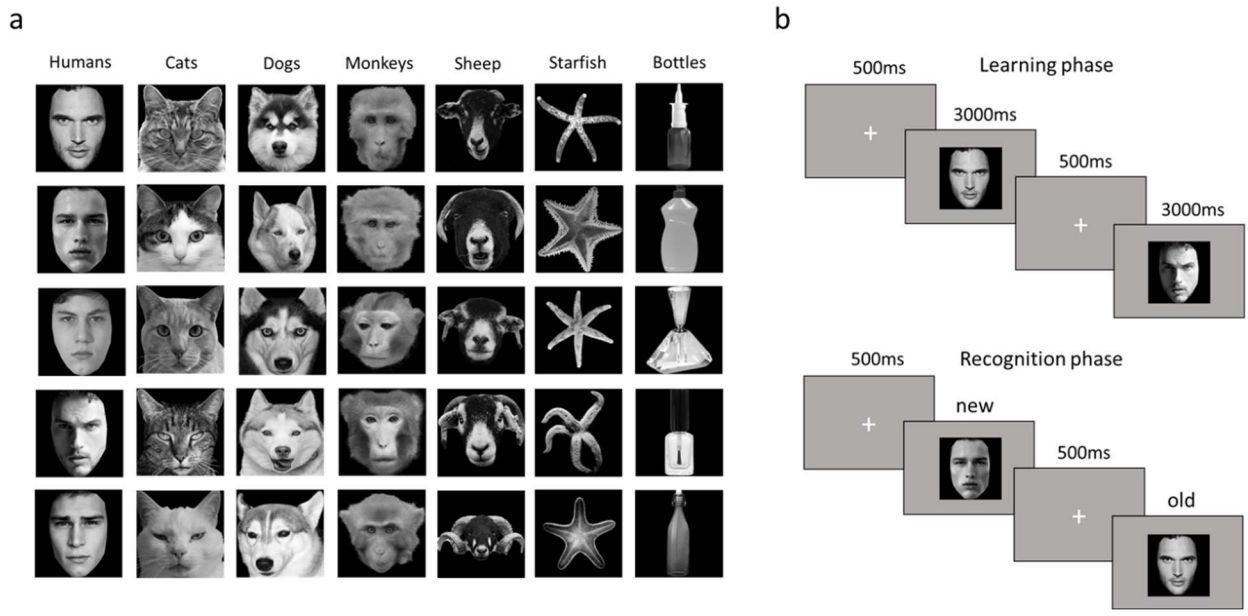

Figure 4.1. a) Example targets from each condition in the old/new recognition task. b) Schematic of the experimental procedure in the old/new recognition task. In the learning phase target images were presented sequentially. Accuracy was then measured in a recognition phase in which the targets were presented among foils. For each image participants had to indicate if the image was old or new.

4.4. Results

We calculated the mean *d*' score for each participant on the old/new recognition task for each condition. The d' scores were entered into a 4 (Animal type: Dog, Sheep, Monkey, Cat) x 2 (Group: DP, Control) was carried out. There was a significant main effect of Group F (1, 248) = 16.25, $p < 0.001$ and Animal type F (3, 248) = 8.96, $p < 0.001$, but no significant interaction F (3, 248) = 1.01, $p = 0.390$, hence we averaged the d' scores across the different animal face types. We then performed a 2 (Group: Control, DP) x 3 (Category: Human, Animal, Objects) mixed ANOVA. There was a significant effect of Group ($F(1, 186) = 23.68$, $p < 0.001$) and Condition ($F(2, 186) = 64.15$, $p < 0.001$). There was also a significant interaction between Group and Condition ($F(2, 186) = 7.20$, $p = 0.001$). To explore the interaction further, we

conducted pairwise comparisons of d' scores for the 3 conditions between the groups (Fig. 4.2). The *d*' scores seen for human faces were significantly lower in the DP group compared to the control group (M_C = 2.66, SD_C = 1.05, M_{DP} = 1.52, SD_{DP} = 0.90, t(62) = 4.66, p < 0.001, Cohen's *d* = 1.17). We found that DPs had a significantly lower *d'* scores for animal faces, (M_C = 1.28, SD_C = 0.56, M_{DP} = 0.90, SD_{DP} = 0.35, t(62) = 3.33, p = 0.002, Cohen's *d* = 0.81). However, there was no difference in *d'* scores between DPs and controls for objects (M_C = 2.71, SD_C = 0.80, M_{DP} = 2.58, SD_{DP} = 0.82, t(62) = 0.64, p = 0.524, Cohen's *d* = 0.16).

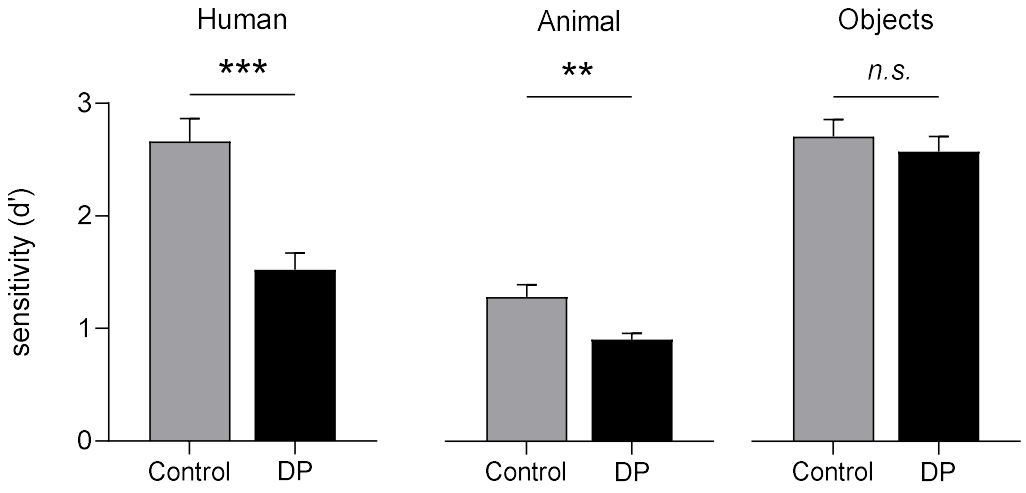

Figure 4.2. Mean sensitivity (*d'*) scores for the Control and DP groups for human faces, animal faces and objects. An average score for the animal faces was calculated by combining the *d*' scores for the cat, dog, monkey and sheep face conditions. An average score for objects was calculated by combining the *d*' scores for starfish and bottles. Error bars represent ± 1 SEM. ***p<0.001, **p<0.01, $^{n.s}$ p>0.05

Next, we calculated the median reaction time (RT) for correct trials. A 2 (Group: Control, DP) x 3 (Category: Human, Animal, Objects) mixed ANOVA showed significant effects of Group (F(1, 186) = 5.44, p = 0.021) and Condition (F(2, 186) = 15.85, p < 0.001), but no interaction between Group and Condition (F(2, 186) = 2.42, p = 0.092). Pairwise comparisons

showed that DPs had a significantly higher RT for human faces, (M_C = 1.05, SD_C = 0.26, M_{DP} = 1.29, SD_{DP} = 0.44, t(62) = 2.53, p = 0.014, Cohen's *d* =0.66), but not for animal faces (M_C = 1.25, SD_C = 0.29, M_{DP} = 1.31, SD_{DP} = 0.34, t(62) = 0.82, p = 0.417, Cohen's *d* = 0.19) or objects, (M_C = 0.97, SD_C = 0.25, M_{DP} = 0.98, SD_{DP} = 0.18, t(62) = 0.16, p = 0.870, Cohen's *d* = 0.05).

We then compared sensitivity (d') of the DPs and Controls in each animal face condition (Fig. 3). A 2 (Group: Control, DP) x 5 (Category: Human, Dog, Sheep, Monkey, Cat) mixed ANOVA revealed a significant effect of Group (F(1, 310) = 35.01, p <0.001) and Condition (F(4, 310) = 64.15, p < 0.001). There was also a significant interaction between Group and Condition (F(4, 310) = 3.55, p = 0.008). To explore the interaction further, we performed pairwise comparisons (Fig. 4.3). DPs had a significantly lower d' score for dogs (M_C = 1.69, SD_C = 0.95, M_{DP} = 1.03, SD_{DP} = 0.52, t(62) = 3.52, p < 0.001, Cohen's *d* = 0.86) and monkeys (M_C = 0.90, SD_C = 0.70, M_{DP} = 0.58, SD_{DP} = 0.51, t(62) = 2.13, p = 0.037, Cohen's *d* = 0.52). However, d' scores were not significantly different for sheep (M_C = 1.17, SD_C = 0.78, M_{DP} = 0.84, SD_{DP} = 0.79, t(62) = 1.67, p =0.101, Cohen's *d* = 0.42) and cats (M_C = 1.38, SD_C = 0.87, M_{DP} = 1.17, SD_{DP} = 0.81, t(62) = 1.01, p = 0.320, Cohen's *d* = 0.25).

To examine response bias in the different face conditions, we calculated a criterion score - *C* (Fig 4.3b). The higher the criterion, the more perceptual evidence is required to make a decision (i.e. a conservative response bias). Criterion scores were entered into 2 (Group: Control, DP) x 5 (Category: Human, Dog, Sheep, Monkey, Cat) mixed ANOVA. The main effect of Group was not significant (F(1, 310) = 0.01, p = 0.918), but there was a significant effect of Condition (F(4, 310) = 3.91, p = 0.004) and a significant interaction (F(4, 310) = 3.97, p = 0.004). DPs had a significantly higher criterion score for human faces (M_C = 0.06, SD_C = 0.41, M_{DP} =

0.47, SD_{DP} = 0.64, t(62) = 2.98, p = 0.004, Cohen's *d* = 0.76). However, there was no significant difference in criterion score with any of the animal faces and objects at $p < 0.05$.

To further explore the mechanisms underlying the impairments with human and animal faces, we analysed hits (Fig. 4.3c) and false alarms (Fig 4.3d). Hit and false alarm rates were entered into a 2 (Group: Control, DP) x 5 (Condition: Human, Dog, Sheep, Monkey, Cat) x 2 (Outcome: Hits, False alarms) mixed ANOVA. There was a significant effect of Condition ($F(4, 620) = 3.94$, $p = 0.004$) and Outcome ($F(1, 620) = 829.10$, $p < 0.001$), but no effect of Group ($F(1, 620) = 0.23$, $p = 0.635$). However, there were significant interactions between Group and Outcome ($F(1, 620) = 28.31$, $p < 0.001$) and Group and Condition ($F(4, 620) = 4.09$, $p = 0.003$). Individual comparisons showed that DPs had a significantly lower hit rate for human faces compared to Controls ($M_C = 0.85$, $SD_C = 0.13$, $M_{DP} = 0.60$, $SD_{DP} = 0.24$, $t(62) = 4.83$, $p < 0.001$, Cohen's *d* = 1.30). However, there was no significant difference in hit rate with any of the animal faces. Conversely, DPs and Controls did not show a difference in false alarm rates for human faces ($M_C = 0.11$, $SD_C = 0.09$, $M_{DP} = 0.16$, $SD_{DP} = 0.15$, $t(62) = 1.55$, $p = 0.127$, Cohen's *d* = 0.40), but there was a significant difference in false alarm rates for dogs ($M_C = 0.21$, $SD_C = 0.14$, $M_{DP} = 0.30$, $SD_{DP} = 0.17$, $t(62) = 2.21$, $p = 0.031$, Cohen's *d* = 0.58), sheep ($M_C = 0.27$, $SD_C = 0.13$, $M_{DP} = 0.36$, $SD_{DP} = 0.17$, $t(62) = 2.14$, $p = 0.036$, Cohen's *d* = 0.59), monkeys ($M_C = 0.35$, $SD_C = 0.15$, $M_{DP} = 0.43$, $SD_{DP} = 0.16$, $t(62) = 2.02$, $p = 0.047$, Cohen's *d* = 0.52) and cats ($M_C = 0.24$, $SD_C = 0.14$, $M_{DP} = 0.34$, $SD_{DP} = 0.21$, $t(62) = 2.09$, $p = 0.041$, Cohen's *d* = 0.56).

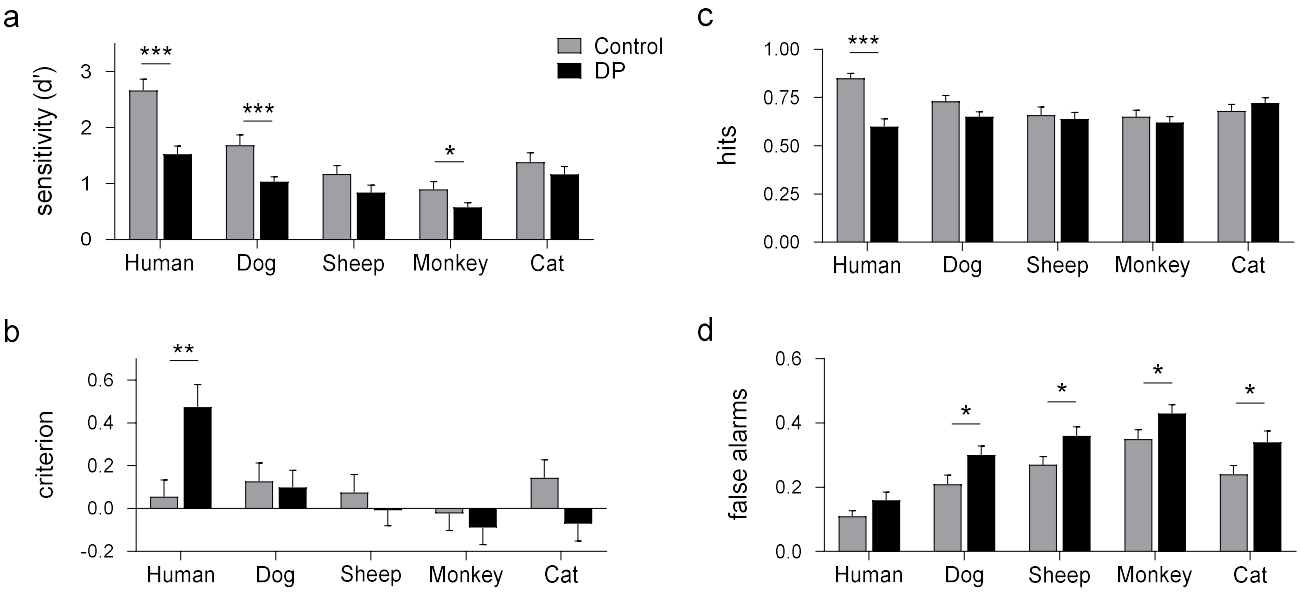

Figure 4.3. (a) Mean sensitivity (d'), (b) criterion, (c) hit rate and (d) false alarm rate for the control and DP groups with human and animal faces. Error bars represent ± 1 SEM. ***p<0.001, **p<0.01, *p<0.05

We also compared DPs and Controls in the two object conditions. There was no significant difference in sensitivity (d') for either starfish (M_C = 2.21, SD_C = 1.04, M_{DP} = 1.88, SD_{DP} = 0.93, t(62) = 1.35, p = 0.183, Cohen's *d* = 0.33) or bottles (M_C = 3.21, SD_C = 0.96, M_{DP} = 3.28, SD_{DP} = 1.00, t(62) = 0.33, p = 0.746, Cohen's *d* = 0.07).

4.4.1. Patterns of recognition dissociations

We investigated the number of DPs with dissociations in impairment. First, we calculated an *A* score for each condition (non-parametric measure of *d'*) (Zhang & Mueller, 2005). As a group, DPs had significantly lower *A* scores for human, t(62) = 5.08, p < 0.001 and animal faces t(62) = 2.94, p = 0.005, but not objects t(62) = 0.49, p = 0.629. Next, we selected the DPs who scored ≤ 2SD from the Control mean *A* score on the human face condition in the old/new recognition task. On this basis, 15 out of 37 DPs (40.54 %) exhibited evidence of impaired human face recognition at the single-case level. We then used Crawford & Garthwaite's

(2005) Bayesian criteria for a dissociation test to estimate the number of individuals exhibiting associations and dissociations between the human face and animal face conditions, and between the human face and object conditions. The Bayesian criteria for a dissociation considers the *A* scores for both conditions in the Control sample, whether the standardised difference in *A* scores differs significantly from the standardized difference in the control sample, and the correlation in *A* scores between the two conditions in the control sample. A strong dissociation was recorded if an individual has a deficit on both conditions and has a significant between-conditions difference. A classical dissociation was recorded if the individual has a deficit on only one of the conditions and has a significant between-conditions difference. An association (no dissociation) was recorded if the individual does not meet the criteria for either a strong or classical dissociation (Table 4.2). Of the 15 DP individuals impaired in face recognition, 9 individuals (60%) showed an associated impairment with animal faces, whereas only 5 DPs (33%) had an associated impairment with objects (Fig. 4.4).

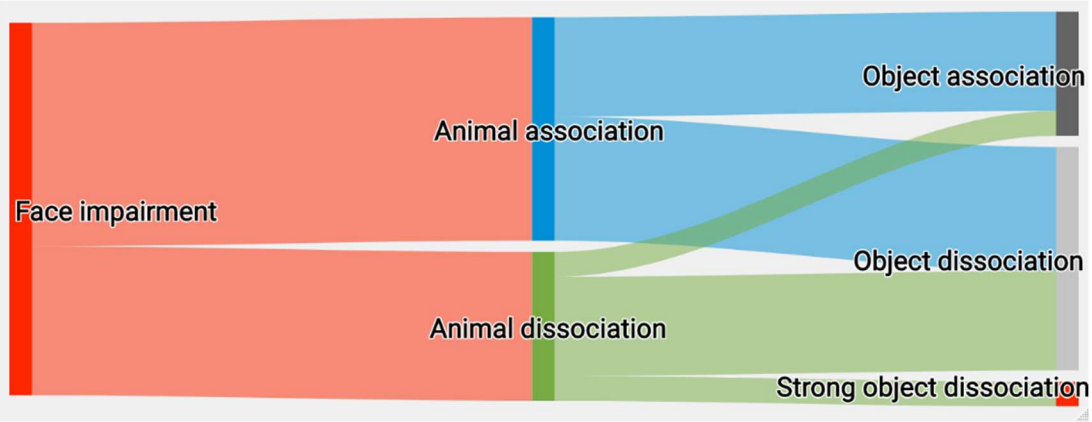

Figure 4.4. A Sankey diagram visualising the number of DP individuals with face recognition impairment and associations and dissociations (classical and strong) with animal faces and objects. The widths of the nodes are proportional to the number of individuals flowing between the categories

Table 4.2. Z scores for human and animal faces and objects and the results of Bayesian criteria for dissociations test for the 15 DP individuals who were impaired with human face recognition on the old/new recognition task.

DPs	Humans z score	Animals z score	Objects z score	Animals association/dissociation	Objects association/dissociation
DP1	-2.78	-1.88	-2.5	Association	Association
DP2	-2.22	-1.75	-1.5	Association	Association
DP3	-3.11	-0.25	0.31	Classical dissociation	Classical dissociation
DP4	-2.11	-1.5	0.83	Association	Classical dissociation
DP5	-2.11	0.5	1.33	Classical dissociation	Classical dissociation
DP6	-2.33	-1.5	-1.33	Association	Association
DP7	-3.22	-4.00	0.17	Association	Classical dissociation
DP8	-3.22	0.13	0.33	Classical dissociation	Classical dissociation
DP9	-2.56	0.13	-0.5	Classical dissociation	Association
DP10	-3.22	-1	-0.33	Association	Classical dissociation
DP13	-7.33	-1.25	-3.17	Classical dissociation	Strong dissociation
DP12	-2.11	-0.38	-1.17	Association	Association
DP13	-2.33	-0.38	1	Association	Classical dissociation
DP14	-4.33	0	-0.83	Classical dissociation	Classical dissociation
DP15	-2	-0.5	1.17	Association	Classical dissociation

4.5. Discussion

The aim of this study was to investigate whether the deficit in human face recognition evident in DP extends to animal faces. Studies of acquired prosopagnosia have found mixed evidence for a deficit in animal face recognition. McNeil and Warrington (1993) reported the case of a sheep farmer (WJ), who acquired prosopagnosia after a stroke, but was still able to differentiate between different sheep identities. On the other hand, other cases of prosopagnosia have been reported with deficits in the recognition of animal faces (Bornstein et al., 1969; Landis, 1986; Toftness, 2019). To date, however, no studies have investigated whether the deficit in human faces in DP extends to animal faces. In this study, we found that at a group level, individuals with DP had recognition deficits with both human and animal faces. The selectivity of the deficit in recognition was shown by the lack of any difference between DPs and controls in the recognition of objects that did not have faces. Although DPs were impaired with recognising animal faces, the magnitude of group-level impairment was different for the different animal faces. While in the current study, the recognition deficits in DP for dog and monkey faces reached significance, we note that there is a similar trend of reduced performance for sheep and cat faces. Low-level image properties cannot fully account for the magnitude of recognition deficits, as DPs were only significantly impaired with dogs and monkeys, whereas the low-level properties analysis shows highest similarity of sheep and monkeys to human faces.

These findings suggest that the deficit in DP involves a shared representation of human and animal faces. This is consistent with neurophysiological and neuroimaging studies showing a similar representation of human and animal faces in the temporal lobe (Decramer et al., 2021; Kriegeskorte et al., 2008; Tong et al., 2000; Kanwisher et al., 1999). For example,

single neuron recordings have shown that neurons in human brain that are selective for human faces are also selective for monkey faces (Decramer et al., 2021). Neuroimaging studies have reported similar findings with regions showing selectivity for human faces also showing selective responses to animal faces (Kanwisher et al., 1999; Tong et al., 2000) and studies using multi-voxel pattern analysis (MVPA) further report similar patterns of neural response between human and animal faces (Kriegeskorte et al., 2008).

There were, however, some differences in the way DPs and controls recognised human and animal faces. The impaired recognition of human faces in DPs reflected a lower hit rate, but no difference in false alarms. On the other hand, recognition impairments in animal faces in DPs reflected a higher incidence of false alarms, but no difference in hit rate. One explanation is that these differences between human and animal faces result from a difference in response bias. Our criterion analysis fits with this account as DPs had a more conservative bias for human face recognition. That is, they required more perceptual evidence to indicate that a target was present. It is possible that a lifetime of face recognition problems and the associated social embarrassment causes DPs to adopt a conservative decision criterion. This may not generalise to animal faces because the social cost of misidentification (i.e., the potential for embarrassment) is substantially lower. Overall, this suggests that the lower recognition of human faces in DPs may reflect a somewhat different processing strategy to that found for the deficit in animal faces.

We did not find any group level deficits in the recognition of simple animate (starfish) or inanimate objects (bottles). Although our findings suggest that DP is selective for faces, the extent to which prosopagnosia selectively affects the perception of non-face objects remains contentious (Geskin & Behrmann, 2018). A number of studies have suggested that deficits in

the human face identification occur in the absence of any deficits in the recognition of non-face objects (Barton et al., 2019; Bate et al., 2019; Garrido et al., 2018; Shah, Gaule, Gaigg, et al., 2015). However, there is now increasing evidence that individuals can have co-occurring deficits in non-face object recognition (Duchaine et al., 2007; Barton et al., 2019; Barton & Corrow, 2016; Biotti et al., 2017; de Haan & Campbell, 1991; Gray et al., 2019; Epihova et al., 2022). Nevertheless, it is not clear why only particular objects are affected in DP. In a recent study, we showed a deficit in the perception of pareidolic objects (that are perceived as being face-like) in DP (Epihova et al., 2022). However, this was only with pareidolic objects that had similar image properties to faces. Further studies that reveal which objects are or are not affected in DP may help uncover the functional organising principles involved in object perception.

Next, we investigated the dissociations/associations between performance for human faces and either animal faces or objects. We selected only the DPs who performed ≤2 SD on the human face condition on the old/new recognition task for this analysis. 60% of this sample showed an association between human and animal face recognition, whereas only 33% of this sample showed an association between human faces and objects. Nevertheless, one third of the DP sample did have associated object agnosia, despite the fact that, at group level, DPs performed equally to controls with objects. This is consistent with previous reports demonstrating that even in the absence of reduced performance with object recognition, at a group level, some DP individuals in the group exhibit object deficits (Barton et al., 2019; Bate et al., 2019) and provides support for a heterogenous profile of DP (Minnebusch et al., 2007).

In the present study, we classified individuals as DP based on their scores on the PI20 and CFMT. Although there is no formal guidance on the diagnosis of DP, we acknowledge that this approach is relatively liberal. In particular, it has been argued that diagnostic decisions should be informed by performance on multiple objective tests of face recognition performance in addition to any self-report evidence (Bate & Tree, 2017; Dalrymple & Palermo, 2016). It is true that liberal diagnostic criteria can complicate the interpretation of null effects of group (DPs vs controls). For example, subtle perceptual deficits may be harder to detect in milder cases. However, it is unlikely that clear evidence of a perceptual deficit – such as that described here – can be attributed to the presence of milder cases within the DP sample. If anything, a more liberal approach would be expected to reduce the chance of a significant group difference (DPs vs controls).

In conclusion, we provide the first systematic evidence for a deficit in the recognition of animal faces in DP. These findings converge with other studies showing similar patterns of neural response to human and animal faces in the temporal lobe. Nevertheless, we did find some differences in the manifestation of the deficit in recognition with human and animal faces - deficits in human face recognition were linked to lower ability to recognize targets and a more conservative response bias, while impairments with animal faces reflected higher misidentification of foils. Our results suggest a heterogenous recognition profile of DP, as one third of the DPs who were impaired with human faces were also impaired with objects, despite normal group-level performance with objects.

4.6. Data accessibility

Experimental stimuli, code and anonymised data are publicly available at https://osf.io/jymqv/

Chapter 5

Alterations in functional connectivity and face identity representations in developmental prosopagnosia

5.1. Abstract

Developmental prosopagnosia (DP) is a neurodevelopmental disorder, characterised by impairments in recognising face identities. However, the neural correlates of DP are currently not well understood. Here, we combined fMRI univariate, functional connectivity and multi-voxel pattern analyses (MVPA) to investigate the organization of face-selectivity, functional connectivity and representations of individual faces in DP and neurotypical individuals. We show that DP is associated with atypical functional connectivity organisation despite normal face-selectivity. Namely, the anterior temporal cortex was less functionally connected to the rest of the brain in DP and exhibited an atypical connectivity pattern. Moreover, we found distinct response patterns to individual face identities in the anterior temporal cortex in neurotypical, but not in DP individuals. The alterations in connectivity and identity representations were specific to faces. Together, these findings suggest that poor face recognition ability in DPs is associated with poor quality of neural representations of individual face identities and reduced global functional connectivity. These results offer new insights for the critical role of the anterior temporal cortex in supporting face recognition abilities.

5.2. Introduction

Developmental prosopagnosia (DP) a neurodevelopmental disorder, characterised by deficits in face identity recognition, despite normal intelligence, low-level vision and no history of brain damage (Cook & Biotti, 2016; Duchaine & Nakayama, 2006; Susilo & Duchaine, 2013). Regions in the ventral temporal cortex have been functionally defined as face-selective to reflect their preferential response for faces, compared to other visual categories (Haxby et al., 2000; Kanwisher, 2010). The occipital face area (OFA), fusiform face area (FFA) and superior temporal sulcus (STS) are thought to comprise the core face system responsible for visual analysis of faces (Haxby et al., 2000). The face-selectivity found in these regions has focused research efforts to these face-specific areas as probable candidates of the neural correlates of individual differences in face recognition and deficits in DP. Some studies have shown that face selectivity in the FFA predicts individual differences of face recognition ability in the neurotypical population (Elbich & Scherf, 2017; Ramot et al., 2019), however, others have found no association (McGugin & Gauthier, 2016; Jiang et al., 2013). These mixed results extend into DP - while some studies show reduced face-selectivity in DPs (Jiahui, Yang, & Duchaine, 2018; Hadjikhani & De Gelder, 2002; Furl, Garrido, Dolan, Driver, & Duchaine, 2011), others find face-selectivity comparable to that of neurotypical individuals (Rivolta et al., 2014; Avidan, Hasson, Malach, & Behrmann, 2005; Hasson, Avidan, Deouell, Bentin, & Malach, 2003). The integrity of information flow expressed as functional connectivity, rather than face selectivity *per se*, might be a better predictor of face recognition abilities. In a large study of neurotypical individuals, Levakov et al., (2022) demonstrated that reduced functional connectivity to the anterior temporal cortex is associated with worse face recognition performance. Consistent with this, DPs also show reduced functional connectivity to the anterior temporal cortex (Rosenthal et al., 2017).

However, these approaches might be limited for the investigation of DP. Firstly, DP is a neurodevelopmental disorder. Unlike acquired prosopagnosia, resulting from core localised damage (Barton, 2008; Davies-Thompson et al., 2014), atypical face recognition skills in DP emerge over the course of development. As such, impaired face recognition has the potential to be arrived at through different neural routes – the principle of equifinality (Bishop, 1997). The plasticity of face recognition development is demonstrated by a recent study showing that patients whose entire hemisphere was removed in childhood can achieve 80% of the neurotypical face recognition performance (Granovetter et al., 2022). Importantly, this effect was independent of which hemisphere was removed. This suggest that even though in adult neurotypical participants the right hemisphere is dominant for face processing (Kanwisher et al., 1997; Pitcher et al., 2007), the functional processing of faces can be reorganized, such that equal performance can be achieved. Thus, neural correlates of DP should not be necessarily assumed to have one-to-one mapping with the neural correlates implicated in acquired face recognition deficits or in neurotypical individuals. Exploring functional connectivity of the whole brain has the potential to uncover reorganizations in brain areas not typically associated with face recognition in acquired disorders. Related to this, is the notion that the connectivity of an area need not necessarily be reduced or increased to be atypical. Similarly to the fact that atypical representation of faces can be achieved even if face selectivity is typical (Rivolta et al., 2014), typical functional connectivity strength does not necessarily imply that the pattern of connectivity will be intact. For example, it is possible that a brain area in DP has the same connectivity strength with the rest of the brain as neurotypicals, but the pattern of connections differ. Further, the approach of exploring the pattern of connectivity can be utilised to move beyond traditional neurobiological measures of

"increased/decreased" activity and connectivity and allows for a greater understanding of how neural responses are expressed at the large-scale level of the brain.

Secondly, so far investigations of the neural correlates of DP have largely focused on face selectivity. However, DPs' difficulties with faces stem from inability to recognise individual face identities, rather than not recognising faces as such. For example, Natu et al., (2016) demonstrated that in the neurotypical population perceptual discriminability of face-identity was associated with the magnitude of neural sensitivity to face identity, but not with activity for faces in face-selective regions. An alternative hypothesis therefore is that DP will be associated with the quality of neural pattern discrimination between individual face identities. As identity recognition might be achieved through a significant overlap between the output of the structural encoding for a stimulus and the already stored representation of the same stimulus (Wing et al., 2020; Wing et al., 2015; Ritchey et al., 2013; Sommer & Sander, 2022), successful face recognition might manifest as a higher neural representational similarity for the same face identity compared to two different identities. Conversely, impairments in face recognition, such as those found in DP, might stem from a less distinct representation of individual identities, where the neural pattern shows lower discrimination between same and different identities.

Here, we combined univariate, functional connectivity and MVPA fMRI analyses to investigate the neural correlates of DP. Specifically, the study had 3 aims. Firstly, to determine whether the organization of face-selectivity in terms of location and magnitude differs in DP. Secondly, we explored potential alterations in whole-brain functional connectivity when viewing faces and a control category of flowers. In a data-driven analysis, we compared voxel-based global functional connectivity organization between DPs and controls. The aim of this

approach was to uncover areas with altered functional topology in DP – areas with different number and pattern of connections without pre-defined regions of interest assumptions. Finally, we investigated the similarity in neural signatures elicited by different face identities. We hypothesised that controls would show higher similarity in neural representations of the same face identity compared to different face identities. In contrast, the representational difference between same and different face identities will be less distinct in DPs.

5.3. Methods

5.3.1. Participants

Twenty-two DPs (4 males, M_{age} = 41.59, SD_{age} = 11.82, 20 right-handed, 2 left-handed) and 20 Controls (8 males, M_{age} = 34.10, SD_{age}=12.62, 20 right-handed) participated in the study. DP participants were recruited through www.troublewithfaces.org. Some of the DP and control participants recruited for the current study have already participated in the experiments from Chapters 2, 3, and 4. Diagnostic evidence for the presence of DP was collected using the PI20 questionnaire - a 20-item self-report measure of face recognition abilities (Shah et al., 2015) and the Cambridge Face Memory Test (CFMT) – an objective measure of face recognition (Duchaine & Nakayama, 2006). To be classified with DP, a participant had to score both > 65 on the PI20 and < 65% on the CFMT (Supplementary Table 1 shows diagnostic information for all DPs). Conversely, all control participants had to score <65 on the PI20 and > 65% on the CFMT, (Figure 5.1). Where a participant has completed the PI20 and CFMT as part of the selection criteria in a previous experiment, the score from their first attempt was taken to avoid practice effects. The use of convergent diagnostic evidence from self-report and objective computer-based measure of face recognition ability provides reliable identification

of DP; for example, less than 2% of the population score > 65 on the PI20 and < 65% on the CFMT (Gray et al., 2017). All participants were over 18 years-old, had normal or corrected-to-normal vision and had no history of psychiatric and neurological conditions and Autism Spectrum Disorder. All participants provided written informed consent and the experiment was approved by the York Neuroimaging Centre (YNiC) Ethics Committee.

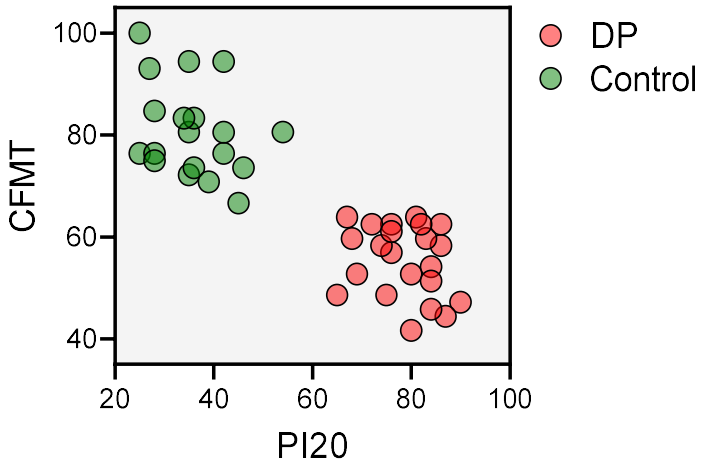

Figure 5.1. Individual scores on the diagnostic tests: self-report of face recognition abilities (PI20) and face recognition abilities (CFMT) in Control and DP participants. Each point represents one participant.

5.3.2. Functional localiser scan

36 faces, 36 scenes and 36 scrambled images were used for the localiser scan. Images were in colour, superimposed on a mid-gray background and had a resolution of 400x400 pixels. Faces were front-, left- and right-facing white male and female images and were taken from the Radboud face database (Langner et al., 2010). Scene images consisted of natural outdoor, man-made outdoor and indoor scenes and were taken from the SUN database (Xiao et al., 2010). The scrambled images were generated through global phase scrambling of the

face images, which rendered them unrecognisable. Example images are shown on Supplementary Figure 1. The 3 object categories were presented in a block design, with 9 blocks per each category. In each block, 4 images from the same category were presented individually for 600ms, with a 200ms. inter-stimulus-interval. This was followed by an inter-block interval lasting 6s. The order of blocks presentation was pseudorandomised such that each triplet of blocks contained 3 different conditions. To maintain attention during the scan, participants were required to press a button when the fixation cross changes from black to green, which occurred randomly 60 times throughout the scan. The total length of the scan was 4.5mins.

5.3.3. Experimental scans

15 different face and flower identities were used for the face and flower scans, respectively. All face and flower images were gray-scale on a mid-gray background with a resolution of 400x400 pixels. All faces were front-facing white males and were taken from the Radboud face database (Langner et al., 2010). All flowers were from the *Asteraceae* family and were taken from the SOLID database (Frank et al., 2020). Examples of face and flower images are shown in Figure 5.2a. The faces and flowers scans had block designs, with 4 blocks per each unique face or flower identity. In each block, an image of the same identity was repeated 4 times for 600ms, with a 200ms. inter-stimulus-interval. This was followed by an inter-block interval lasting 6s. The order of blocks presentation was pseudorandomised such that in each 15 blocks the same exemplar was never repeated. To maintain attention during the scan, participants were required to press a button when the fixation cross changes from

black to green, which occurred randomly 60 times throughout the scan. The total length of each scan was 9mins.

To ensure that the face and flower exemplars were comparable on low-level similarity among them, we measured low-level properties of the 15 face and 15 flower exemplars and calculated similarity among the within-category exemplars using a GIST descriptor an image analysis tool that captures the spectral and spatial properties of an image (Torralba & Oliva, 2001). Each image was spatially divided into 64 (8x8) locations. The GIST descriptor calculates low-level properties by convolving the image with 32 Gabor filters at 4 spatial scales, each with 8 orientations, producing 32 feature maps for each of the 64 spatial locations. This produces a total of 2048 values describing the low-level properties of each image. First, we measured the GIST for all 15 face and flower images. Next, we correlated the resulting vector of each face with the other 14 faces and each flower with the other 14 flowers, producing 105 values describing the similarity in low-level properties between each pair of images for the face and flower categories, thus measuring the low-level homogeneity of images in the two conditions. Next, we compared the homogeneity of low-level properties between the faces and flowers. There was no significant difference in low-level homogeneity between the face and flower categories, $t(208) = 0.03$, $p = 0.979$, (Figure 5.2b).

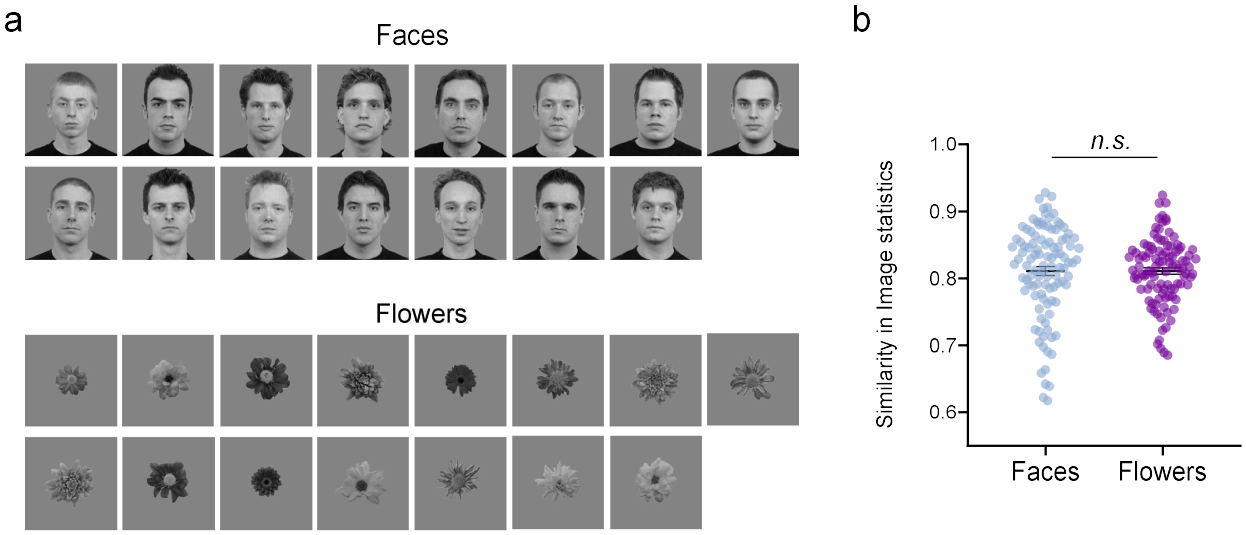

Figure 5.2 (a) The 15 face and flower identities used in the fMRI experiment, (b) No difference in the similarity of image properties between the faces and flowers stimuli. Each dot represent similarity in image statistics between a pair of images (105 similarities within a category).

5.3.4. fMRI data acquisition and pre-processing

fMRI data were acquired with a GE 3T HD Excite MRI scanner at YNiC at the University of York, fitted with an eight-channel phased-array, head-dedicated gradient insert coil tuned to 127.4 Hz. A gradient echo-planar imaging (EPI) was used to collect data from 38 contiguous slices (TR= 3000 ms, TE = 25 ms, FOV = 288 x 288 mm, matrix size = 128 x 128, slice thickness = 3mm). The fMRI data was initially analysed with FEAT v5.98 (http://www.fmrib.ox.ac.uk/fsl). In all scans, the initial 9 sec. of data was removed to reduce the effects of magnetic saturation. Registration of the functional data to the structural image was conducted using the boundary-based registration algorithm (Greve & Fischl, 2009). Motion correction was applied using MCFLIRT (Jenkinson et al., 2002), non-brain tissue removal was applied using BET (Smith, 2002) and slice-timing correction were applied followed by temporal high-pass filtering (Gaussian-weighted least squares straight line fitting, sigma = 100s). Gaussian spatial smoothing was applied at 5 mm FWHM. Parameter estimates were generated for each condition (localiser scan- 3 conditions: face, scrambled, scene; face scan – 15 conditions: 15

face identities; flowers scan - 15 conditions: 15 flower identities) by regressing the homodynamic response of each voxel against a box-car function convolved with a single gamma HRF. There were no significant differences in head movement between the groups in the localiser scan, $t(40) = 1.43$, $p = 0.162$, faces scan, $t(40) = 0.70$, $p = 0.488$ and flowers scan, $t(40) = 1.00$, $p = 0.323$. One Control participant was excluded from further analysis for excessive head motion (Supplementary Figure 2).

5.3.5. Functional connectivity (FC) pre-processing

FC pre-processing and analysis was carried out with the CONN toolbox (Whitfield-Gabrieli & Nieto-Castanon, 2012). The faces and flowers scans were pre-processed using CONN's default pre-processing pipeline, which includes realignment and unwrapping, slice-timing correction, outlier detection, structural and functional segmentation and normalization and spatial smoothing (8mm Gaussian kernel). Next, functional data was denoised by applying CONN's default denoising pipeline. This included the anatomical component-based noise correction aCompCor (Behzadi et al., 2007) by modelling out the sources of noise from white matter, gray matter, and cerebro-spinal fluid as nuisance parameters within the first-level general-linear model (GLM). Scrubbing (as many regressors as identified invalid scans), motion regression (12 regressors: 6 motion parameters + 6 first-order temporal derivatives) and a temporal band-pass filter (0.008–0.09 Hz) were applied.

5.4. Results

5.4.1. Univariate analyses

First, we asked whether there was a difference in face selectivity between DPs and Controls. We compared the magnitude of face selectivity by comparing the response to faces with the response to scenes and scrambled images. Figure 5.3 shows face-selectivity for each group of participants. The location of face-selective areas was similar across both groups (Table 1, Suppl. Table 2). We then contrasted the face-selectivity from both groups across the whole brain. We did not find large differences between the control and DP group (Figure 5.3).

The OFA, FFA and STS were functionally present at both groups. Analysis of group peak coordinates within these areas showed a striking similarity in the location of the face-selective regions between both groups (Supplementary Table 2).

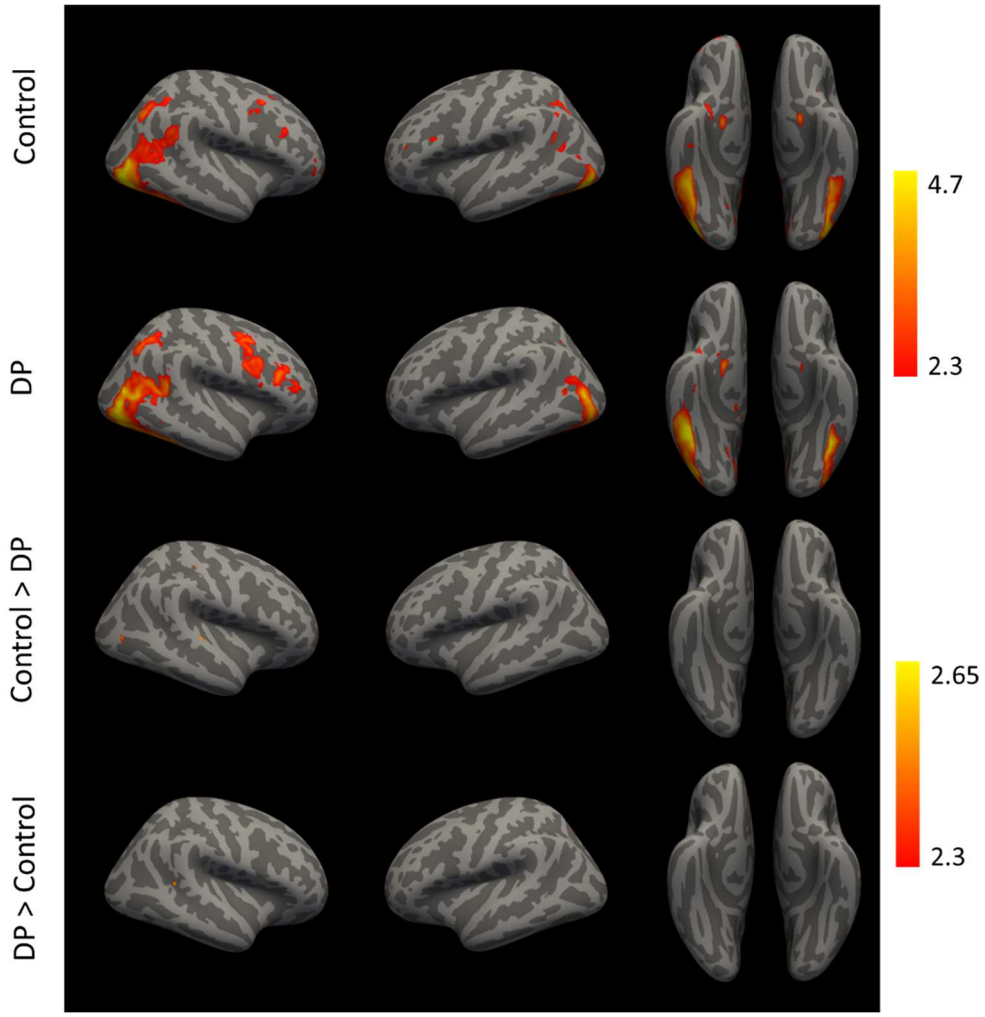

Figure 5.3. Face selectivity in Controls, DPs and the Controls > DPs and DPs > Controls whole brain contrasts

Next, to check for individual differences in the location and presence of face-selective regions between the groups, we identified individual regions of interest (ROIs) in each participant. Table 1 shows the mean and SD of coordinates of the face-selective ROIs and the number of DP and Control participants in which each ROI was functionally present. Similar to the group analysis, individually defined face-selective regions shared similar locations in DPs and Controls. Next, we determined whether there are any differences in the presence of each region between the groups. Fisher's exact tests showed no difference between the groups in the presence of rOFA ($p = 0.209$), rFFA ($p = 0.463$), rSTS ($p = 0.390$), rAFTP ($p = 0.758$), lOFA ($p = 0.463$), lFFA ($p = 0.321$), lSTS ($p = 0.354$), lAFTP ($p = 0.999$).

Taken together, these findings do not appear to show significant differences in the selectivity for faces compared to non-face images in controls compared to DPs.

Table 5.1. Control (n = 19) and DP (n = 22) mean and standard deviation of peak voxel coordinates for each ROI. Individual regions defined by localiser scan (Faces > Scrambled + Scenes). Coordinates were transformed from individual space into MNI-ICBM1522 mm space.

		MNI mean coordinates			SD		
		x	y	z	x	y	Z
rFFA	Control(*n*=18)	40.11	-55.56	-14.56	3.03	7.53	3.42
	DP (*n*=22)	40.27	-52.36	-16.64	3.72	6.25	2.92
lFFA	Control (*n*=16)	-39.63	-53.38	-16.25	3.74	6.05	3.34
	DP (*n*=21)	-40.57	-56.67	-17.14	4.25	7.16	3.26
rOFA	Control (*n*=17)	41.88	-78.94	-7.53	3.64	5.92	6.15
	DP (*n*=22)	44.73	-75.45	-6.73	3.47	5.76	6.49
lOFA	Control (*n*=18)	-40.24	-80.82	-8.82	4.99	4.61	5.91
	DP (*n*=22)	-41.27	-82.18	-7.18	5.18	4.70	4.73
rSTS	Control (*n*=15)	44.80	-58.80	16.13	5.80	6.27	6.99
	DP (*n*=20)	46.10	-57.40	15.90	5.17	9.63	4.75
lSTS	Control (*n*=8)	-43.75	-66.25	15.25	3.77	6.96	5.65
	DP (*n*=13)	-42.00	-60.62	16.46	4.83	13.07	7.26
rATFP	Control (*n*=10)	36.90	-4.60	-28.60	6.61	12.04	6.33
	DP (*n*=10)	38.60	-14.20	-25.20	5.08	10.97	8.95
lATFP	Control (*n*=6)	-35.67	-12.67	-24.33	9.91	10.41	5.43
	DP (*n*=7)	-36.00	-14.57	-22.29	8.33	11.65	8.75

5.4.2. Whole-brain global functional connectivity

We measured connectivity differences between Controls and DPs for the face and flowers scans. A whole-brain voxel-based functional intrinsic connectivity contrast (ICC) (Martuzzi et al., 2011) was computed. This analysis measures the strength of functional connectivity between each voxel and every other voxel and then calculates the strength of connectivity between each voxel and the average of the rest of the voxels in the brain (root mean square of correlation coefficient values between a voxel and the rest of the brain), thus providing a measure of the functional centrality at each voxel. Centrality is a graph theory-based measure used to identify the degree of connections of each voxel with all other voxels. Voxels with higher connections to the rest of the brain are regarded as functionally central and thus more globally connected. Individual-level ICCs were calculated and combined into Control and DP group-level analyses. Next, we performed a group contrast to identify any regions that are less globally connected in DPs compared to Controls (voxel-threshold $p<0.005$, cluster-size FDR-corrected $p<0.05$). Areas with significantly lower global connectivity in DP compared to controls are shown on Figure 5.4. Most voxels fell within the left temporal pole. Full details of the overlap of the area with anatomical structures from the Harvard Oxford atlas can be found in Supplementary Table 3.

In contrast, for the flowers scan, there was no difference in global connectivity between controls and DPs in any region (Fig. 5.4). This shows that there is a selective reduction in global connectivity during face processing for DPs.

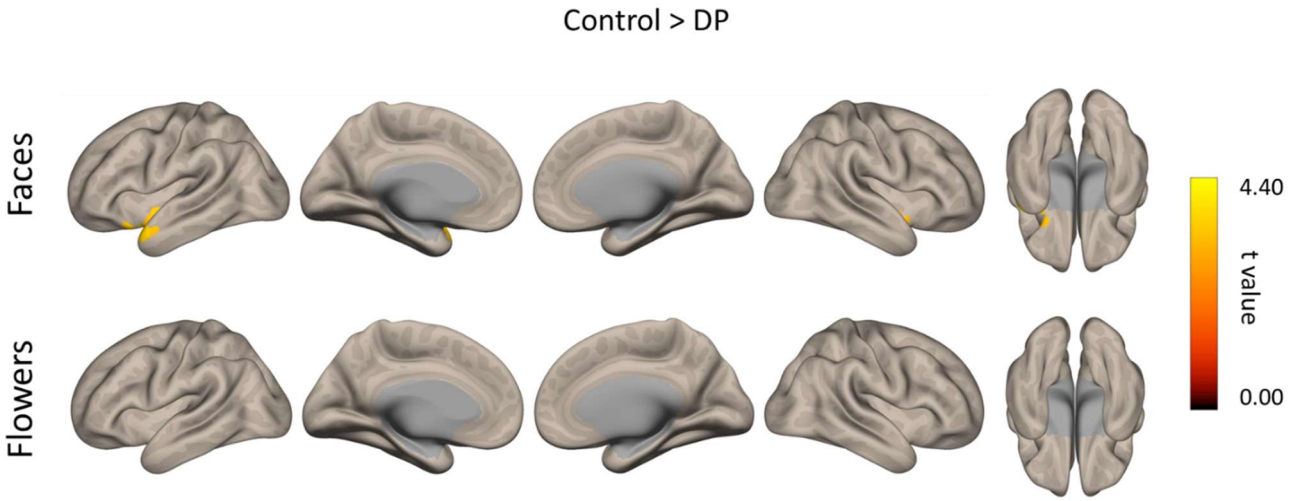

Figure 5.4. Difference in whole-brain global connectivity between controls and DP groups for the faces and flowers scans.

5.4.3. Seed-based functional connectivity

To identify potential regions for further seed-based connectivity analysis, we ran the global connectivity contrast between Controls and DPs with a more liberal threshold of voxel-threshold $p<0.05$, cluster-size FDR-corrected $p<0.05$. The rationale for this was based on the fact that a region will show as significantly less globally connected (less central) in DPs only if it is significantly less connected to sufficiently large number of voxels. As such, if a region has a reduced connection to only one other region, this might not be sufficient to result in reduced global connectivity. Repeating the analysis with a higher threshold allows for exploration of regions that might not be less connected with the rest of the whole brain, but nevertheless less connected to a set of other regions. Regions with lower global connectivity identified with the more liberal threshold are shown in Supplementary Table 4. We used the top 4 anatomical regions from the Harvard Oxford atlas falling within the identified overall lower global connectivity area as seeds to perform a classic seed-to-voxel functional connectivity analysis. These seed regions were the left temporal pole, right putamen, left insular cortex and left

hippocampus. The reference time series for each seed were obtained by averaging the time series of all voxels within the seed region. First, a seed-to-voxel functional connectivity was calculated for Controls and DPs and then a group contrast was carried out. Figure 5.5 shows regions that have lower connectivity with the respective seed in DPs compared to controls. In DPs the left temporal pole had weaker connections to the right posterior middle temporal gyrus, left frontal pole and left superior frontal gyrus. The right putamen was less connected to the left and right insular cortices. The left insular cortex was less connected to the right cuneal cortex, precuneous cortex and the right putamen. The left hippocampus had less connections with the right anterior middle temporal gyrus and right anterior superior temporal gyrus. Full details of the regions with lower connectivity to the 4 seeds are presented in in Supplementary Tables 5-8. Next, we asked whether the seed-based reductions in connectivity were specific for faces by repeating the 4 seed-based connectivity analysis with the flowers experiment. We found that only the right putamen had reduced connectivity in DPs for flowers, whereas the left temporal pole, hippocampus and insular cortex showed connectivity comparable to controls. The pattern of reduced connections to the right putamen was similar to the face scan, with lower connections found to the right central opercular cortex, right precentral gyrus and right insular cortex (Supplementary Table 9).

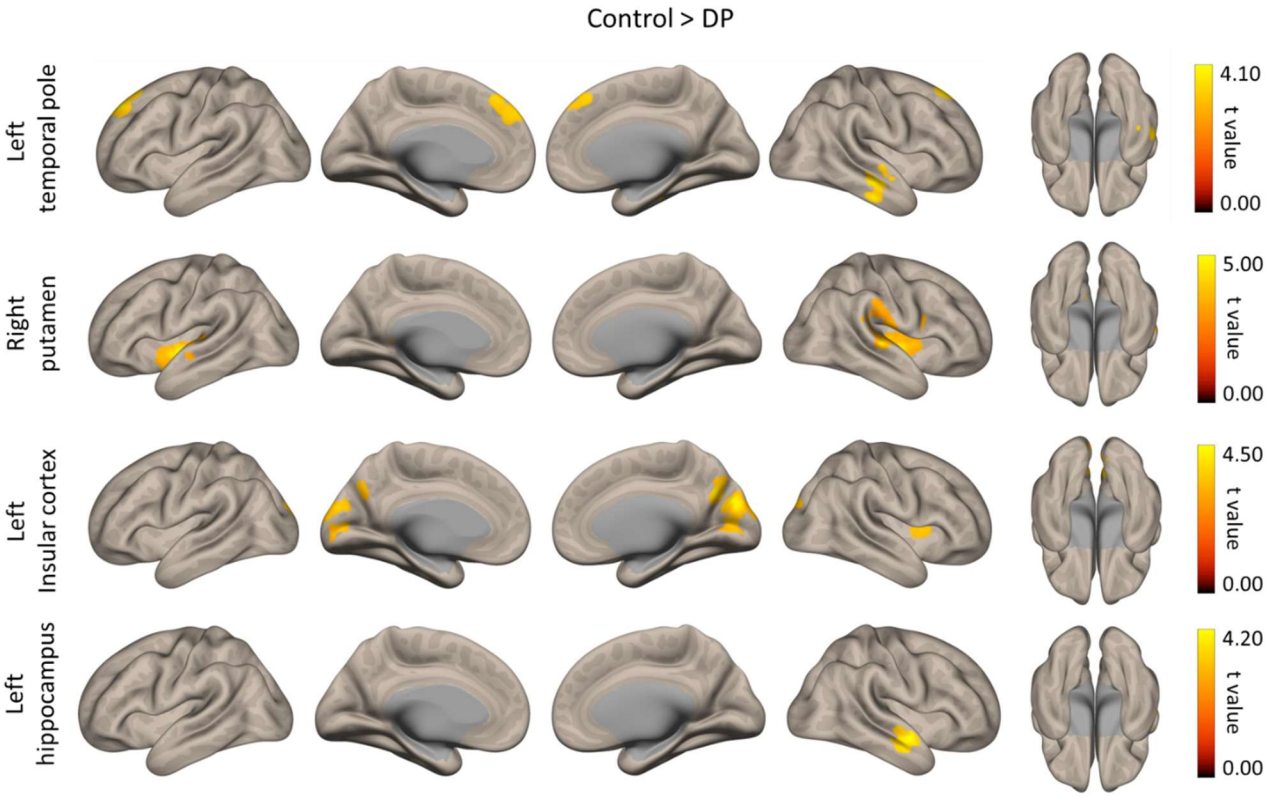

Figure 5.5. Seed-based functional connectivity reductions for the Controls > DPs contrast. The 4 seeds were the left temporal pole, right putamen, left insular cortex and left hippocampus.

5.4.4. Multivariate pattern analysis of functional connectivity

The global connectivity analysis aims to uncover *quantitative* group differences in the strength of connectivity. However, atypical functionality of a region may not necessarily be linked to lower connectivity strength, but rather *qualitatively* different pattern of connections. To explore this, we carried out a functional connectivity multi-variate pattern analysis (fc-MVPA). This analysis computes the connectivity patterns characterising the connectivity between each voxel and the rest of the brain (Nieto-Castanon, 2022). That is, the connectivity of a particular area does not necessarily need to be lower (quantitatively different), but the pattern of functional projections might be (qualitative difference). The fc-MVPA calculates functional connectivity between each voxel and the rest of the voxels in the brain for each subject and computes a reduced set of eigenpattern (principal component)

scores best characterizing relevant spatial features of these maps across subjects. In the current analysis we used the first 4 components. Cumulatively the first 4 components explained 90.02% and 89.70% of the variance in connectivity profiles across all gray matter voxels in the faces and flowers scans, respectively. Once each subject's functional connectivity profiles are represented in terms of the 4 lower-dimensional eigenpattern scores, group-level functional connectivity analyses are computed by entering these scores into a standard General Linear Model that evaluates the hypothesis that there will be a group difference (Control vs DP) in the connectivity pattern of a given voxel using the Likelihood Ratio Test. Lastly, this procedure is repeated for each voxel sequentially, constructing a statistical parametric map across the entire brain. We performed a group contrast to identify any regions with different pattern of connectivity in DPs compared to controls (voxel-threshold $p<0.005$, cluster-size FDR-corrected $p<0.05$). Areas with significantly different pattern of functional connections in DP are shown on Figure 5.6. Most voxels fell within the left temporooccipital middle temporal gyrus, precuneous cortex, brain stem, right temporooccipital fusiform cortex and the left temporal pole. Full details of the overlap of the area with anatomical structures from the Harvard Oxford atlas can be found in Supplementary Table 10. Next, we repeated the fc-MVPA with the flowers scan. For the flowers scan significantly different pattern of functional connections in DPs was found in the precuneous cortex, right lingual gyrus, and the left cerebellum (Supplementary Table 11). This shows that the difference in connectivity pattern associated with the anterior, posterior, and inferior temporal cortex is selective for face processing.

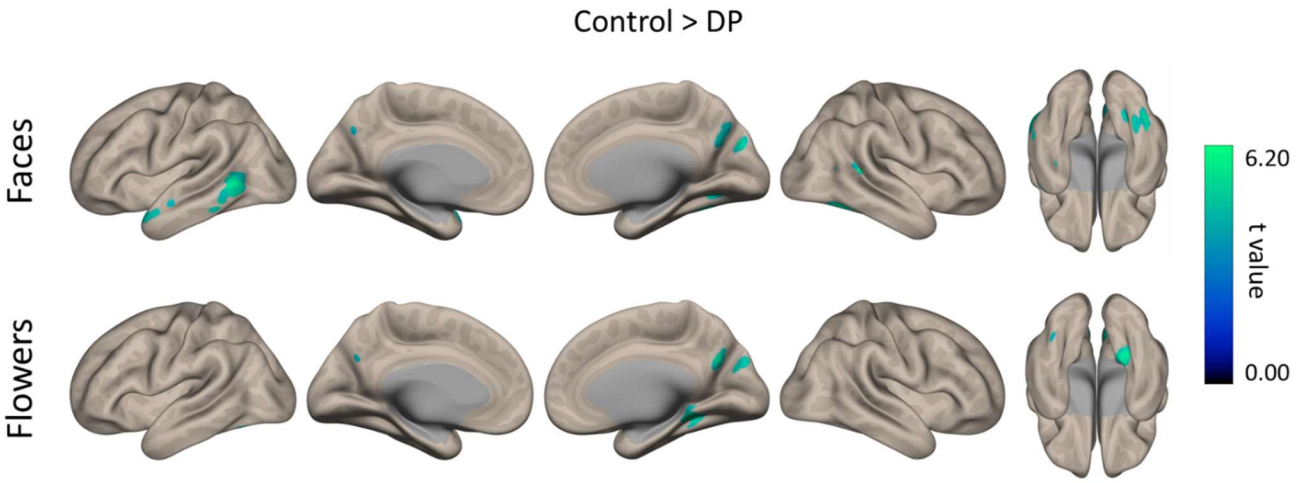

Figure 5.6. Difference in whole-brain fc-MVPA between controls and DP groups for the faces and flowers scans.

5.4.5. Representational MVPA

Next, we asked whether there was any difference in the pattern of activity to individual face identities in DPs and controls. To determine whether the pattern of activity could discriminate between individual exemplars, we compared responses to odd and even repetitions of individual face or flower images. If there is a distinct representation of individual exemplars in these regions, we would expect higher similarity for the same identity compared to different identities faces. First, we calculated the within-identity and between-identities similarities for each participant and subtracted the between-identities similarity from the within-identity similarity. We identified 5 large anatomical ROIs from the Harvard-Oxford atlas based on the areas in which the functionally face-selective ROIs (OFA, FFA, STS, ATFP) fall within. Based on this, we selected the temporal-occipital fusiform cortex (TOFC), posterior and anterior temporal fusiform cortex (pTFC, aTFC) and the posterior and anterior inferior temporal gyrus (pITG, aITG) for analysis. Figure 5.7 shows the magnitude of face identity representations across the different regions. One-sample t-tests (two-tailed) showed that

controls had distinct representations of individual face identities in anterior regions of the temporal lobe (aITG: t =2.51, p = 0.022; pITG: t = 2.34, p = 0.031; aTFC, t = 2.17, p = 0.043), but not in posterior regions (pTFC: t =1.88, p = 0.077; TOFC: t: 1.18, p = 0.255). In contrast, DPs did not show any distinct face identity representations in any of these regions (TOFC: t = 0.29, p = 0.771; pTFC: t = 0.04, p = 0.968; aTFC: t = 0.96, p = 0.347; pITG: t = 0.67, p = 0.511; aITG: t = 0.31, p = 762). A 2 (Groups) x 5 (ROIs) ANOVA showed that Controls had significantly higher identity representations across all regions compared to DPs, F(1, 195) = 10.84, p = 0.001. We next asked whether the magnitude of face identity representations could be predicted by performance on the CFMT. None of the correlations were significant at $p < 0.05$ after correcting for multiple comparisons.

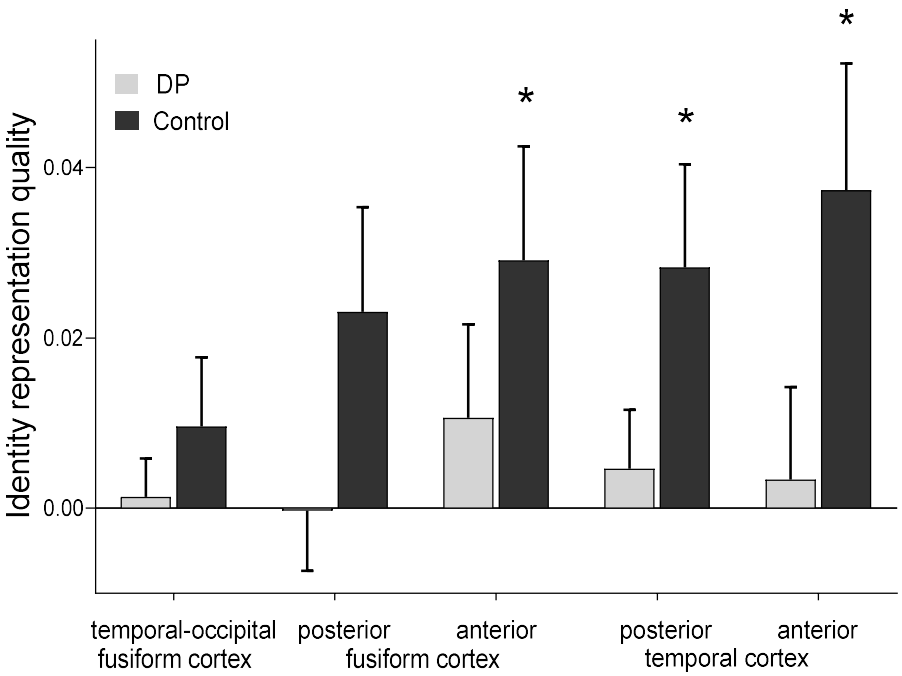

Figure 5.7. Mean (± 1 SEM) difference of within minus between identity representations in DP and Control participants

Next, we repeated this analysis for the flowers scan. There were no distinct representations for individual flower exemplars in Controls and DPs in any of the regions, Controls: TOFC: t = 0.72, p = 0.479; pTFC: t = 1.92, p = 0.072; aTFC: t = 1.13, p = 0.273; pITG: t = 1.66, p = 0.115; aITG: t = 0.18, p = 857; DPs: TOFC: t = 2.01, p = 0.058; pTFC: t = 0.47, p = 0.640; aTFC: t = 1.03, p = 0.316; pITG: t = 1.85, p = 0.405; aITG: t = 0.52, p = 0.608. A 2 (Groups) x 5 (ROIs) ANOVA showed that there was no difference in magnitude of identity representations between Controls and DPs, F(1, 195) = 0.49, p = 0.483, Supplementary Figure 3.

5.5. Discussion

Here we combined univariate, MVPA and functional connectivity fMRI analyses to investigate the organization of face-selectivity, functional connectivity, and representations of individual faces in DP and neurotypical individuals. Overall, we found similar organization of face-selectivity maps in DP and neurotypical participants. Namely, the presence, location and activity magnitude of face-selective regions did not differ between the groups. These results add to previous reports of typical face selectivity in DP (Rivolta et al., 2014; Avidan, Hasson, Malach, & Behrmann, 2005; Hasson, Avidan, Deouell, Bentin, & Malach, 2003), but see (Jiahui, Yang, & Duchaine, 2018; Hadjikhani & De Gelder, 2002; Furl, Garrido, Dolan, Driver, & Duchaine, 2011).

Instead, DP was characterised by altered functional connectivity organization. Quantitatively, the left anterior temporal cortex was less functionally connected to the rest of the brain when DPs were presented with faces, but not flowers. Seed-based connectivity analyses showed that the global reduction in connectivity of the anterior temporal cortex is

mainly contributed by interhemispheric connectivity reductions to the contralateral middle temporal cortex and reduction in spatially distant ipsilateral connections to the left frontal pole and superior frontal gyrus. DPs had further face-specific interhemispheric reductions in connectivity between the right anterior temporal cortex and the left hippocampus, and between the left insular cortex and the right cuneal and precuneous cortex – regions comprising the extended face processing system (Gobbini & Haxby, 2007). Our results suggest that alterations in integrity of interhemispheric functional connectivity is involved in poor face recognition abilities. We further analysed the pattern of functional connectivity using fc-MVPA analysis. This analysis aims to uncover alterations in the whole-brain connectivity pattern, rather than connectivity strength. Similarly, to the global connectivity analysis, we found that the left anterior temporal lobe had different pattern of connections to the rest of the brain in DP. We also observed altered connectivity in left posterior middle temporal cortex and right temporooccipital fusiform cortex. Importantly, the difference in functional organization observed in these areas was specific to face processing. These results are consistent with the previously demonstrated functional disruptions in the anterior temporal lobe associated with DP (Rosenthal et al., 2017) and poor face recognition skills in neurotypical populations (Levakov et al., 2022). Our findings further demonstrate that reduced connectivity *and* different pattern of connectivity to the anterior temporal cortex are involved in DP. Importantly, these alterations are evident at the large-scale whole-brain level, without restriction of analysis to pre-defined face-selective regions and point to the significance of integration across the whole-brain functional connectivity in supporting typical face recognition abilities.

We measured the discriminability of individual face identities by comparing the representational patterns for the same face identity compared to different face identities.

Controls exhibited distinct response patterns to individual face identities in the anterior temporal fusiform cortex, posterior, and anterior inferior temporal cortex. Read-out of individual-level face information was progressively more pronounced anteriorly along the ventral stream, reaching the highest discriminability in the anterior temporal cortex. In contrast to neurotypical controls, DPs showed no identity discrimination in any of the areas we analysed, including the anterior temporal cortex. That is, the similarity in neural representations for the same face identity was equal to that of two different faces. The lack of face-identity information in anterior temporal cortex suggests that DP do not have a population code in the temporal cortex representing the subtle differences between individual faces. These results are consistent with previous reports, supporting the functional role of anterior temporal cortex in distinguishing individual face identities (Kriegeskorte et al., 2007; Anzellotti et al., 2014; Yang et al., 2016).

Successful face recognition entails distinguishing and recognising a face as familiar among other highly similar face identities. This process is supported by accumulating perceptual experience with different face identities through repetitive exposure. Indeed, pattern similarity, as measured by fMRI across repetitions of a stimulus, is higher when stimuli are subsequently remembered (Xue et al., 2010; Ward et al., 2013), demonstrating that successful memory encoding occurs when the same neural representations are more precisely reactivated across repetitions. In the current study none of the face identities were perceptually familiar to participants. The fact that we observed an above chance identity representation with only 4 repetitions of each previously unfamiliar identity suggest that this process operates early on and likely underpins identity learning. This is consistent with the proposed role of the anterior temporal cortex in both mnemonic and perceptual functions. For example, activity in the anterior temporal cortex is sensitive to previously familiar faces

(Gobbini & Haxby, 2007; Sugiura et al., 2001) but also supports fine-grained perceptual discrimination in previously unfamiliar faces (Anzellotti et al., 2014) and is proposed to act as a bridge between high-level visual perception and memory (Collins et al., 2016). Importantly, these results are also consistent with the behavioural profile of DPs, whose impairments are specific to distinguishing and recognising face *identities*, rather than recognising faces as a category.

Our results can be illustrated with reference to the face-space framework, whereby individual faces are encoded as mean-relative vectors within a multi-dimensional space (Valentine, 1991). With exposure to faces during development the face-space dimensionality is increasingly optimised to represent the variability of face features and best capture the difference between faces in reference the average face. Neural evidence further supports this view that individual faces are encoded by their direction (facial identity) and distance (distinctiveness) from a prototypical (mean) face (Loffler et al., 2005). Behavioural evidence demonstrates that DPs show atypical mechanisms of face identity coding in a multi-dimensional faces space (Palermo et al., 2011), suggesting a distortion of representations within the multidimension face space. The current results demonstrating that DPs show the same representational similarity for two different face identities as for the same repeated identity, provide neural evidence for alterations of the coding of face identity within the face space in DP. It should be noted, however, that the current results cannot infer about the particular process that results in altered face space in DP. Identity recognition might be achieved through a significant overlap between the output of the structural encoding for a stimulus and the already stored representation of the same stimulus (Wing et al., 2020; Wing et al., 2015; Ritchey et al., 2013; Sommer & Sander, 2022). Thus, the lack of identity representation in DP might result from alterations in the structural encoding process,

alterations in storing an otherwise intact representation, and/or the process of matching the structural encoding with the already stored representation.

One limitation of our experimental task is that all faces were shown from front-view. This was done to maximise the number of different identities shown. Although face representations have been shown to gradually change from view-specific to view-invariant along the posterior-anterior gradient of the temporal cortex (Yang et al., 2016), it is possible that the representations we observed here are specific to the image, rather than the face identity more generally. Future studies should include face identities with varying identity-irrelevant properties such as viewpoint and expression. For example, the similarity in response between two different viewpoints of the same identity compared to two similar viewpoints from different identities would constitute a more accurate neural representation of face identity.

One interesting result we observed in the lack of individual-level flower discrimination in any of the areas we analysed. This fits with previous reports demonstrating identity representations in anterior inferotemporal cortex for faces, but not houses (Kriegeskorte et al., 2007), and suggests that the representation of the anterior temporal cortex is not entirely domain-general. Probing the identity-level representations of the anterior temporal cortex with a more diverse and comprehensive set of categories will be required before drawing strong conclusions about its role in face-specific identity representations.

Here we explored the organization in face-selectivity and functional connectivity and face identity representations in DP. Overall, our results show comparable location and presence of face-selective regions across DPs and Controls. In contrast, DP was marked by alteration in functional connectivity specific for face processing. These alterations included

reduced global connectivity and different connectivity pattern to the left anterior temporal cortex. Additionally, we found that areas in the anterior, posterior, and inferior temporal cortex were differently connected to the rest of the brain in DP. Further, using MVPA, we showed that face identity representations are hosted in the anterior temporal cortex and their strength correlated with face recognition abilities. However, the neural quality of identity representation for individual faces was distorted in DP. These results show that typical face recognition abilities are underpinned by the process of reactivation of the same neural representation during visual repetitions and failure of pattern reactivation is associated with face recognition deficits in DP. Together, these results point to the functional significance of the anterior temporal cortex in supporting typical face recognition abilities.

Chapter 6

Structural connectivity analysis in developmental prosopagnosia

6.1. Abstract

Developmental prosopagnosia (DP) is a neurodevelopmental disorder characterised by deficits in the recognition of face identity. The majority of studies investigating structural connectivity correlates in DP have focussed on the occipital and temporal lobe. However, the overall connectivity across the whole brain is largely unexplored in DP. Using network-based analyses, we explored the organization of the structural connectome in a group of DPs who had previously shown altered whole-brain functional organization. We show that the overall structural topology in DP was comparable to that of neurotypical controls. Instead, DP was characterised by reduced local connections between the inferior, middle, and superior temporal cortex. Together these findings demonstrate that global functional connectivity is more predictive of face recognition deficits in DP than global structural connectivity. However, we also show that DP is associated with altered local structural connectivity in regions of the temporal lobe that are important for face recognition.

6.2. Introduction

Developmental prosopagnosia (DP) is a neurodevelopmental disorder associated with life-long difficulties in the recognition of faces. Unlike acquired prosopagnosia, DP manifests in the absence of any apparent brain damage. The neural correlates of DP are still a subject to

debate - while some studies have found reduced activity in face-selective areas when viewing faces (Jiahui, Yang, & Duchaine, 2018; Hadjikhani & De Gelder, 2002; Furl, Garrido, Dolan, Driver, & Duchaine, 2011), others find activity comparable to that of neurotypical individuals (Rivolta et al., 2014; Avidan, Hasson, Malach, & Behrmann, 2005; Hasson, Avidan, Deouell, Bentin, & Malach, 2003). More recently, it has been proposed that DP might results from reduced communication between areas that are functionally important for face processing (Avidan et al., 2014; Song et al., 2015; Rosenthal et al., 2017; Levakov et al., 2022). Evidence supports the idea that this reduction in functional connectivity might, to some extent, be a consequence of a structural alteration in white matter tracts. Alterations in the connectivity of two white matter tracts - the inferior longitudinal fasciculus (ILF), connecting the occipital and temporal lobes, and the inferior fronto-occipital fasciculus (IFOF) projecting between the occipital and frontal cortex, have been shown in DP (Thomas et al., 2009; Herbet et al., 2018). More specifically, DP has been linked to aberrant structural connectivity between regions in the ventral temporal cortex functionally involved in face processing (Gomez et al., 2015; Song et al., 2015).

To date, only connections of specific tracts or between regions that show functional selectivity for faces have been explored in DP. However, a recent study found widespread functional connectivity patterns extending beyond the face network can predict face recognition abilities in neurotypical individuals (Levakov et al., 2022). This fits with findings (see Chapter 5), in which we showed reduced functional connectivity in DPs across the whole brain – that is there are brain areas that are less functionally connected to the rest of the brain. Importantly, this reduced functional connectivity was evident when participants viewed faces but not when they viewed non-face objects (flowers). However, it is unclear

whether this abnormal pattern of functional organization at the whole-brain level is a result of alternations in the structural organization.

Investigating whole-brain organization is particularly important when studying neurodevelopmental disorders such as DP. Unlike acquired deficits, the same cognitive difficulties that emerge over the course of development can manifest through miswiring in different neural routes – a phenomenon known as the principle of equifinality (Bishop, 1997). The plasticity of the developing brain in relation to face recognition abilities is demonstrated by a recent study showing that patients whose entire hemisphere was removed in childhood can achieve 80% of the neurotypical face recognition performance (Granovetter et al., 2022). Importantly, this effect was independent of which hemisphere was removed. This suggests that even though in adult neurotypical participants the right hemisphere is dominant for face processing (Kanwisher et al., 1997; Pitcher et al., 2007), the functional processing of faces can be reorganized, such that equal performance can be achieved. Thus, neural investigations of DP should not be directly assumed to have one-to-one mapping with the neural correlates implicated in acquired face recognition deficits. Exploring the connectome of the whole brain has the potential to investigate potential structural reorganizations and altered topology in DP.

In the current study, we investigated structural connectivity across the brain using diffusion tensor imaging (DTI). DTI is an MRI technique that measures the directionality of water molecule diffusion to determine the structure of white matter tracts in the brain (Basser et al., 2000). Here, we utilise graph theory analysis to explore the pattern of structural organization across the whole brain in DP. Graph theory has been widely used to investigate the topology of brain connectomes and uncover abnormal patterns of structural and

functional connectivity (Farahani et al., 2019; Guye et al., 2010). A graph's information represents connections (edges) between regions (nodes). Edges can be weighted (representing the quantity of connections) or binary (representing the presence or absence of a connection). Characterising the structural connectome at the macroscopic level typically involves parcellating the brain into nodes using a range of brain atlases. Graph theory measures can thus provide insight into the overall structural organization of the connectome (Rubinov & Sporns, 2010).

6.3. Methods

6.3.1. Participants

Data was collected from the same Control (*n*=19) and DP (*n*=22) participants that participated in Chapter 5. All participants provided written informed consent and the experiment was approved by the York Neuroimaging Centre (YNiC) Ethics Committee.

6.3.2. Diffusion MRI (dMRI) data acquisition and pre-processing

dMRI data were acquired with a GE 3T HD Excite MRI scanner with an 8 channel whole head High Resolution Brain Array. Two diffusion-weighted MRI scans were acquired, with opposing phase encoding directions. The first fMRI scan lasted ~ 9 minutes with posterior-to-anterior phase encoding direction. A single-shot pulsed gradient spin-echo echo-planar imaging sequence was used with the following parameters: b = 1000 s/mm^2, 25 unique diffusion directions, 60 slices, FOV = 192mm, TR= 12s, TE = 88.5ms (minimum full), voxel size = 2 x 2 x 2 mm^3, matrix size = 96 × 96, flip angle = 90 degrees. 3 volumes without diffusion

weighting (b0) were acquired at the start of the scan. The second dMRI scan was ~4.5 minutes with anterior-to-posterior phase encoding direction and was used to correct distortion and had only 12 diffusion directions. All other scan parameters were the same as the first dMRI scan. Data was split across time and the first 3 baseline volumes with no diffusion were extracted. The b0 volumes were merged across the 2 scans to estimate the amount of susceptibility-induced distortion and Topup (Andersson et al., 2003) was used to correct it by applying the distortion field to the scans and combining them together. Non-brain tissue removal was applied using BET (Smith, 2002).

6.3.3. Whole-brain tractography

The diffusion data were reconstructed using generalised q-sampling imaging, (Fig. 6.1a) (Yeh et al., 2010) with a diffusion sampling length ratio of 1.25. The tensor metrics were calculated using DWI with b-value of 1000 s/mm². A deterministic fibre tracking algorithm (Yeh et al., 2013) was used with augmented tracking strategies (Yeh, 2020) to improve reproducibility. The anisotropy threshold was randomly selected. The angular threshold was randomly selected from 15 degrees to 90 degrees. The step size was randomly selected from 0.5 voxel to 1.5 voxels. Tracks with length shorter than 30 or longer than 300 mm were discarded. A total of 1000000 seeds were placed. Whole-brain tractography was conducted using DSI Studio (http://dsi-studio.labsolver.org).

6.3.4. Connectome construction

The connectome model was constructed by parcellating the whole-brain tracts with 62 cortical regions derived from the Desikan-Killiany-Tourville (DKT) atlas (Klein & Tourville, 2012), (Fig. 6.1b). Full list of the regions from the DKT atlas used in the connectome construction is shown on Supplementary Figure 1. The connectivity matrix was calculated by using the number of tracts connecting each pair of anatomical regions. The weighted connectivity matrix for each participant was thresholded at 10% of the overall count sum and then binarized (Fig. 6.1c). At this threshold mean densities of 10% and 9% were calculated across connectomes in Controls and DPs, respectively, which has previously been found to preserve the most informative edges, enabling the calculation of a range of graph-theoretic measures (Akarca et al., 2021; Zdorovtsova et al., 2022).

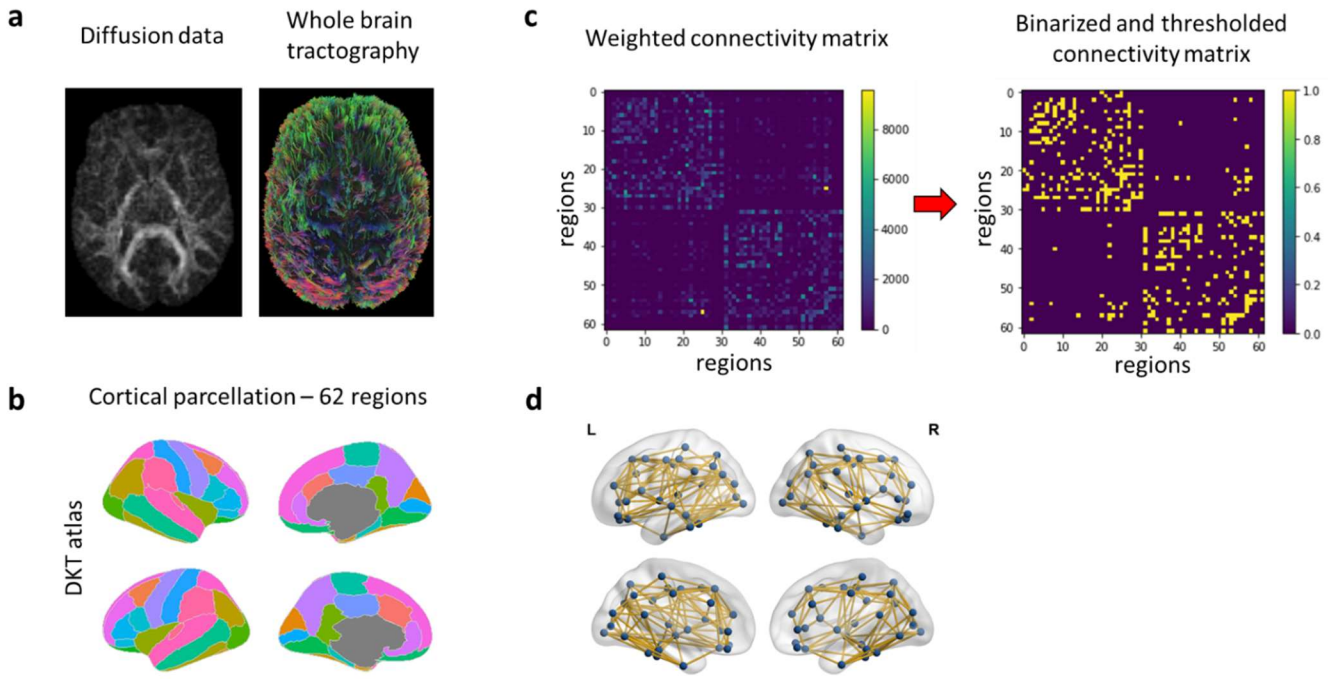

Figure 6.1. Processing workflow for connectome network construction. (a) whole brain tractography, (b) Desikan-Killiany-Tourville (DKT) atlas was used to parcellate the brain into 62 cortical regions, (c) weighted connectivity matrix and binarized, thresholded connectivity matrix, (d) brain network plot representing the 62 nodes and edges between them.

6.3.5. Topological measures

A DTI-derived brain network for each subject can be described as a graph with set of nodes representing regions of brain and edges that form the white matter connections between the nodes, (Fig. 6.1d). Topological measures of brain networks can be represented in a number of ways, all of which capture different features of connectivity. In the current study we used two graph measures (degree and clustering coefficient) at the whole network and nodal levels to investigate the relationship between brain organization and face recognition abilities.

6.3.6. Degree and Clustering coefficient

The degree is the number of edges connected to a node (brain region). The degree of each node measures its' integration with the broader network (global connectivity to the rest of the brain regions). The degree of node i is given by:

$$k(i) = \sum_{j \in N} a(i,j)$$

where $a(i,j)$ is the connection status between the pair of regions i and j.

The clustering coefficient is the fraction of a node's neighbours that are neighbours of each other, thus indicating the level of modularity within a network. High clustering coefficient of a region indicates the region's neighbours are highly clustered together, forming a module. Clustering coefficient values range from 0 to 1. The clustering coefficient for node i is given by:

$$ci = \frac{1}{n}\sum_{i \in N} \frac{2ti}{ki(ki-1)}$$

where ci is the clustering coefficient of a node i.

6.4. Results

We first calculated overall connectivity across the whole brain. We measured the number of connections (edges) to each region (node) at the whole network-level to give a value of degree of connectivity. There was no overall difference in the degree between Controls (M = 5.87, SD = 1.44) and DPs (M = 5.44, SD = 1.48) across the whole brain (t (39) = 0.94, p = 0.353). Next, we determined if there were differences in connectivity across different regions between Controls and DPs across the 62 regions (Fig 6.2a). Although the majority of regions had higher degree in Controls, none of the regions were significantly different at FDR-corrected for multiple-comparisons threshold $p < 0.05$, (Fig 6.2c). Node-based degree values for Controls, DPs and the Control > DP contrast are presented in Supplementary Table 1.

Next, we measured the degree of modularity within the network by measuring the clustering coefficient. There was no significant difference in the network-level clustering coefficient of Controls (M = 0.50, SD = 0.07) and DPs (M = 0.47, SD = 0.10), t (39) = 1.14, p = 0.263. Next, region-level clustering coefficients were calculated for Controls and DPs (Fig 6.2b). We then compared the clustering coefficients across the 62 regions between the groups (Fig 6.2d). Only the left pericalcarine showed a marginally higher clustering coefficient in Controls compared to DPs (p = 0.051, FDR-corrected for 62 multiple-comparisons. Node-based clustering coefficient values for Controls, DPs and the Control > DP contrast are presented in Supplementary Table 2.

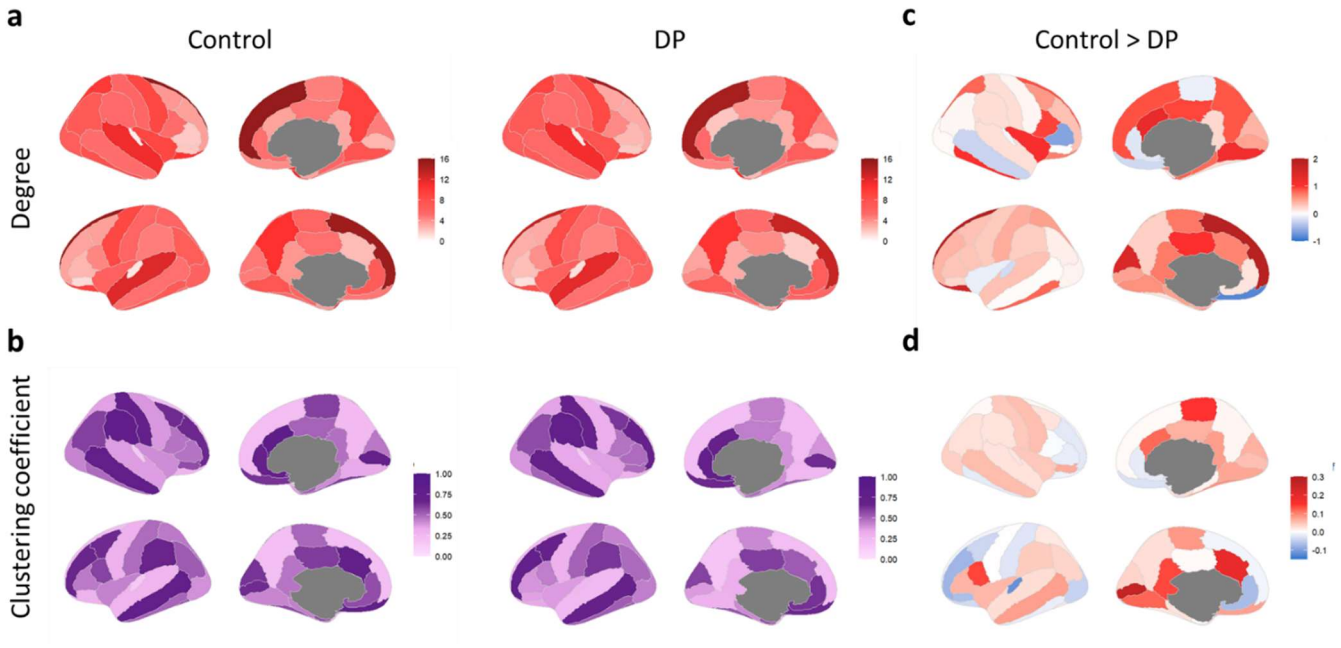

Figure 6.2. (a) Region-level node degree and (b) clustering coefficient values in Control and DP groups, (c) Control > DP difference in region-level node degree (d) and clustering coefficient

The degree of a region measures the overall connectedness of that regions to the rest of the 61 regions in brain. However, as the participants in the study were selected to have face deficits only, it is theoretically plausible that poor recognition abilities specific to faces are associated with reductions in connectedness to a single other region. As such, the overall degree of a region would not significantly differ between groups because the contribution of the reduced connectedness will be only 1 out of 61 connections. To explore this possibility further, we measured the number of connections between the inferior temporal (IT) cortex from the DKT atlas and each of the other brain regions separately. We chose the IT cortex as a seed region due to its functional importance for face processing. Next, to investigate whether poor face recognition is associated with different connection strength between the IT and any other region in the brain, we measured the difference in number of fibers between

the IT and the rest of the 61 brain regions between Controls and DPs. Three regions showed significantly higher connections to the left IT cortex in Controls than DPs: the left fusiform cortex ($p < 0.001$, FDR-corrected for 61 multiple comparisons), left middle temporal cortex ($p < 0.001$, FDR-corrected), and the left superior temporal cortex ($p < 0.001$, FDR-corrected), (Fig. 6.3a). Next, we repeated the between group analysis for the right IT. Five regions showed significantly higher connections to the right IT cortex in Controls than DPs: the right fusiform cortex, $p < 0.001$, right middle temporal cortex ($p < 0.001$, FDR-corrected), right superior temporal cortex ($p < 0.001$, FDR-corrected), right lateral occipital cortex ($p < 0.001$, FDR-corrected) and the right parahippocampal cortex ($p = 0.002$, FDR- cortex), (Fig. 6.3b).

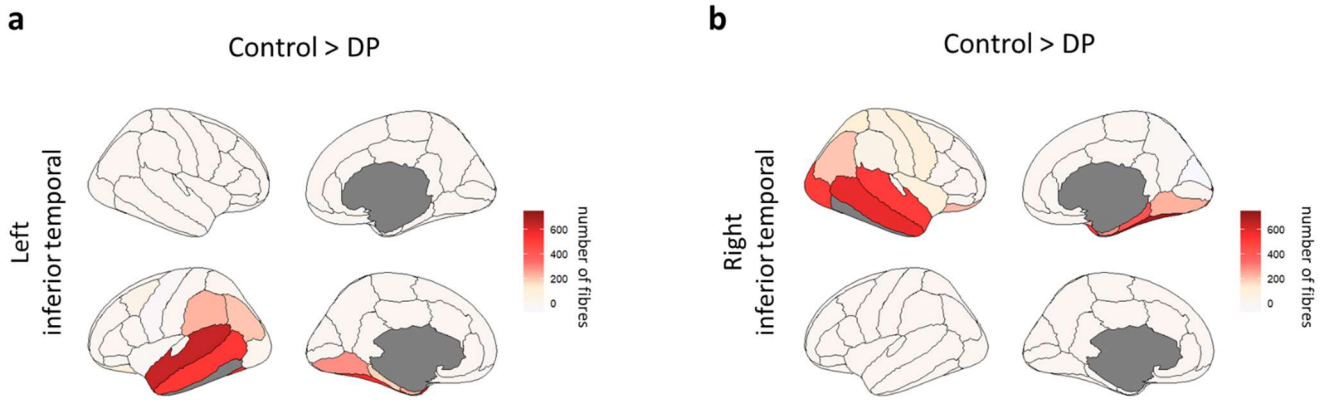

Figure 6.3. Difference between Controls and DPs in the number of fibres linking the (a) left and (b) right inferior temporal region with the rest of the brain regions in the DKT atlas.

6.5. Discussion

Here we used network-based analysis to explore the structural organization across the whole brain in DP. Overall, there was no difference between DP and neurotypical participants in the number of structural connections (degree) and modularity (clustering coefficient) across the

whole network. Region-level analysis of these measures showed that overall many regions were more connected to the rest of the brain as well as having a higher clustering coefficient, however, none of the individual region comparisons between the two groups reached significance. This pattern of results suggests that the association between whole-brain structural organization and face recognition abilities might be weak or highly variable across individuals. However, the fact that the majority of regions showed a higher mean degree in Controls suggests that although they are not significantly more connected to the rest of the whole brain, it is possible that each of the regions might be more connected to another region/limited number of other regions. This would result in a higher mean degree, but not sufficiently higher to reach significance.

We found local reductions in structural connectivity in DP. DPs had fewer projections between the left and right IT cortex and the fusiform, middle, and superior temporal cortex in the ipsilateral hemisphere. Additionally, the right IT cortex also had reduced structural connectivity to the right lateral occipital and parahippocampal cortex. Our findings are consistent with the wider literature reports of local structural alterations in DP. Namely, reduced volume in ILF and IFOF have been previously reported (Grossi et al., 2014; Thomas et al., 2009) as well as reduced local structural connectivity restricted only to areas implicated in face processing (Gomez et al., 2015; Song et al., 2015). In line with this, most of the areas with reduced global functional connectivity we found in Chapter 5 were located in the regions with reduced local structural connectivity found in the current study. The pattern of current result suggests that structural alterations local to the IT cortex might facilitate atypical functional connectivity.

In Chapter 5 we found altered global functional connectivity in multiple regions. For example, areas in the anterior temporal cortex had reduced connectivity to the rest of the brain and areas in the inferior, middle, and superior temporal cortex had qualitatively different connectivity patterns to the rest of the brain in DP. Importantly, these alterations in functional connectivity were present only in the face processing task, with no alterations in functional connectivity for flower processing. This is in line with another report showing atypical functional organization in DP (Rosenthal et al., 2017). Based on the current findings, it is likely that DP is characterised by typical whole-brain structural organization, but atypical functional organization specific for face processing. This is consistent with the findings that functional and structural connectivity in the brain are not often aligned, with many functionally coupled regions lacking direct structural connections (Mišic et al., 2016; Liu et al., 2022; Suárez et al., 2020). In such cases functional communication between structurally uncoupled regions must rely on polysynaptic signalling – connection through intermediate regions. Even in cases where there is an underlying structural connection between functionally coupled regions, structural connectivity can explain only about 50% of the variance in functional connectivity (Honey et al., 2009), meaning that half of the variance in functional connectivity cannot be directly explained by underlying structural connection. It follows that global connectivity deficits in function are not necessarily underlined by structural ones.

In a study directly relevant to face processing, Wang et al., (2020) explored the correspondence between the structural and functional face connectome. The authors functionally defined face-specific network of areas and measured the similarity of functional and structural connections between these areas. Functional and structural connectivity across the entire face network had only weak to moderate correlation (r=0.32), suggesting

that structural connectivity explains no more than 10% of the functional connectivity. Crucially, this relationship was driven by the structural-functional coupling withing the core face pathways (r = 0.36), and no correlation was found in the non-core face pathways (r = 0.01). Given the large gap in correspondence between structural and functional connectivity, a critical question concerns which connectivity measure has a better predictive power for cognitive abilities and behaviour. Although numerous studies have independently linked functional (Seo et al., 2013; Qian et al., 2019; Wang et al., 2009) and structural (Contreras et al., 2015; Shu et al., 2018; Bathelt et al., 2019) whole-brain connectivity to cognitive variability, only a limited number of studies have directly compared them in predicting cognition. Consistent with our current results, these studies demonstrated that whole-brain functional connectivity is a better predictor than structural connectivity of a range of cognitive abilities (Dhamala et al., 2021; Ooi et al., 2022). Our results add to the growing literature by demonstrating that deficits in face recognition in DP are better captured by whole-brain global functional, rather than structural connectivity. Importantly, the deficits in functional connectivity in DP were only evident when the task was relevant to their behavioural deficit – processing face identities. It is worth noting, however, that the functional connectivity alterations found in DP were based on a voxel-level analysis, whereas the structural connectivity used much larger regions, potentially leading to reduced sensitivity for capturing finer-scale effects.

In conclusion, we have used a network-based analyses to explore the structural connectivity in DP. We found that the overall organization of the structural connectome in DP was comparable to that of neurotypical adults. Further, we show that DP is associated with decreased local structural connectivity between the inferior, middle and superior cortices. These results demonstrate that global functional connectivity is more

predictive of face recognition deficits than global structural connectivity and that face recognition deficits in DP is associated with altered local structural connectivity in the temporal lobe.

Chapter 7

General discussion

7.1. Aims of thesis

The overall aim of this thesis is to explore the underlying deficit in developmental prosopagnosia (DP). The first aim of the thesis was to directly address a current controversy in the literature about whether the deficit of face recognition in DP extends to non-face objects. These findings have important implications for understanding whether the perception of faces is based on specialised processes or engage shared mechanisms with other objects. Chapter 2 asked whether DPs have a deficit in the recognition of pareidolic objects (which appear face-like) and whether this was dependent on the perceptual or image similarity with faces. Although face recognition impairments are a hallmark symptom of DP, it was unclear whether face recognition impairments will be influenced by race and species boundaries. Chapters 3 and 4 explored DPs' deficits across different races and animal species. A final aim was to explore the neural correlates of DP. Despite a number of neuroimaging studies of DP, a clear account of which neural processes are impaired is missing. Chapter 5 and 6 explore how the brain may give rise to deficits in face recognition by investigating the whole-brain organization of functional and structural connectivity as well as the integrity of neural signatures elicited by individual faces.

7.2. Findings and theoretical implications

7.2.1. Behavioural profile of developmental prosopagnosia

One common finding across the experiments in this thesis is that the memory, perception and matching of upright faces from different races and species is impaired in DP. Conversely, on a group level DPs did not have deficits with non-face objects. In Chapters 2 and 4 we show that recognition of cars, bottles and starfish was not impaired in DP. Similarly in Chapter 5 we demonstrate that DP is characterised by disrupted functional connectivity when viewing faces, but not flowers. One conclusion that might be drawn on based on these results is that the deficits in DP are face-specific. However, in Chapter 2 we show DPs exhibit a recognition deficit with pareidolic objects (which give rise to the perception of a face), but only when they have similar low-level properties to faces – merely evoking the perception of a face was not enough to impair recognition. Similarly, in the neurotypical population, recognition ability for faces co-varied only with the pareidolic images with similar image properties to faces. This demonstrates the importance of low-level properties in the association of deficits in DP, and recognition mechanisms more broadly. One remaining question stemming from these findings is whether the effect of low-level similarity to faces on recognition would extend to non-pareidolic objects. Evidence from neuroimaging studies have shown that similarity in neural patterns for various object categories co-varied with similarity in their low-level properties (Rice et al., 2014). Similarly, other object properties such as texture, form (Long et al., 2018), animacy (Kriegeskorte et al., 2008) and real-world object's size (Konkle & Oliva, 2012) have also successfully explained variation in neural responses.

While there are numerous studies characterising the neural responses to a large sample of object categories, to date, we lack a systematic investigation of whether these neural findings extend to behavioural recognition. The main reason behind this is practical feasibility. While investigating objects representational space by presenting many (*n*>1000) object categories with differing properties in fast succession has been achieved in neuroimaging (Hebart et al., 2022, Grootswagers et al., 2022), characterising the behavioural recognition of numerous object categories would be considerably more time consuming, as it will involve completing many conditions. Each condition will entail remembering images from a specific category and later recognising them among distractors from the same category. On a practical level, this means that characterising neural similarity between 2 categories might require seconds in an MRI scanner, while investigating the association of recognition mechanisms of these two categories would require minutes. Scaling this over many object categories to estimate behvaioural recognition similarity space will attenuate the time requirements manyfold. Although the predominant body of evidence from the literature, as well as in this thesis, points to a specialised recognition system for faces, and face-specific deficits in DP, characterising the recognition of a diverse set of objects will be required before strong conclusions can be made. One future direction in the exploration of recognition associations and DPs' deficits is to include many diverse categories with varying object properties (low-level image properties, shape, texture, animacy, size, visual experience, semantic relatedness) in order to find and systematise underlying properties driving covariation in recognition.

Another consideration relating to investigation of low and mid-level image properties to recognition, is that faces are a category with a very high intra-category similarity (similarity among faces) and relatively low inter-categories similarity (similarity between faces and other

categories). When investigating the contribution of image properties to recognition associations, it is particularly difficult to find a non-face category with sufficiently similar image properties to faces. In Chapter 2 we show that the similarity in image properties between faces and objects that were specifically chosen to be highly similar to faces is moderate. While it holds generally true that exemplars within a category will be more similar to other exemplars from the same category, compared to exemplars from different categories, this is particularly prominent for faces. The special status of faces, thus, could be subserved by their outlier status in terms of their low- and mid-level image properties. This sentiment is illustrated excellently by the maxim *"The best material model for a cat is another, or preferably the same cat"* (Rosenblueth & Wiener, 1945).

One interesting finding from Chapter 4, in line with the wider literature (Barton et al., 2019; Bate et al., 2019), is that even in the absence of group-level deficits with objects, some DP individuals showed impaired performance. Although DPs were not impaired with non-face objects on a group-level, 33% of DPs with face impairments in the old/new recognition task also had impairments with objects. One explanation for the co-occurrence of face and object deficits in some DPs is provided by the independent disorders hypothesis (Gray & Cook, 2018), stating that shared face and object deficits in some individuals might stem from a shared developmental atypicality and common genetic and environmental factors. Consistent with this, one study investigating 10 genetically related family members with prosopagnosia reported that all of them were also impaired on recognition of cars and guns (Duchaine, Germine, & Nakayama, 2007).

Co-occurrence of neurodevelopmental disorders is the rule, rather than the exception. For example, the presence of prosopagnosia in Autism Spectrum Disorder (ASD) is

substantially higher than in the general population (Gray & Cook, 2018; Minio-Paluello et al., 2020). Similarly, ASD traits are also higher in DP compared to the general population. Importantly, the 2 disorders are regarded as separate, as many individuals with ASD do not have face recognition deficits and many DPs do not exhibit ASD traits (Cook & Biotti, 2016). In fact, a commonly adopted exclusion criteria in case-control studies of DP is the presence of ASD diagnosis (Bate et al., 2019; Biotti et al., 2017; Marsh et al., 2019; Barton et al., 2019; Ulrich et al., 2017). The theoretical justification behind the exclusion is the assumption that face recognition deficits in DP and ASD might be inherently different and exclusion of ASD diagnosis is used to ensure face recognition deficits are explicitly attributable to DP. However, the consequence of this is that it might exaggerate the distinctiveness of DP and artificially decrease the heterogeneity, such that we end up studying the correlates of the inclusion criteria, rather than DP *per se*.

A related aspect amplifying the homogeneity of DP is that participants with difficulties that do not fall below diagnostic thresholds, but who report impairments in their lived experiences, are excluded. A standard practice in DP research is to include participants who self-report face recognition difficulties *and* score below 2SD from the control average on at least two face recognition tasks. Selecting only participants who meet stringent criteria inevitably exaggerates the homogeneity and distinctiveness of the sample relative to the broader underlying population which they are sampled from. A recent study included a large sample (n = 115) of individuals with face-recognition difficulties based on self-report only and found reports of widespread comorbidities with a range of developmental impairments (Svart & Starrfelt, 2022). Importantly, such typically excluded cases demonstrate comparable face recognition deficits to the included samples (Burns et al., 2022), suggesting that including participants who do not fall below the <2SD threshold on face recognition tasks can allow for

a more comprehensive investigation of the developmental comorbidities in DP. Future investigations should adopt a more transdiagnostic approach which will allow for the investigation and characterisation of the behavioural sub-types of DP – for example individuals who have a specific face-selective deficits vs. concurrent face and object deficits. This will aid a more precise estimation of the prevalence of concurrent deficits and investigation of the underlying properties of the objects affected. Further, variability in any cognitive measure is likely an emergent property of multiple structural or functional neural processes (Akarca et al., 2021). Adopting a less restrictive approach will also allow examining structural and functional neural mechanisms underlying the constellation of recognition deficits in DP and the neural processes that may give rise to converging profile of impairments in different disorders, such as those found in DP and ASD.

The hallmark symptom of DP is a deficit in recognising face identities. However, this is typically tested with own-race faces. It is well established that recognition ability for face identities from our own race is better than for faces from other races and species – phenomena known as the Other-Race Effect (ORE) (Malpass & Kravitz, 1969) and the Other-Species-Effect (OSE) (Scott & Fava, 2013), respectively. Chapter 3 explored whether DPs' deficits in face recognition, usually demonstrated with own-race faces, will transfer to other-race faces. In line with the ORE, results in Chapter 3 showed that control participants had worse matching performance with other-race faces compared to own-race faces. Crucially, DPs performed worse on both own and other-race faces, suggesting that their face deficits extend to other race-faces. Chapter 4 was similar in its conception, as it explored whether DPs deficits transfer to other-species faces. Results show that DPs had recognition impairments with both own and other-species faces, suggesting that their face impairments also extend to other species. It is worth noting that DPs' deficits for other-races and other-

species faces were of smaller magnitude compared to the deficits for own-race and own-species faces. One explanation for this is the overall lower performance mainly of Controls, and to a lesser extent of DPs with other- race and species faces due to lack of perceptual experience. The smaller difference in performance between own and other- race and species faces in DPs is potentially attributable to their inability to benefit from perceptual experience with own faces, resulting in suboptimal performance.

Nevertheless, DPs' recognition impairments with other- race and species faces are particularly interesting in relation to the structural variation between faces from different races and species. Faces from different races have slight variations in facial components and configurations, but importantly, they share the same morphology, while faces from different species have different morphological structure altogether. Our results suggest that the face deficits in DP encompass different configural and morphological structure of faces. These behavioural results are consistent with neuroimaging studies probing the representational space of various visual categories. Using representational similarity analysis, Kriegeskorte et al., (2008) showed that neural representations for faces from different races and species cluster together, while differing from non-face images. Our behavioural results link these neural findings with the behavioural profile of DP by demonstrating that DPs have associated race and species recognition impairments. This neural-behavioural correspondence further shows the utility of using neural representational patterns as a guide to probe the co-variance of recognition mechanisms of different categories and generate predictions about behavioural recognition deficits in DP.

7.2.2. Neural profile of developmental prosopagnosia

Chapter 5 and 6 explored the neural correlates of DP. The first objective in Chapter 5 was to investigate the organization of face selectivity in DP by comparing the response to faces with the response to non-face images (scenes and scrambled faces). Consistent with previous studies, we found that DPs exhibit a typical network of face-selective areas. There was no difference in the location and presence of face-selective regions as well as the magnitude of face-selectivity. One conclusion from these results is that face-selectivity might not reflect face recognition (dis)abilities. The general assumption when probing the neural correlates of DP is that face-selectivity will be reduced relative to control participants, however, little theoretical justification is provided for this assumption. Face selectivity reflects the amount of BOLD activity in response to seeing faces over and above the activity for non-face categories (often places, bodies and scenes). If it is associated with any behavioural ability, theoretically the most probable candidate will be the advantage in performance with faces relative to non-faces. Indeed, Huang et al., (2014) demonstrated that face selectivity in the FFA was correlated with the magnitude of recognition advantage for faces over objects. However, these results do not infer about the relationship between face selectivity and face recognition abilities *per se*.

Related to the previous argument, face-selective regions have been the locus of investigations even when studies assess the neural patterns of activity for face identities, rather than face-selectivity. In studies of neurotypical participants a common analysis method is to use univariate methods to localise face-selective regions and then investigate face identity representations in these regions using MVPA (Kriegeskorte et al., 2007; Natu et al., 2009; Jeong & Xu, 2016; Nestor et al., 2011; Axelrod & Yovel, 2015). However, regions

exhibiting preferential activity for faces are not necessarily co-localized with regions hosting identity representations - they might just provide necessary input. Similarly, regions that do not exhibit face-selectivity may still be involved in functional networks supporting face processing. Indeed, the behavioural relevance of the global organization of functional connectivity across distributed networks has been demonstrated in both healthy populations and a range of disorders (Ooi et al., 2022; Ramasubbu et al., 2014; Xu et al., 2021; Yeager et al., 2022; Qian et al., 2019; Seo et al., 2013; Wang et al., 2009).

Limiting neural investigation only to areas which are face-selective is problematic for exploring the neural correlates in DP for two reasons. Firstly, DP is characterised by deficits in recognising face identities, not faces as such. Face-selective regions are appropriate targets for exploring the neural basis of face recognition *on a categorical level* (recognising faces from other categories) but not necessarily about face identity recognition. For example, electrical stimulation of the fusiform gyrus results in metamorphosed appearance of faces (Parvizi et al., 2012). While it is theoretically clear why face-selective regions may be candidates for investigations of disorders where the perception of faces is distorted such as prosopometamorphosia (Blom et al., 2021), it is unclear why this is the case in DP. Chapter 5 directly addressed this by investigating the neural correlates of DPs' behavioural deficits with identities recognition. We found that in neurotypical controls, identity representations are hosted in the anterior inferior temporal cortex. In contrast, DPs lacked identity representations. That is, the similarity in the neural pattern of activity was not higher for the same identity faces, compared to different identities.

Secondly, DP is a *neurodevelopmental* disorder characterised by face recognition deficits that have emerged over the course of a development. Typical cognitive development,

and by extension atypical development, are emergent properties of a plastic and dynamic system. The developmental plasticity of face recognition is illustrated by a recent study showing that patients whose entire hemisphere was removed in childhood can achieve 80% of the neurotypical face recognition performance (Granovetter et al., 2022), regardless of which hemisphere was removed. This suggest that even though in adult neurotypical participants the right hemisphere is dominant for face processing (Kanwisher et al., 1997; Pitcher et al., 2007), the functional processing of faces can be reorganized, such that equal performance can be achieved. It follows that atypical functioning in a particular cognitive domain may not necessarily mirror the cause for the loss of that function in an otherwise typically developed brain (acquired cases). Within this framework, attempts to understand the brain organization that may govern behavioural face recognition deficits emerging over the course of development should explore areas beyond the ones exhibiting a face-selective response profile. To this end, the final objective in Chapter 5 and 6 was to explore the functional and structural connectivity organization. We used a whole-brain assumptions-free approach to characterise the connectivity in DP. The aim of this was to move beyond the "increased/decreased activity" approach and investigate potential deficits in how different brain areas are functionally and structurally integrated, resulting in face recognition impairments. Across Chapters 5 and 6 we measured the degree centrality of each voxel/region – that is, the magnitude of functional and structural connectivity of each voxel/region with the rest of the brain. This measure provides insight about quantitative differences in functional and structural connectivity strength. In Chapter 5 we also performed a voxel-wise functional connectivity MVPA analysis to characterise the pattern of functional connectivity. We found widespread alterations specific to face processing in both the strength and pattern of functional connectivity. Namely, the anterior temporal cortex in DP was less

connected and had a different pattern of connections to the rest of the brain. This is consistent with the lack of representation of face identities we found in the anterior temporal cortex, demonstrating the functional importance of the anterior temporal cortex in supporting face recognition abilities. DPs also had reductions in connectivity involving areas which do not exhibit face-selectivity such as the putamen, insular cortex, and hippocampus. Results from Chapter 6 demonstrate that in contrast to global functional connectivity reductions in DP, there were no global reductions in structural connectivity. Instead, DP was characterised by local structural connectivity reductions between the inferior, middle and superior temporal cortex. These results suggests that global functional, rather than structural connectivity is a better predictor of face recognition impairments in DP.

7.4. Concluding remarks

An on-going debate in psychology and neuroscience concerns the way faces and objects are represented. Domain-specific theories suggest that faces are processed via a specialised mechanism, separate from objects. This debate extends to DP and the degree to which the condition is face-specific or engages a shared recognition mechanism (domain-general). Across 2 Experiments, Chapter 2 investigated the extent of association between recognition abilities of neurotypical adults as well as the recognition deficits in DP for faces and face-like objects varying in their low-level similarity to faces. The results from Chapter 2 demonstrated that DPs have recognition deficits only for objects with similar low-level properties to faces. These results point to a shared recognition mechanism between faces and objects based on image statistics.

The specialisation of the mechanism for face recognition is a gradual experience-dependent process, not fully present at birth. Thus, it was unclear whether DPs' impairments in this mechanism will be influenced by visual experience. In Chapters 3 and 4 investigated recognition performance in DPs with own-race, other-race and other-species faces. Results demonstrated that DPs had deficits in the recognition across all types of faces. Together, these results show that DPs have a general, experience-independent, deficit in face recognition, encompassing a range of configural and morphological structures.

Current theories of the neural basis of DP focus on the face processing network in the temporal lobe. While the face network is specialised for face perception, the multiplex task of recollecting and linking familiar identities and person-related knowledge, requires the neural architectures to increasingly integrate signals beyond the face network. To address this Chapter 5 and 6 explored the extent to which the deficit in face processing may involve interactions with brain regions beyond the face processing network. We used whole-brain analyses in which we compared the magnitude and pattern of functional and structural connectivity across the whole brain between DPs and control participants. Chapter 5 found an overall alteration in the magnitude and the pattern of functional connectivity between the anterior temporal lobe and the rest of the brain in DP. Importantly, the anterior temporal lobe hosted representations to individual face identities in neurotypical, but not in DP individuals. Chapter 6 further demonstrated reductions in structural connectivity within the temporal lobe and between temporal lobe and frontal regions. Together, these findings offer new insights for the critical role of integration of information across the whole brain in supporting face recognition abilities.

In conclusion, this thesis contributes to the growing literature on developmental prosopagnosia by demonstrating that face recognition deficits in DP extend the boundaries of race and species. Furthermore, low-level image properties are an important component to consider when probing the organizational space of recognition deficits in DP. Finally, neural investigations of developmental prosopagnosia should be explored in light of the specific behavioural difficulties that have emerged over the course of development in DPs. Taken together, the experiments in this thesis contribute to the wider effort to understand the behvaioural and neural mechanisms of typical and atypical face recognition abilities.

Appendices

Appendix A.1. Chapter 2.

Supplementary Table 1. Individual scores on the diagnostic tests used to validate developmental prosopagnosia (PI20 questionnaire and Cambridge Face Memory Test (CFMT))

Participant	Age	Gender	Dominant hand	PI20 questionnaire score	CFMT score (%)
1	39	M	R	86	40.28
2	52	M	R	84	51.39
3	37	F	R	81	56.94
4	47	F	R	81	63.89
5	45	F	R	79	62.5
6	43	F	R	78	56.94
7	57	F	R	78	34.72
8	52	F	L	75	41.67
9	19	M	R	75	51.39
10	49	F	R	70	62.5
11	49	M	R	70	54.17
12	33	M	R	67	48.61
13	19	F	R	67	56.94
14	54	F	R	74	58.33
15	46	M	L	71	55.55
16	35	F	L	87	56.94
17	40	F	R	82	62.5
18	60	M	R	84	43.05

19	42	F	R	69	59.72
20	50	F	R	84	54.16
21	51	F	L	79	55.55
22	26	F	R	81	51.38
23	46	M	R	77	56.94
24	22	F	R	77	59.72
25	42	F	R	68	56.94
26	28	F	R	67	63.89
27	27	M	R	73	62.5
28	41	F	R	75	48.61
29	37	F	R	90	47.22
30	47	F	R	88	44.44

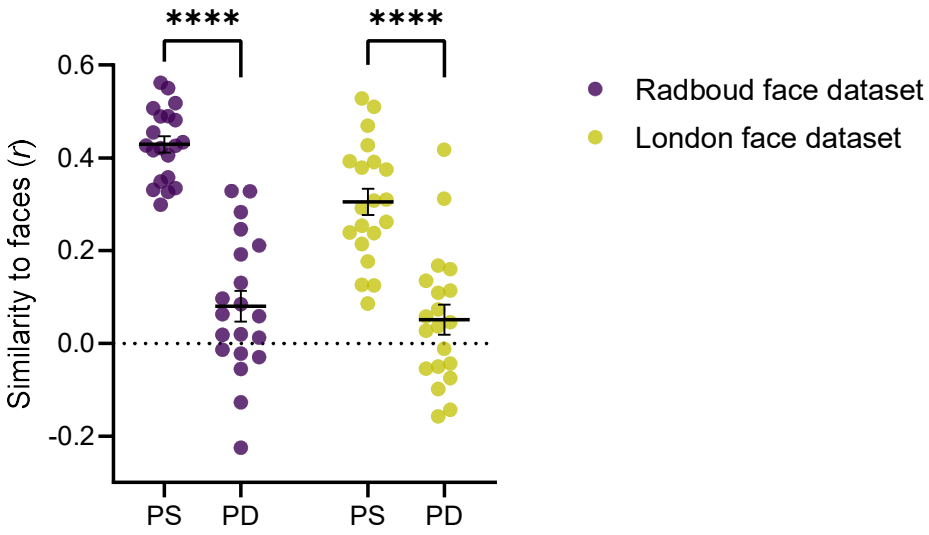

Supplementary Figure 1. Low-level similarity of PS and PD images to faces from the Radboud (Langner et al., 2010) and London (DeBruine et al., 2017) face datasets.

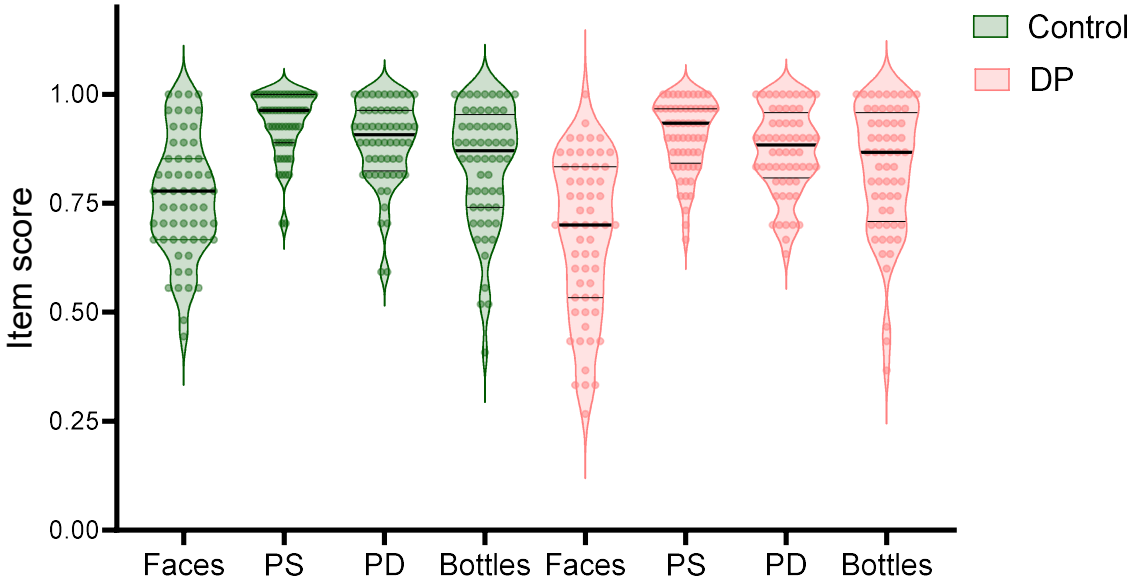

Supplementary Figure 2. Variation of accuracy scores for each image in the 4 conditions of the old/new recognition paradigm for controls and DP participants. The ranges for PS and PD are comparable and cannot explain the difference in the strength of correlations between faces and PS (r = 0.62) and faces and PD (*r* = 0.76). Moreover, the highest range is with faces, but our results show that the lowest correlation (*r* = 0.54) is in the face condition

Supplementary Table 2. Reliability (Cronbach's alpha) values for the 4 conditions of the old/new recognition paradigm for controls and DP participants

Reliability (Cronbach's alpha)	Control	DP
Faces	0.68	0.80
PS	0.58	0.62
PD	0.63	0.64
Bottles	0.78	0.81

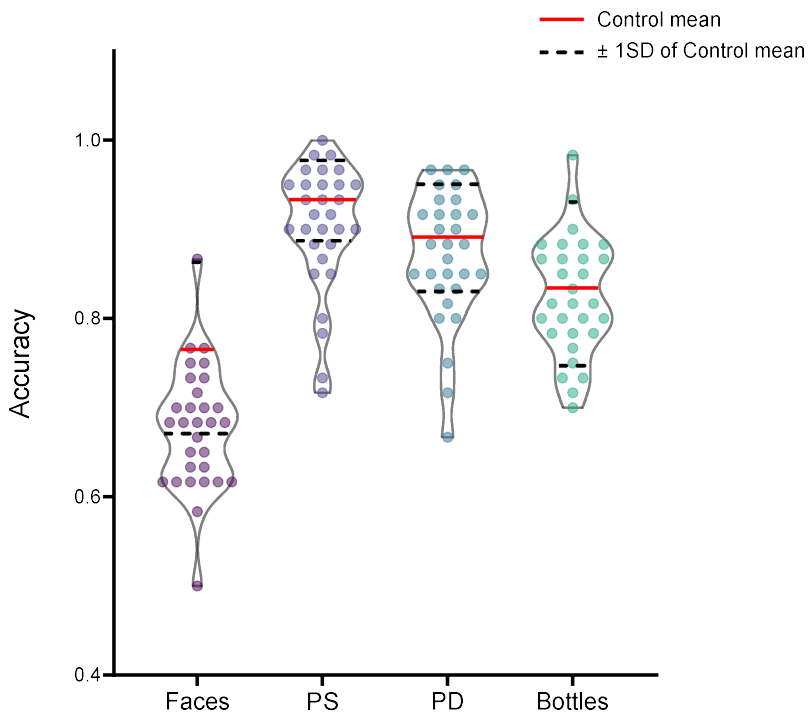

Figure 3. Accuracy scores of individual DP participants relative to the average and ± 1SD of the Control average scores in the 4 tasks of the old/new recognition paradigm.

Supplementary Table 3. Correlation values of multi-item patterns between DPs and controls for faces, PS, PD, bottles, most face-like and least face-like conditions.

Condition	DP-Control correlation (Person's *r*)
Faces	0.51
PS	**0.48**
PD	**0.79**
Bottles	0.66
Most face-like	**0.66**
Least face-like	**0.71**

Appendix A.2. Chapter 5.

Supplementary Table 1. Demographic information and individual scores on the diagnostic tests used to validate developmental prosopagnosia (PI20 questionnaire and Cambridge Face Memory Test (CFMT)). One DP participant (DP13) scored 64 on the PI20 questionnaire (1 point below the threshold of 65) but was included in the final sample as their score on the PI20 was more than 3 SDs above the mean of the control score and their CFMT score (48.60) was more than 3 SDs below the mean control score.

Participant	Age	Gender	PI20	CFMT
DP1	41	F	68	59.72
DP2	34	F	76	56.94
DP3	38	F	90	47.22
DP4	55	F	74	58.33
DP5	46	M	86	58.33
DP6	47	F	87	44.44
DP7	22	F	69	52.77
DP8	26	F	83	59.72
DP9	38	M	76	62.5
DP10	52	F	84	54.17
DP11	31	F	80	52.78
DP12	59	F	72	62.5
DP13	68	M	65	48.6
DP14	30	F	67	63.89
DP15	30	F	84	45.83
DP16	28	F	80	41.67
DP17	49	F	81	63.89
DP18	42	F	75	48.61
DP19	49	F	86	62.5
DP20	42	F	82	62.5
DP21	54	M	84	51.39
DP22	34	F	76	61.11
DPs Mean	**41.59**		**78.41**	**55.43**
DPs SD	**11.82**		**7.10**	**6.99**
Control Mean	**34.10**		**36.55**	**81.04**
Control SD	**12.62**		**8.29**	**8.89**

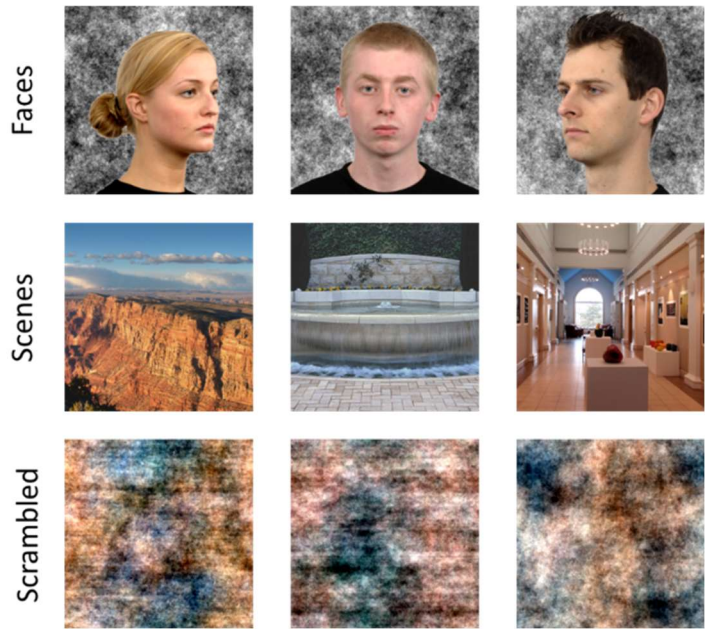

Supplementary Figure 1. Example face, scene and scrambled images used in the localiser scan.

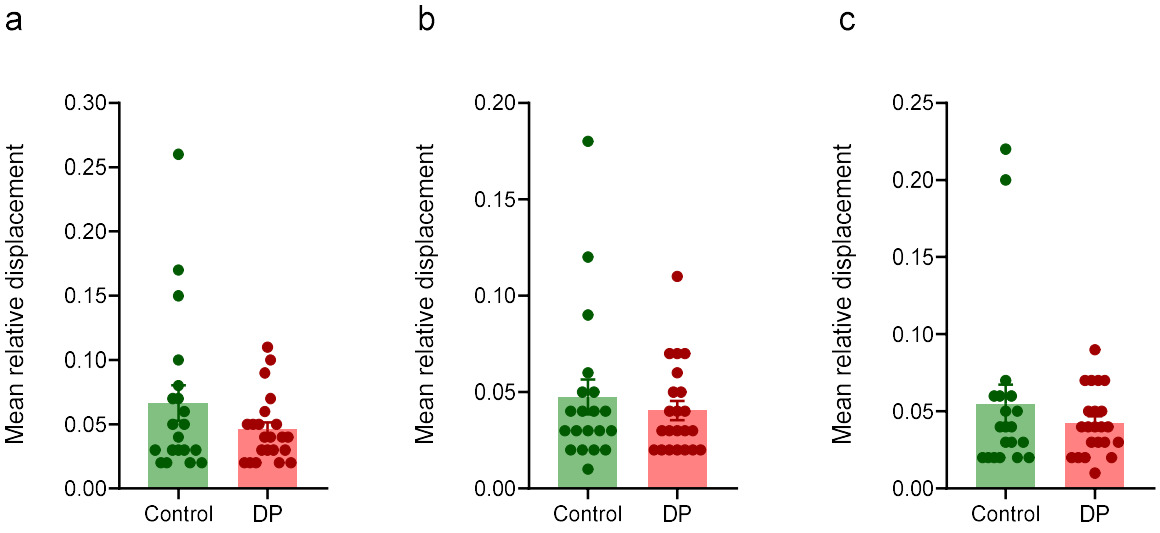

Supplementary Figure 2. Mean relative head displacement for Control and DP participants in the **a.** localiser scan, **b.** faces scan, **c.** flowers scan. Mean relative displacement for Controls and DPs was calculated to examine head movement. There were no significant differences in head movement between the groups in the localiser scan, $t(40) = 1.43$, $p = 0.162$, faces scan, $t(40) = 0.70$, $p = 0.488$ and flowers scan, $t(40) = 1.00$, $p = 0.323$. However, one control participant had a consistently high mean relative displacement across the 3 scans (Localiser scan: M = 0.26, Faces scan: M = 0.18, Flowers scan: M = 0.22), (Fig. 2a, b, c) and was excluded from further analysis.

Supplementary Table 2. Control and DP group peak voxel coordinates derived from the face > (scrambled + scene) contrast. rFFA – right fusiform face area, lFFA – left fusiform face area, rOFA – right occipital face area, lOFA – left occipital face area, rSTS – right superior temporal sulcus, lSTS – left superior temporal sulcus.

		Peak MNI coordinates		
ROI		x	y	z
rFFA	Control	44	-42	-20
	DP	46	-52	-22
lFFA	Control	-46	-60	-18
	DP	-42	-50	-20
rOFA	Control	46	-78	-12
	DP	48	-76	4
lOFA	Control	-44	-74	-12
	DP	-46	-82	2
rSTS	Control	44	-60	16
	DP	46	-68	12
lSTS	Control	-48	-68	20
	DP	-48	-70	16

Supplementary Table 3. Breakdown of the number of voxels and their corresponding anatomical structure identified as showing higher global functional connectivity in the Control>DP contrast for faces at voxel-wise threshold of uncorrected $p<0.005$, cluster-size FDR-corrected $p<0.05$

All voxels combined:
187 voxels (24%) covering 8% of atlas.TP l (Temporal Pole Left)
106 voxels (13%) covering 13% of atlas.Putamen r
58 voxels (7%) covering 17% of atlas.Amygdala r
52 voxels (7%) covering 16% of atlas.Amygdala l
43 voxels (5%) covering 3% of atlas.FOrb l (Frontal Orbital Cortex Left)
29 voxels (4%) covering 2% of atlas.IC l (Insular Cortex Left)
27 voxels (3%) covering 10% of atlas.Pallidum r
12 voxels (2%) covering 4% of atlas.Pallidum l
8 voxels (1%) covering 1% of atlas.Hippocampus r
5 voxels (1%) covering 1% of atlas.PP l (Planum Polare Left)
2 voxels (0%) covering 0% of atlas.IC r (Insular Cortex Right)
2 voxels (0%) covering 0% of atlas.Putamen l
257 voxels (33%) covering 0% of atlas.not-labeled

Supplementary Table 4. Breakdown of the number of voxels and their corresponding anatomical structure identified as showing higher global functional connectivity in the Control>DP contrast for faces at voxel-wise threshold of uncorrected $p<0.05$, cluster-size FDR-corrected $p<0.05$. The top 4 regions were selected for further seed-to-voxel functional connectivity analysis.

All voxels combined:
549 voxels (6%) covering 23% of atlas.TP l (Temporal Pole Left)
457 voxels (5%) covering 57% of atlas.Putamen r
382 voxels (4%) covering 29% of atlas.IC l (Insular Cortex Left)
307 voxels (4%) covering 40% of atlas.Hippocampus l
286 voxels (3%) covering 33% of atlas.Putamen l
263 voxels (3%) covering 16% of atlas.FOrb l (Frontal Orbital Cortex Left)
236 voxels (3%) covering 19% of atlas.Thalamus r
198 voxels (2%) covering 20% of atlas.CO l (Central Opercular Cortex Left)
179 voxels (2%) covering 43% of atlas.pSTG r (Superior Temporal Gyrus, posterior division Right)
147 voxels (2%) covering 21% of atlas.Hippocampus r

143 voxels (2%) covering 12% of atlas.pSMG r (Supramarginal Gyrus, posterior division Right)
141 voxels (2%) covering 10% of atlas.pMTG l (Middle Temporal Gyrus, posterior division Left)
132 voxels (2%) covering 40% of atlas.Amygdala l
122 voxels (1%) covering 39% of atlas.HG l (Heschl's Gyrus Left)
121 voxels (1%) covering 35% of atlas.Amygdala r
115 voxels (1%) covering 32% of atlas.PP l (Planum Polare Left)
113 voxels (1%) covering 8% of atlas.pMTG r (Middle Temporal Gyrus, posterior division Right)
106 voxels (1%) covering 39% of atlas.Pallidum r
97 voxels (1%) covering 7% of atlas.IC r (Insular Cortex Right)
93 voxels (1%) covering 31% of atlas.Pallidum l
91 voxels (1%) covering 20% of atlas.aMTG l (Middle Temporal Gyrus, anterior division Left)
88 voxels (1%) covering 16% of atlas.PT l (Planum Temporale Left)
77 voxels (1%) covering 19% of atlas.aMTG r (Middle Temporal Gyrus, anterior division Right)
75 voxels (1%) covering 19% of atlas.pSTG l (Superior Temporal Gyrus, posterior division Left)
70 voxels (1%) covering 5% of atlas.Thalamus l
66 voxels (1%) covering 2% of atlas.PreCG l (Precentral Gyrus Left)
56 voxels (1%) covering 20% of atlas.aSTG r (Superior Temporal Gyrus, anterior division Right)
52 voxels (1%) covering 8% of atlas.SMA L(Juxtapositional Lobule Cortex -formerly Supplementary Motor Cortex- Left)
52 voxels (1%) covering 2% of atlas.PC (Cingulate Gyrus, posterior division)
47 voxels (1%) covering 4% of atlas.toMTG r (Middle Temporal Gyrus, temporooccipital part Right)
47 voxels (1%) covering 11% of atlas.PT r (Planum Temporale Right)
44 voxels (1%) covering 4% of atlas.pSMG l (Supramarginal Gyrus, posterior division Left)
44 voxels (1%) covering 16% of atlas.HG r (Heschl's Gyrus Right)
38 voxels (0%) covering 2% of atlas.TP r (Temporal Pole Right)
32 voxels (0%) covering 4% of atlas.pTFusC r (Temporal Fusiform Cortex, posterior division Right)
32 voxels (0%) covering 6% of atlas.PO r (Parietal Operculum Cortex Right)
30 voxels (0%) covering 1% of atlas.AC (Cingulate Gyrus, anterior division)
27 voxels (0%) covering 10% of atlas.aSTG l (Superior Temporal Gyrus, anterior division Left)
24 voxels (0%) covering 7% of atlas.aITG l (Inferior Temporal Gyrus, anterior division Left)
22 voxels (0%) covering 7% of atlas.FO r (Frontal Operculum Cortex Right)
18 voxels (0%) covering 5% of atlas.PP r (Planum Polare Right)
16 voxels (0%) covering 3% of atlas.PO l (Parietal Operculum Cortex Left)
10 voxels (0%) covering 1% of atlas.toMTG l (Middle Temporal Gyrus, temporooccipital part Left)
10 voxels (0%) covering 2% of atlas.aPaHC r (Parahippocampal Gyrus, anterior division Right)
9 voxels (0%) covering 1% of atlas.pTFusC l (Temporal Fusiform Cortex, posterior division Left)
6 voxels (0%) covering 1% of atlas.Caudate r
5 voxels (0%) covering 6% of atlas.Accumbens r
4 voxels (0%) covering 1% of atlas.pPaHC l (Parahippocampal Gyrus, posterior division Left)
3 voxels (0%) covering 1% of atlas.aTFusC r (Temporal Fusiform Cortex, anterior division Right)
2 voxels (0%) covering 0% of atlas.FOrb r (Frontal Orbital Cortex Right)

2 voxels (0%) covering 0% of atlas.aPaHC l (Parahippocampal Gyrus, anterior division Left)
2 voxels (0%) covering 0% of atlas.LG l (Lingual Gyrus Left)
2 voxels (0%) covering 2% of atlas.Accumbens l
1 voxels (0%) covering 0% of atlas.Precuneous (Precuneous Cortex)
1 voxels (0%) covering 0% of atlas.pPaHC r (Parahippocampal Gyrus, posterior division Right)
1 voxels (0%) covering 0% of atlas.CO r (Central Opercular Cortex Right)
3300 voxels (38%) covering 1% of atlas.not-labeled

Supplementary Table 5. Breakdown of the number of voxels and their corresponding anatomical structure identified as showing higher connectivity to the left temporal pole in the Control>DP contrast for faces at voxel-wise threshold of uncorrected $p<0.005$, cluster-size FDR-corrected $p<0.05$

All voxels combined:
219 voxels (24%) covering 16% of atlas.pMTG r (Middle Temporal Gyrus, posterior division Right)
190 voxels (21%) covering 3% of atlas.FP l (Frontal Pole Left)
132 voxels (14%) covering 5% of atlas.SFG l (Superior Frontal Gyrus Left)
59 voxels (6%) covering 2% of atlas.SFG r (Superior Frontal Gyrus Right)
37 voxels (4%) covering 0% of atlas.FP r (Frontal Pole Right)
22 voxels (2%) covering 2% of atlas.pITG r (Inferior Temporal Gyrus, posterior division Right)
9 voxels (1%) covering 2% of atlas.aMTG r (Middle Temporal Gyrus, anterior division Right)
248 voxels (27%) covering 0% of atlas.not-labeled

Supplementary Table 6. Breakdown of the number of voxels and their corresponding anatomical structure identified as showing higher connectivity to the right putamen in the Control>DP contrast for faces at voxel-wise threshold of uncorrected $p<0.005$, cluster-size FDR-corrected $p<0.05$

All voxels combined:
312 voxels (14%) covering 23% of atlas.IC r (Insular Cortex Right)
305 voxels (14%) covering 23% of atlas.IC l (Insular Cortex Left)
173 voxels (8%) covering 39% of atlas.PT r (Planum Temporale Right)

137 voxels (6%) covering 10% of atlas.Thalamus l
124 voxels (6%) covering 14% of atlas.CO r (Central Opercular Cortex Right)
118 voxels (5%) covering 33% of atlas.PP l (Planum Polare Left)
109 voxels (5%) covering 9% of atlas.Thalamus r
86 voxels (4%) covering 28% of atlas.HG l (Heschl's Gyrus Left)
75 voxels (3%) covering 14% of atlas.PO r (Parietal Operculum Cortex Right)
64 voxels (3%) covering 15% of atlas.pSTG r (Superior Temporal Gyrus, posterior division Right)
50 voxels (2%) covering 18% of atlas.HG r (Heschl's Gyrus Right)
46 voxels (2%) covering 6% of atlas.aSMG r (Supramarginal Gyrus, anterior division Right)
34 voxels (2%) covering 4% of atlas.Hippocampus l
29 voxels (1%) covering 8% of atlas.PP r (Planum Polare Right)
16 voxels (1%) covering 0% of atlas.Brain-Stem
12 voxels (1%) covering 1% of atlas.Putamen r
11 voxels (0%) covering 1% of atlas.CO l (Central Opercular Cortex Left)
9 voxels (0%) covering 0% of atlas.PC (Cingulate Gyrus, posterior division)
9 voxels (0%) covering 1% of atlas.Putamen l
4 voxels (0%) covering 0% of atlas.PostCG r (Postcentral Gyrus Right)
4 voxels (0%) covering 1% of atlas.Amygdala l
3 voxels (0%) covering 1% of atlas.aSTG l (Superior Temporal Gyrus, anterior division Left)
2 voxels (0%) covering 0% of atlas.PT l (Planum Temporale Left)
521 voxels (23%) covering 0% of atlas.not-labeled

Supplementary Table 7. Breakdown of the number of voxels and their corresponding anatomical structure identified as showing higher connectivity to the left insular cortex in the Control>DP contrast for faces at voxel-wise threshold of uncorrected $p<0.005$, cluster-size FDR-corrected $p<0.05$

All voxels combined:
183 voxels (25%) covering 29% of atlas.Cuneal r (Cuneal Cortex Right)
146 voxels (20%) covering 3% of atlas.Precuneous (Precuneous Cortex)
119 voxels (16%) covering 15% of atlas.Putamen r
71 voxels (10%) covering 3% of atlas.OP l (Occipital Pole Left)
38 voxels (5%) covering 14% of atlas.Pallidum r
25 voxels (3%) covering 3% of atlas.ICC r (Intracalcarine Cortex Right)
15 voxels (2%) covering 1% of atlas.OP r (Occipital Pole Right)
11 voxels (1%) covering 2% of atlas.Cuneal l (Cuneal Cortex Left)

8 voxels (1%) covering 1% of atlas.IC r (Insular Cortex Right)
7 voxels (1%) covering 1% of atlas.ICC l (Intracalcarine Cortex Left)
1 voxels (0%) covering 1% of atlas.SCC r (Supracalcarine Cortex Right)
111 voxels (15%) covering 0% of atlas.not-labeled

Supplementary Table 8. Breakdown of the number of voxels and their corresponding anatomical structure identified as showing higher connectivity to the left hippocampus in the Control>DP contrast for faces at voxel-wise threshold of uncorrected $p<0.005$, cluster-size FDR-corrected $p<0.05$

All voxels combined:
120 voxels (32%) covering 29% of atlas.aMTG r (Middle Temporal Gyrus, anterior division Right)
95 voxels (25%) covering 34% of atlas.aSTG r (Superior Temporal Gyrus, anterior division Right)
65 voxels (17%) covering 5% of atlas.pMTG r (Middle Temporal Gyrus, posterior division Right)
13 voxels (3%) covering 3% of atlas.pSTG r (Superior Temporal Gyrus, posterior division Right)
1 voxels (0%) covering 0% of atlas.TP r (Temporal Pole Right)
1 voxels (0%) covering 0% of atlas.PP r (Planum Polare Right)
79 voxels (21%) covering 0% of atlas.not-labeled

Supplementary Table 9. Breakdown of the number of voxels and their corresponding anatomical structure identified as showing higher connectivity to right putamen in the Control>DP contrast for flowers at voxel-wise threshold of uncorrected $p<0.005$, cluster-size FDR-corrected $p<0.05$

All voxels combined:
201 voxels (22%) covering 23% of atlas.CO r (Central Opercular Cortex Right)
183 voxels (20%) covering 4% of atlas.PreCG r (Precentral Gyrus Right)
128 voxels (14%) covering 10% of atlas.IC r (Insular Cortex Right)
100 voxels (11%) covering 3% of atlas.PostCG r (Postcentral Gyrus Right)
309 voxels (34%) covering 0% of atlas.not-labeled

Supplementary Table 10. Breakdown of the number of voxels and their corresponding anatomical structure identified as showing different pattern of functional connectivity in the Control>DP contrast for faces at voxel-wise threshold of uncorrected $p<0.005$, cluster-size FDR-corrected $p<0.05$

All voxels combined:
225 voxels (21%) covering 26% of atlas.toMTG l (Middle Temporal Gyrus, temporooccipital part Left)
127 voxels (12%) covering 2% of atlas.Precuneous (Precuneous Cortex)
111 voxels (10%) covering 3% of atlas.Brain-Stem
109 voxels (10%) covering 13% of atlas.TOFusC r (Temporal Occipital Fusiform Cortex Right)
69 voxels (6%) covering 3% of atlas.TP l (Temporal Pole Left)
51 voxels (5%) covering 2% of atlas.iLOC l (Lateral Occipital Cortex, inferior division Left)
34 voxels (3%) covering 5% of atlas.Cuneal r (Cuneal Cortex Right)
13 voxels (1%) covering 1% of atlas.LG r (Lingual Gyrus Right)
7 voxels (1%) covering 0% of atlas.AG r (Angular Gyrus Right)
7 voxels (1%) covering 1% of atlas.OFusG r (Occipital Fusiform Gyrus Right)
4 voxels (0%) covering 1% of atlas.aSTG l (Superior Temporal Gyrus, anterior division Left)
4 voxels (0%) covering 0% of atlas.pSMG r (Supramarginal Gyrus, posterior division Right)
3 voxels (0%) covering 0% of atlas.toITG l (Inferior Temporal Gyrus, temporooccipital part Left)
1 voxels (0%) covering 0% of atlas.pSMG l (Supramarginal Gyrus, posterior division Left)
1 voxels (0%) covering 0% of atlas.aTFusC l (Temporal Fusiform Cortex, anterior division Left)
323 voxels (30%) covering 0% of atlas.not-labeled

Supplementary Table 11. Breakdown of the number of voxels and their corresponding anatomical structure identified as showing different pattern of functional connectivity in the Control>DP contrast for flowers at voxel-wise threshold of uncorrected $p<0.005$, cluster-size FDR-corrected $p<0.05$

All voxels combined:
130 voxels (19%) covering 2% of atlas.Precuneous (Precuneous Cortex)
97 voxels (14%) covering 6% of atlas.LG r (Lingual Gyrus Right)
83 voxels (12%) covering 4% of atlas.Cereb1 l (Cerebelum Crus1 Left)
45 voxels (7%) covering 3% of atlas.Cereb6 l (Cerebelum 6 Left)
34 voxels (5%) covering 5% of atlas.Cuneal r (Cuneal Cortex Right)
25 voxels (4%) covering 1% of atlas.Brain-Stem
22 voxels (3%) covering 1% of atlas.Cereb8 l (Cerebelum 8 Left)

8 voxels (1%) covering 2% of atlas.Amygdala r
5 voxels (1%) covering 1% of atlas.TOFusC r (Temporal Occipital Fusiform Cortex Right)
5 voxels (1%) covering 1% of atlas.OFusG l (Occipital Fusiform Gyrus Left)
3 voxels (0%) covering 1% of atlas.pPaHC r (Parahippocampal Gyrus, posterior division Right)
2 voxels (0%) covering 0% of atlas.Hippocampus r
1 voxels (0%) covering 0% of atlas.TOFusC l (Temporal Occipital Fusiform Cortex Left)
219 voxels (32%) covering 0% of atlas.not-labeled

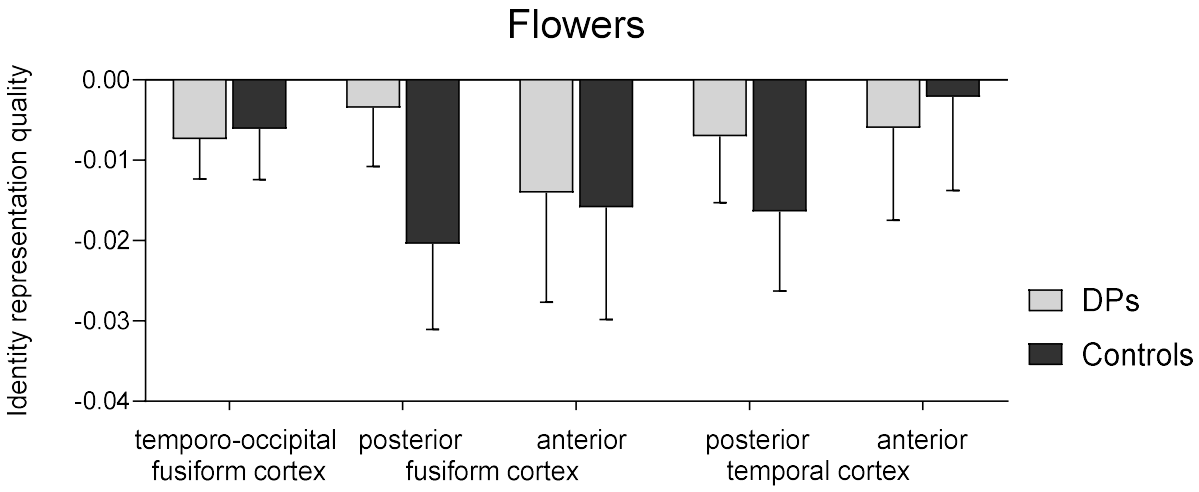

Supplementary Figure 3. Mean difference of within > between flower identity representations in Controls and DPs. Error bars represent ± 1 SEM.

Appendix A.3. Chapter 6.

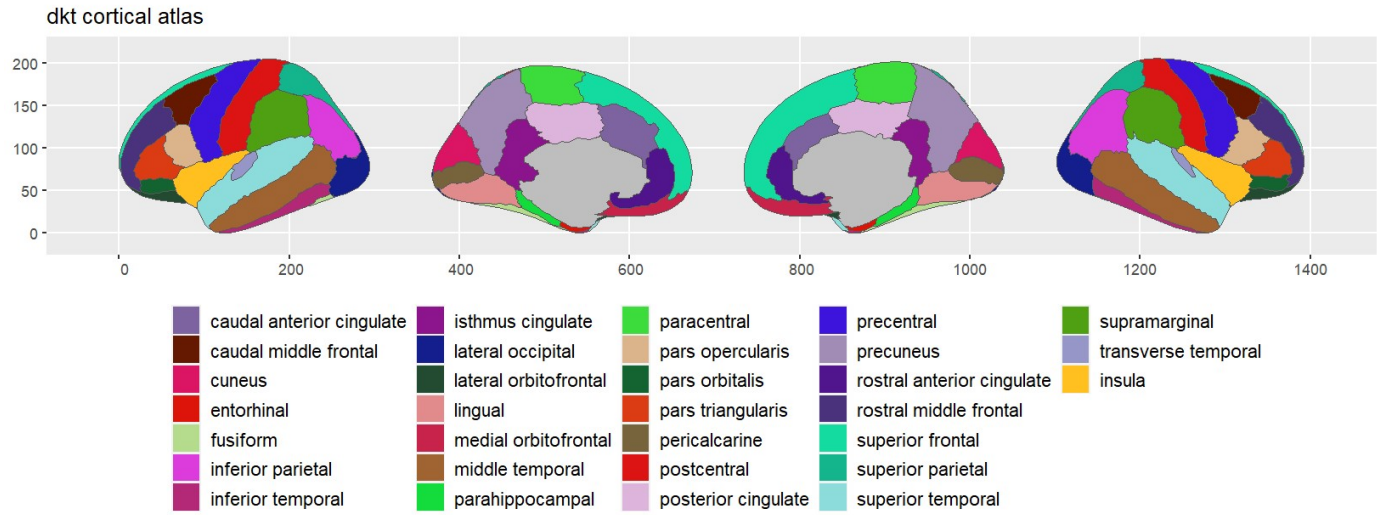

Supplementary Figure 1. 62 regions (31 in each hemisphere) from the Desikan-Killiany-Tourville (DKT) atlas used as nodes for the network connectome analysis

Supplementary Table 1. Region-level mean node degree values in Control and DP groups and the Control > DP difference

DKT region	Left hemisphere			Right hemisphere		
	Mean degree					
	Control	DP	Control > DP	Control	DP	Control > DP
caudal anterior cingulate	2.53	1.86	0.66	3.42	2.14	1.28
caudal middle frontal	3.47	3.14	0.34	3.79	3.23	0.56
cuneus	4.84	3.36	1.48	4.68	4.27	0.41
entorhinal	3.58	3.14	0.44	3.37	2.55	0.82
fusiform	5.37	5.23	0.14	5.05	4.86	0.19
inferior parietal	6.68	6.59	0.09	7.00	6.95	0.05
inferior temporal	6.89	6.09	0.80	7.79	6.77	1.02
isthmus cingulate	3.84	3.14	0.71	3.21	3.00	0.21
lateral occipital	6.16	6.09	0.07	6.58	6.55	0.03
lateral orbitofrontal	9.37	7.77	1.60	10.32	9.64	0.68
lingual	7.37	6.77	0.60	7.58	6.41	1.17
medial orbitofrontal	4.84	5.68	-0.84	4.16	4.41	-0.25
middle temporal	5.16	5.14	0.02	5.21	5.50	-0.29
parahippocampal	5.74	5.23	0.51	5.74	4.95	0.78
paracentral	5.95	5.23	0.72	4.58	4.68	-0.10
pars opercularis	4.37	4.05	0.32	5.26	4.32	0.94
pars orbitalis	1.37	1.14	0.23	2.05	2.05	0.01
pars triangularis	2.68	2.36	0.32	2.00	2.64	-0.64
pericalcarine	4.74	4.23	0.51	2.68	2.18	0.50
postcentral	5.95	5.50	0.45	5.68	5.50	0.18
posterior cingulate	5.16	4.14	1.02	4.84	3.91	0.93
precentral	8.79	8.50	0.29	8.74	8.68	0.06
precuneus	10.58	10.32	0.26	9.37	8.50	0.87
rostral anterior cingulate	6.79	6.64	0.15	5.16	5.32	-0.16
rostral middle frontal	3.37	2.95	0.41	3.47	3.14	0.34
superior frontal	15.11	13.18	1.92	15.53	14.64	0.89
superior parietal	5.79	5.27	0.52	9.89	9.09	0.80
superior temporal	12.16	11.82	0.34	11.26	11.09	0.17
supramarginal	4.68	4.41	0.28	5.37	5.18	0.19
transverse temporal	0.95	1.18	-0.23	0.63	0.68	-0.05
insula	6.21	6.32	-0.11	8.89	7.82	1.08

Supplementary Table 2. Region-level mean node clustering coefficient values in Control and DP groups and the Control > DP difference

DKT region	Left hemisphere			Right hemisphere		
	Mean clustering coefficient					
	Control	DP	Control > DP	Control	DP	Control > DP
caudal anterior cingulate	0.72	0.53	0.19	0.82	0.70	0.12
caudal middle frontal	0.65	0.69	-0.04	0.64	0.62	0.02
cuneus	0.63	0.59	0.04	0.46	0.40	0.06
entorhinal	0.56	0.55	0.00	0.52	0.49	0.03
fusiform	0.56	0.54	0.02	0.60	0.51	0.09
inferior parietal	0.53	0.49	0.04	0.59	0.57	0.03
inferior temporal	0.51	0.52	-0.02	0.49	0.51	-0.02
isthmus cingulate	0.47	0.33	0.14	0.48	0.40	0.08
lateral occipital	0.40	0.45	-0.04	0.43	0.39	0.04
lateral orbitofrontal	0.31	0.34	-0.04	0.29	0.30	-0.01
lingual	0.43	0.31	0.12	0.34	0.27	0.07
medial orbitofrontal	0.73	0.65	0.08	0.63	0.65	-0.03
middle temporal	0.76	0.68	0.08	0.76	0.71	0.06
parahippocampal	0.44	0.41	0.02	0.41	0.40	0.01
paracentral	0.50	0.42	0.08	0.59	0.44	0.15
pars opercularis	0.59	0.45	0.14	0.47	0.47	0.00
pars orbitalis	0.30	0.36	-0.07	0.56	0.49	0.07
pars triangularis	0.45	0.39	0.06	0.47	0.49	-0.02
pericalcarine	0.64	0.38	0.27	0.70	0.64	0.05
postcentral	0.49	0.51	-0.02	0.73	0.68	0.05
posterior cingulate	0.60	0.60	0.01	0.51	0.45	0.07
precentral	0.31	0.31	0.00	0.38	0.33	0.05
precuneus	0.22	0.19	0.03	0.25	0.24	0.01
rostral anterior cingulate	0.56	0.63	-0.07	0.71	0.73	-0.02
rostral middle frontal	0.66	0.73	-0.08	0.65	0.67	-0.02
superior frontal	0.22	0.23	-0.01	0.23	0.22	0.01
superior parietal	0.46	0.44	0.02	0.36	0.36	0.01
superior temporal	0.29	0.26	0.03	0.37	0.35	0.02
supramarginal	0.66	0.62	0.04	0.78	0.76	0.02
transverse temporal	0.16	0.27	-0.11	0.16	0.14	0.02
insula	0.43	0.38	0.06	0.41	0.36	0.05

References

Akarca, D., Vértes, P. E., Bullmore, E. T., Baker, K., Gathercole, S. E., Holmes, J., Kievit, R. A., Manly, T., Bathelt, J., Bennett, M., Bignardi, G., Bishop, S., Bottacin, E., Bridge, L., Brkic, D., Bryant, A., Butterfield, S., Byrne, E. M., Crickmore, G., … Astle, D. E. (2021). A generative network model of neurodevelopmental diversity in structural brain organization. Nature Communications, 12(1).

Alais, D., Xu, Y., Wardle, S. G., & Taubert, J. (2021). A shared mechanism for facial expression in human faces and face pareidolia. *Proceedings of the Royal Society B: Biological Sciences*, *288*(1954).

Andersson, J. L. R., Skare, S., & Ashburner, J. (2003). How to correct susceptibility distortions in spin-echo echo-planar images: Application to diffusion tensor imaging. *NeuroImage*, *20*(2), 870–888.

Andrews, T. J., Watson, D. M., Rice, G. E., & Hartley, T. (2015). Low-level properties of natural images predict topographic patterns of neural response in the ventral visual pathway. *Journal of Vision*, *15*(7), 1–12.

Anzellotti, S., Fairhall, S. L., & Caramazza, A. (2014). Decoding representations of face identity that are tolerant to rotation. *Cerebral Cortex*, *24*(8), 1988–1995.

Avidan, G., Hasson, U., Malach, R., & Behrmann, M. (2005). Detailed exploration of face-related processing in congenital prosopagnosia: 2. Functional neuroimaging findings. *Journal of Cognitive Neuroscience*, *17*(7), 1150–1167.

Avidan, G., Tanzer, M., Hadj-Bouziane, F., Liu, N., Ungerleider, L. G., & Behrmann, M. (2014). Selective dissociation between core and extended regions of the face processing network in congenital prosopagnosia. *Cerebral Cortex*, *24*(6), 1565–1578.

Axelrod, V., & Yovel, G. (2015). Successful decoding of famous faces in the fusiform face area. *PLoS ONE*, *10*(2), e0117126.

Barton, J. J. S. (2008). Structure and function in acquired prosopagnosia: lessons from a series of 10 patients with brain damage. *Journal of Neuropsychology*, *2*(1), 197–225.

Barton, J. J. S., Albonico, A., Susilo, T., Duchaine, B., & Corrow, S. L. (2019). Object recognition in acquired and developmental prosopagnosia. *Cognitive Neuropsychology*, *36*(1–2), 54–84.

Barton, J. J. S., & Corrow, S. L. (2016). The problem of being bad at faces. *Neuropsychologia*, *89*, 119–124.

Basser, P. J., Pajevic, S., Pierpaoli, C., Duda, J., & Aldroubi, A. (2000). In vivo fiber tractography using DT-MRI data. *Magnetic resonance in medicine*, *44*(4), 625-632.

Bate, S., & Bennetts, R. (2015). The independence of expression and identity in face-processing: evidence from neuropsychological case studies. *Frontiers in Psychology*, *6*, 770.

Bate, S., Bennetts, R., Hasshim, N., Portch, E., Murray, E., Burns, E., & Dudfield, G. (2019). The limits of super recognition: An other-ethnicity effect in individuals with extraordinary face recognition skills. *Journal of Experimental Psychology: Human Perception and Performance*, *45*(3), 0–363.

Bate, S., Bennetts, R. J., Tree, J. J., Adams, A., & Murray, E. (2019). The domain-specificity of face matching impairments in 40 cases of developmental prosopagnosia. *Cognition*, *192*, 104031.

Bate, S., & Tree, J. J. (2017). The definition and diagnosis of developmental prosopagnosia. In *Quarterly Journal of Experimental Psychology* (Vol. 70, Issue 2, pp. 193–200). Psychology Press Ltd.

Bathelt, J., Scerif, G., Nobre, A. C., & Astle, D. E. (2019). Whole-brain white matter organization, intelligence, and educational attainment. Trends in neuroscience and education, 15, 38-47.

Behrmann, M., Avidan, G., Marotta, J. J., & Kimchi, R. (2005). Detailed exploration of face-related processing in congenital prosopagnosia: 1. Behavioral findings. *Journal of Cognitive Neuroscience*, *17*(7), 1130–1149.

Behrmann, M., & Plaut, D. C. (2013). Distributed circuits, not circumscribed centers, mediate visual recognition. *Trends in Cognitive Sciences*, *17*(5), 210–219.

Behrmann, M., & Plaut, D. C. (2014). Bilateral hemispheric processing of words and faces: Evidence from word impairments in prosopagnosia and face impairments in pure alexia. *Cerebral Cortex*, *24*(4), 1102–1118.

Behzadi, Y., Restom, K., Liau, J., & Liu, T. T. (2007). A component based noise correction method (CompCor) for BOLD and perfusion based fMRI. *NeuroImage*, *37*(1), 90–101.

Biotti, F., & Cook, R. (2016). Impaired perception of facial emotion in developmental prosopagnosia. *Cortex*, *81*, 126–136.

Biotti, F., Gray, K. L. H., & Cook, R. (2017). Impaired body perception in developmental prosopagnosia. *Cortex*, *93*, 41–49.

Biotti, F., Gray, K. L. H., & Cook, R. (2019). Is developmental prosopagnosia best characterised as an apperceptive or mnemonic condition? *Neuropsychologia*, *124*, 285–298.

Bishop, D. V. M. (1997). Cognitive neuropsychology and developmental disorders: Uncomfortable bedfellows. *Quarterly Journal of Experimental Psychology Section A: Human Experimental Psychology*, *50*(4), 899–923.

Blom, J. D., ter Meulen, B. C., Dool, J., & ffytche, D. H. (2021). A century of prosopometamorphopsia studies. In *Cortex* (Vol. 139, pp. 298–308). Masson SpA.

Bornstein, B., Sroka, H., & Munitz, H. (1969). Prosopagnosia with animal face agnosia. *Cortex*, *5*(2), 164–169.

Bothwell, R. K., Brigham, J. C., & Malpass, R. S. (1989). Cross-racial identification. *Personality and Social Psychology Bulletin*, *15*(1), 19–25.

Bracci, S., Ritchie, J. B., & Beeck, H. Op De. (2017). Neuropsychologia On the partnership between neural representations of object categories and visual features in the ventral visual pathway. *Neuropsychologia*, *105*(June), 153–164.

Bracci, S., Ritchie, J. B., Kalfas, I., & Op de Beeck, H. P. (2019). The ventral visual pathway represents animal appearance over animacy, unlike human behavior and deep neural networks. *Journal of Neuroscience*, *39*(33), 6513–6525.

Brincat, S. L., & Connor, C. E. (2004). Underlying principles of visual shape selectivity in posterior inferotemporal cortex. *Nature Neuroscience*, *7*(8), 880–886.

Burns, E. J., Gaunt, E., Kidane, B., Hunter, L., & Pulford, J. (2022). A new approach to diagnosing and researching developmental prosopagnosia: Excluded cases are impaired too. *Behavior Research Methods*, 1–24.

Caldara, R., Seghier, M. L., Rossion, B., Lazeyras, F., Michel, C., & Hauert, C. A. (2006). The fusiform face area is tuned for curvilinear patterns with more high-contrasted elements in the upper part. *NeuroImage*, *31*(1), 313–319.

Carey, S., & Diamond, R. (1977). From piecemeal to configurational representation of faces. *Science*, *195*(4275), 312-314.

Cenac, Z., Biotti, F., Gray, K. L. H., & Cook, R. (2019). Does developmental prosopagnosia impair identification of other-ethnicity faces? *Cortex*, *119*, 12–19.

Chatterjee, G., & Nakayama, K. (2012). Normal facial age and gender perception in developmental prosopagnosia. *Cognitive Neuropsychology*, *29*(5–6), 482–502.

Chien, S. H.-L., Wang, J.-F., & Huang, T.-R. (2016). Developing the own-race advantage in 4-, 6-, and 9-month-old Taiwanese infants: A perceptual learning perspective. *Frontiers in Psychology*, *7*, 1606.

Coggan, D. D., Baker, D. H., & Andrews, T. J. (2016). The role of visual and semantic properties in the emergence of category-specific patterns of neural response in the human brain. *ENeuro*, *3*(4).

Coggan, D. D., Giannakopoulou, A., Ali, S., Goz, B., Watson, D. M., Hartley, T., Baker, D. H., & Andrews, T. J. (2019). A data-driven approach to stimulus selection reveals an image-based representation of objects in high-level visual areas. *Human Brain Mapping*, *40*(16), 4716–4731.

Coggan, D. D., Liu, W., Baker, D. H., & Andrews, T. J. (2016). Category-selective patterns of neural response in the ventral visual pathway in the absence of categorical information. *NeuroImage*, *135*(May), 107–114.

Collins, J. A., Koski, J. E., & Olson, I. R. (2016). More than meets the eye: The merging of perceptual and conceptual knowledge in the anterior temporal face area. *Frontiers in Human Neuroscience*, *10*(MAY2016).

Connolly, A. C., Swaroop Guntupalli, J., Gors, J., Hanke, M., Halchenko, Y. O., Wu, Y. C., Abdi, H., & Haxby, J. V. (2012). The representation of biological classes in the human brain. *Journal of Neuroscience*, *32*(8), 2608–2618.

Contreras, J. A., Goñi, J., Risacher, S. L., Sporns, O., & Saykin, A. J. (2015). The structural and functional connectome and prediction of risk for cognitive impairment in older adults. Current behavioral neuroscience reports, 2(4), 234-245.

Cook, R., & Biotti, F. (2016). Developmental prosopagnosia. *Current Biology*, *26*(8), R312–R313.

Crawford, J. R., & Garthwaite, P. H. (2005). Testing for suspected impairments and dissociations in single-case studies in neuropsychology: evaluation of alternatives using monte carlo simulations and revised tests for dissociations. *Neuropsychology*, *19*(3), 318–331.

Dalrymple, K. A., Garrido, L., & Duchaine, B. (2014). Dissociation between face perception and face memory in adults, but not children, with developmental prosopagnosia. *Developmental Cognitive Neuroscience*, *10*, 10–20.

Dalrymple, K. A., & Palermo, R. (2016). Guidelines for studying developmental prosopagnosia in adults and children. *Wiley Interdisciplinary Reviews: Cognitive Science*, *7*(1), 73–87.

Davies-Thompson, J., Pancaroglu, R., & Barton, J. (2014). Acquired prosopagnosia: structural basis and processing impairments. *Frontiers in Bioscience-Elite*, *6*(1), 159–174.

Davis, J. M., McKone, E., Dennett, H., O'Connor, K. B., O'Kearney, R., & Palermo, R. (2011). Individual differences in the ability to recognise facial identity are associated with social anxiety. *PLoS ONE*, *6*(12).

de Haan, E. H. F., & Campbell, R. (1991). A fifteen year follow-up of a case of developmental prosopagnosia. *Cortex*, *27*(4), 489–509.

de Renzi, E., Faglionii, P., Grossi, D., & Nichelli, P. (1991). Apperceptive and associative forms of prosopagnosia. *Cortex*, *27*(2), 213–221.

DeBruine, L., & Jones, B. (2017). Face Research Lab London Set. Retrieved from Figshare: https://figshare.com/articles/dataset/Face_Research_Lab_London_Set/5047666

Decramer, T., Premereur, E., Zhu, Q., van Paesschen, W., van Loon, J., Vanduffel, W., Taubert, J., Janssen, P., & Theys, T. (2021). Single-unit recordings reveal the selectivity of a human face area. *The Journal of Neuroscience*, *41*(45), 9340–9349.

Dennett, H. W., McKone, E., Tavashmi, R., Hall, A., Pidcock, M., Edwards, M., & Duchaine, B. (2012). The Cambridge Car Memory Test: A task matched in format to the Cambridge Face Memory Test, with norms, reliability, sex differences, dissociations from face memory, and expertise effects. *Behavior Research Methods*, *44*(2), 587–605.

Dhamala, E., Jamison, K. W., Jaywant, A., Dennis, S., & Kuceyeski, A. (2021). Distinct functional and structural connections predict crystallised and fluid cognition in healthy adults. *Human Brain Mapping*, *42*(10), 3102–3118.

Downing, P. E., Jiang, Y., Shuman, M., & Kanwisher, N. (2001). A Cortical Area Selective for Visual Processing of the Human Body. *Science*, *293*(5539), 2470–2473.

Dowsett, A. J., & Burton, A. M. (2015). Unfamiliar face matching: Pairs out-perform individuals and provide a route to training. *British Journal of Psychology*, *106*(3), 433–445.

Duchaine, B. C., & Nakayama, K. (2006). Developmental prosopagnosia: a window to content-specific face processing. *Current Opinion in Neurobiology*, *16*(2), 166–173.

Duchaine, B. C., Yovel, G., Butterworth, E. J., & Nakayama, K. (2006). Prosopagnosia as an impairment to face-specific mechanisms: Elimination of the alternative hypotheses in a developmental case. *Cognitive Neuropsychology*, *23*(5), 714–747.

Duchaine, B., Germine, L., & Nakayama, K. (2007). Family resemblance: Ten family members with prosopagnosia and within-class object agnosia. *Cognitive Neuropsychology*, *24*(4), 419–430.

Duchaine, B., & Nakayama, K. (2006). The Cambridge Face Memory Test: Results for neurologically intact individuals and an investigation of its validity using inverted face stimuli and prosopagnosic participants. *Neuropsychologia*, *44*(4), 576–585.

Elbich, D. B., & Scherf, K. S. (2017). Beyond the FFA: Brain-behavior correspondences in face recognition abilities. *NeuroImage*, *147*, 409–422.

Epihova, G., Cook, R., & Andrews, T. J. (2022). Recognition of pareidolic objects in developmental prosopagnosic and neurotypical individuals. *Cortex*, *153*, 21–31.

Epstein, R., & Kanwisher, N. (1998). A cortical representation of the local visual environment. *Nature*, *392*(6676), 598–601.

Esins, J., Schultz, J., Stemper, C., & Bülthoff, I. (2014). Do congenital prosopagnosia and the other-race effect affect the same face recognition mechanisms? *Frontiers in Human Neuroscience*, *8*, 759.

Esins, J., Schultz, J., Stemper, C., Kennerknecht, I., & Bülthoff, I. (2016). Face perception and test reliabilities in congenital prosopagnosia in seven tests. *I-Perception*, *7*(1), 2041669515625797.

Farahani, F. v., Karwowski, W., & Lighthall, N. R. (2019). Application of graph theory for identifying connectivity patterns in human brain networks: A systematic review. *Frontiers in Neuroscience*, *13*(585).

Fine, D. R. (2012). A life with prosopagnosia. *Cognitive Neuropsychology*, *29*(5–6), 354–359.

Frank, D., Gray, O., & Montaldi, D. (2020). SOLID-Similar object and lure image database. *Behavior Research Methods*, *52*(1), 151–161.

Fry, R., Wilmer, J. B., Xie, I., Verfaellie, M., & DeGutis, J. (2020). *Evidence for normal novel object recognition abilities in developmental prosopagnosia*.

Furl, N., Garrido, L., Dolan, R. J., Driver, J., & Duchaine, B. (2011). Fusiform gyrus face selectivity relates to individual differences in facial recognition ability. *Journal of Cognitive Neuroscience*, *23*(7), 1723–1740.

Garrido, L., Duchaine, B., & DeGutis, J. (2018). Association vs dissociation and setting appropriate criteria for object agnosia. *Cognitive Neuropsychology*, *35*(1–2), 55–58.

Germine, L., Cashdollar, N., Düzel, E., & Duchaine, B. (2011). A new selective developmental deficit: Impaired object recognition with normal face recognition. *Cortex*, *47*(5), 598–607.

Geskin, J., & Behrmann, M. (2018). Congenital prosopagnosia without object agnosia? A literature review. *Cognitive Neuropsychology*, *35*(1–2), 4–54.

Gobbini, M. I., & Haxby, J. v. (2007). Neural systems for recognition of familiar faces. *Neuropsychologia*, *45*(1), 32–41.

Goldstein, A. G., & Chance, J. E. (1985). Effects of training on Japanese face recognition: Reduction of the other-race effect. *Bulletin of the Psychonomic Society*, *23*(3), 211–214.

Gomez, J., Pestilli, F., Witthoft, N., Golarai, G., Liberman, A., Poltoratski, S., Yoon, J., & Grill-Spector, K. (2015). Functionally defined white matter reveals segregated pathways in human ventral temporal cortex associated with category-specific processing. *Neuron*, *85*(1), 216–227.

Granovetter, M. C., Robert, S., Ettensohn, L., & Behrmann, M. (2022). With childhood hemispherectomy, one hemisphere can support-but is suboptimal for-word and face recognition recordings. *Proceedings of the National Academy of Sciences*, *119*(44), e2212936119.

Gray, K. L. H., Biotti, F., & Cook, R. (2019). Evaluating object recognition ability in developmental prosopagnosia using the Cambridge Car Memory Test. *Cognitive Neuropsychology*, *36*(1–2), 1–8.

Gray, K. L. H., Bird, G., & Cook, R. (2017). Robust associations between the 20-item prosopagnosia index and the Cambridge Face Memory Test in the general population. *Royal Society Open Science*, *4*(3), 160923.

Gray, K. L. H., & Cook, R. (2018). Should developmental prosopagnosia, developmental body agnosia, and developmental object agnosia be considered independent neurodevelopmental conditions? *Cognitive Neuropsychology*, *35*(1–2), 59–62.

Greve, D. N., & Fischl, B. (2009). Accurate and robust brain image alignment using boundary-based registration. *NeuroImage*, *48*(1), 63–72.

Grootswagers, T., Zhou, I., Robinson, A. K., Hebart, M. N., & Carlson, T. A. (2022). Human EEG recordings for 1,854 concepts presented in rapid serial visual presentation streams. *Scientific Data*, *9*(1), 3.

Grossi, D., Soricelli, A., Ponari, M., Salvatore, E., Quarantelli, M., Prinster, A., & Trojano, L. (2014). Structural connectivity in a single case of progressive prosopagnosia: The role of the right inferior longitudinal fasciculus. *Cortex*, *56*, 111–120.

Guye, M., Bettus, G., Bartolomei, F., & Cozzone, P. J. (2010). Graph theoretical analysis of structural and functional connectivity MRI in normal and pathological brain networks. In *Magnetic Resonance Materials in Physics, Biology and Medicine* (Vol. 23, Issue 5, pp. 409–421).

Hadjikhani, N., & De Gelder, B. (2002). Neural basis of prosopagnosia: An fMRI study. *Human Brain Mapping*, *16*(3), 176–182.

Harris, R. J., Rice, G. E., Young, A. W., & Andrews, T. J. (2015). Distinct but overlapping patterns of response to words and faces in the fusiform gyrus. *Cerebral Cortex*, *26*(7), 3161–3168.

Hasson, U., Avidan, G., Deouell, L. Y., Bentin, S., & Malach, R. (2003). Face-selective activation in a congenital prosopagnosic subject. *Journal of Cognitive Neuroscience*, *15*(3), 419–431.

Haxby, J. v., Gobbini, M. I., Furey, M. L., Ishai, A., Schouten, J. L., & Pietrini, P. (2001a). Distributed and Overlapping Representations of Faces and Objects in Ventral Temporal Cortex. *Science*, *293*(5539), 2425–2430.

Haxby, J. V., Gobbini, M. I., Furey, M. L., Ishai, A., Schouten, J. L., & Pietrini, P. (2001b). Distributed and overlapping representations of faces and objects in ventral temporal cortex. *Science*, *293*(5539), 2425–2430.

Haxby, J. V., Grady, C. L., Horwitz, Barry., Ungerleider, L. G., Mishkin, M., Carson, R. E., Herscovitch, P., Schapiro, M. B., & Rapoport, S. I. (1991). Dissociation of object and spatial visual processing pathways in human extrastriate cortex. *Proceedings of the National Academy of Sciences of the United States of America*, *88*(5), 1621–1625.

Haxby, J. v., Hoffman, E. A., & Gobbini, M. I. (2000). The distributed human neural system for face perception. *Trends in Cognitive Sciences*, *4*(6), 223–233.

Hebart, M. N., Contier, O., Teichmann, L., Rockter, A. H., Zheng, C. Y., Kidder, A., Corriveau, A., Vaziri-Pashkam, & Baker, &. (2022). THINGS-data: A multimodal collection of large-scale datasets for investigating object representations in brain and behavior. *BioRxiv*.

Hecaen, H., & Angelergues, R. (1962). Agnosia for faces (prosopagnosia). *Archives of Neurology*, *7*(2), 92–100.

Herbet, G., Zemmoura, I., & Duffau, H. (2018). Functional anatomy of the inferior longitudinal fasciculus: from historical reports to current hypotheses. *Frontiers in Neuroanatomy*, *12*, 77.

Honey, C. J., Sporns, O., Cammoun, L., Gigandet, X., Thiran, J. P., Meuli, R., & Hagmann, P. (2009). Predicting human resting-state functional connectivity from structural connectivity. *Proceedings of the National Academy of Sciences*, *106*(6), 2035–2040.

Huang, L., Song, Y., Li, J., Zhen, Z., Yang, Z., & Liu, J. (2014). Individual differences in cortical face selectivity predict behavioral performance in face recognition. *Frontiers in Human Neuroscience*, *8*, 483.

Jenkinson, M., Bannister, P., Brady, M., & Smith, S. (2002). Improved Optimization for the Robust and Accurate Linear Registration and Motion Correction of Brain Images. *NeuroImage*, *17*(2), 825–841.

Jeong, S. K., & Xu, Y. (2016). Behaviorally relevant abstract object identity representation in the human parietal cortex. *Journal of Neuroscience*, *36*(5), 1607–1619.

Jiahui, G., Yang, H., & Duchaine, B. (2018). Developmental prosopagnosics have widespread selectivity reductions across category-selective visual cortex. *Proceedings of the National Academy of Sciences*, *115*(28), E6418–E6427.

Jiang, X., Bollich, A., Cox, P., Hyder, E., James, J., Gowani, S. A., Hadjikhani, N., Blanz, V., Manoach, D. S., Barton, J. J. S., Gaillard, W. D., & Riesenhuber, M. (2013). A quantitative link between face discrimination deficits and neuronal selectivity for faces in autism. *NeuroImage: Clinical*, *2*(1), 320–331.

Kanwisher, N. (2010). Functional specificity in the human brain: A window into the functional architecture of the mind. *Proceedings of the National Academy of Sciences*, *107*(25), 11163–11170.

Kanwisher, N., Mcdermott, J., & Chun, M. M. (1997). The fusiform face area: a module in human extrastriate cortex specialized for face perception. *Journal of Neuroscience*, *17*(11), 4302–4311.

Kanwisher, N., Stanley, D., & Harris, A. (1999). The fusiform face area is selective for faces not animals. *Neuroreport*, *10*(1), 183–187.

Kanwisher, N., & Yovel, G. (2006). The fusiform face area: a cortical region specialized for the perception of faces. *Philosophical Transactions of the Royal Society B: Biological Sciences*, *361*(1476), 2109–2128.

Keys, R. T., Taubert, J., & Wardle, S. G. (2021). A visual search advantage for illusory faces in objects. *Attention, Perception, & Psychophysics*, 1–12.

Kiani, R., Esteky, H., Mirpour, K., & Tanaka, K. (2007). Object category structure in response patterns of neuronal population in monkey inferior temporal cortex. *Journal of Neurophysiology*, *97*(6), 4296–4309.

Klargaard, S. K., Starrfelt, R., & Gerlach, C. (2018). Inversion effects for faces and objects in developmental prosopagnosia: A case series analysis. *Neuropsychologia*, *113*, 52-60.

Klein, A., & Tourville, J. (2012). 101 labeled brain images and a consistent human cortical labeling protocol. *Frontiers in Neuroscience*, *6*(171).

Kokje, E., Bindemann, M., & Megreya, A. M. (2018). Cross-race correlations in the abilities to match unfamiliar faces. *Acta Psychologica*, *185*, 13–21.

Konkle, T., & Oliva, A. (2012). A real-world size organization of object responses in occipitotemporal cortex. *Neuron*, *74*(6), 1114–1124.

Kriegeskorte, N., Formisano, E., Sorger, B., & Goebel, R. (2007). Individual faces elicit distinct response patterns in human anterior temporal cortex. *Proceedings of the National Academy of Sciences*, *105*(51), 20600–20605.

Kriegeskorte, N., Mur, M., Ruff, D. A., Kiani, R., Bodurka, J., Esteky, H., Tanaka, K., & Bandettini, P. A. (2008). Matching categorical object representations in inferior temporal cortex of man and monkey. *Neuron*, *60*(6), 1126–1141.

Landis, T., Cummings, J. L., Christens, L., Bogen4, J. E., & Imhof, H.-G. (1986). Are unilateral right posterior cerebral lesions sufficient to cause prosopagnosia? Clinical and radiological findings in six additional patients. *Cortex*, *22*(2), 243–252.

Latini, F., Mårtensson, J., Larsson, E. M., Fredrikson, M., Åhs, F., Hjortberg, M., ... & Ryttlefors, M. (2017). Segmentation of the inferior longitudinal fasciculus in the human brain: A white matter dissection and diffusion tensor tractography study. *Brain Research*, *1675*, 102-115.

Langner, O., Dotsch, R., Bijlstra, G., Wigboldus, D. H. J., Hawk, S. T., & van Knippenberg, A. (2010). Presentation and validation of the Radboud Faces Database. *Cognition and Emotion*, *24*(8), 1377–1388.

Levakov, G., Sporns, O., & Avidan, G. (2022). Fine-scale dynamics of functional connectivity in the face processing network during movie watching. *BioRxiv*.

Liu, J., Li, J., Feng, L., Li, L., Tian, J., & Lee, K. (2014). Seeing Jesus in toast: neural and behavioral correlates of face pareidolia. *Cortex*, *53*, 60–77.

Liu, Z. Q., Betzel, R. F., & Misic, B. (2022). Benchmarking functional connectivity by the structure and geometry of the human brain. *Network Neuroscience*, *6*(4), 937–949.

Loffler, G., Yourganov, G., Wilkinson, F., & Wilson, H. R. (2005). fMRI evidence for the neural representation of faces. Nature neuroscience, 8(10), 1386-1391.

Long, B., Yu, C.-P., & Konkle, T. (2018). Mid-level visual features underlie the high-level categorical organization of the ventral stream. *Proceedings of the National Academy of Sciences*, *115*(38), E9015–E9024.

Malach, R., Levy, I., & Hasson, U. (2002). The topography of high-order human object areas. *Trends in Cognitive Sciences*, *6*(4), 176–184.

Malaspina, M., Albonico, A., Toneatto, C., & Daini, R. (2017). What do eye movements tell us about the visual perception of individuals with congenital prosopagnosia? *Neuropsychology*, *31*(5), 546.

Malpass, R. S., & Kravitz, J. (1969). Recognition for faces of own and other race. *Journal of Personality and Social Psychology*, *13*(4), 330.

Margalit, E., Jamison, K. W., Weiner, K. S., Vizioli, L., Zhang, R.-Y., Kay, K. N., & Grill-Spector, K. (2020). Ultra-high-resolution fMRI of human ventral temporal cortex reveals differential representation of categories and domains. *Journal of Neuroscience*.

Marsh, J. E., Biotti, F., Cook, R., & Gray, K. L. H. (2019). The discrimination of facial sex in developmental prosopagnosia. *Scientific Reports*, *9*(1), 1–8.

Martuzzi, R., Ramani, R., Qiu, M., Shen, X., Papademetris, X., & Constable, R. T. (2011). A whole-brain voxel based measure of intrinsic connectivity contrast reveals local changes

in tissue connectivity with anesthetic without a priori assumptions on thresholds or regions of interest. *NeuroImage*, *58*(4), 1044–1050.

McGugin, R. W., & Gauthier, I. (2016). The reliability of individual differences in face-selective responses in the fusiform gyrus and their relation to face recognition ability. *Brain Imaging and Behavior*, *10*(3), 707–718. https://doi.org/10.1007/s11682-015-9467-4

McKone, E., Hall, A., Pidcock, M., Palermo, R., Wilkinson, R. B., Rivolta, D., Yovel, G., Davis, J. M., & O'Connor, K. B. (2011). Face ethnicity and measurement reliability affect face recognition performance in developmental prosopagnosia: Evidence from the Cambridge Face Memory Test–Australian. *Cognitive Neuropsychology*, *28*(2), 109–146.

McNeil, J. E., & Warrington, E. K. (1993). Prosopagnosia: A face-specific disorder. *The Quarterly Journal of Experimental Psychology*, *46*(1), 1–10.

Megreya, A. M., White, D., & Burton, A. M. (2011). The other-race effect does not rely on memory: Evidence from a matching task. *Quarterly Journal of Experimental Psychology*, *64*(8), 1473–1483.

Milner, A. D., & Goodale, M. A. (1995). *The visual brain in action*. Oxford psychology series, No. 27.

Minio-Paluello, I., Porciello, G., Pascual-Leone, A., & Baron-Cohen, S. (2020). Face individual identity recognition: a potential endophenotype in autism. *Molecular Autism*, *11*(1), 1–16.

Minnebusch, D. A., Suchan, B., Ramon, M., & Daum, I. (2007). Event-related potentials reflect heterogeneity of developmental prosopagnosia. *European Journal of Neuroscience*, *25*(7), 2234–2247.

Mišic, B., Betzel, R. F., de Reus, M. A., van den Heuvel, M. P., Berman, M. G., McIntosh, A. R., & Sporns, O. (2016). Network-level structure-function relationships in human neocortex. *Cerebral Cortex*, *26*(7), 3285–3296.

Moreira, T. P., Perez, M. L., Werneck, R. de O., & Valle, E. (2017). Where is my puppy? Retrieving lost dogs by facial features. *Multimedia Tools and Applications*, *76*(14), 15325–15340.

Moscovitch, M., Winocur, G., & Behrmann, M. (1997). What is special about face recognition? Nineteen experiments on a person with visual object agnosia and dyslexia but normal face recognition. *Journal of Cognitive Neuroscience*, *9*(5), 555–604.

Naselaris, T., Prenger, R. J., Kay, K. N., Oliver, M., & Gallant, J. L. (2009). Bayesian reconstruction of natural images from human brain activity. *Neuron*, *63*(6), 902–915.

Natu, V. S., Barnett, M. A., Hartley, J., Gomez, J., Stigliani, A., & Grill-Spector, K. (2016). Development of neural sensitivity to face identity correlates with perceptual discriminability. *Journal of Neuroscience*, *36*(42), 10893–10907.

Natu, V. S., Jiang, F., Narvekar, A., Keshvari, S., Blanz, V., & O'Toole, A. J. (2009). Dissociable neural patterns of facial identity across changes in viewpoint. *Journal of Cognitive Neuroscience*, *22*(7), 1570–1582.

Nestor, A., Plaut, D. C., & Behrmann, M. (2011). Unraveling the distributed neural code of facial identity through spatiotemporal pattern analysis. *Proceedings of the National Academy of Sciences of the United States of America*, *108*(24), 9998–10003.

Nieto-Castanon, A. (2022). Brain-wide connectome inferences using functional connectivity MultiVariate Pattern Analyses (fc-MVPA). *PLOS Computational Biology*, *18*(11), e1010634.

Nishimura, M., Doyle, J., Humphreys, K., & Behrmann, M. (2010). Probing the face-space of individuals with prosopagnosia. *Neuropsychologia*, *48*(6), 1828–1841.

Omer, Y., Sapir, R., Hatuka, Y., & Yovel, G. (2019). What is a face? Critical features for face detection. *Perception*, *48*(5), 437–446.

Ooi, L. Q. R., Chen, J., Zhang, S., Kong, R., Tam, A., Li, J., Dhamala, E., Zhou, J. H., Holmes, A. J., & Yeo, B. T. T. (2022). Comparison of individualized behavioral predictions across anatomical, diffusion and functional connectivity MRI. *NeuroImage*, *263*(119636).

Palermo, R., Rivolta, D., Wilson, C. E., & Jeffery, L. (2011). Adaptive face space coding in congenital prosopagnosia: Typical figural aftereffects but abnormal identity aftereffects. *Neuropsychologia*, *49*(14), 3801–3812.

Parvizi, J., Jacques, C., Foster, B. L., Withoft, N., Rangarajan, V., Weiner, K. S., & Grill-Spector, K. (2012). Electrical stimulation of Human Fusiform face-selective regions distorts face perception. *Journal of Neuroscience*, *32*(43), 14915–14920.

Pascalis, O., de Haan, M., & Nelson, C. A. (2002). Is face processing species-specific during the first year of life? *Science*, *296*(5571), 1321–1323.

Pascalis, O., Scott, L. S., Kelly, D. J., Shannon, R. W., Nicholson, E., Coleman, M., & Nelson, C. A. (2005). Plasticity of face processing in infancy. *Proceedings of the National Academy of Sciences*, *102*(14), 5297–5300.

Perrett, D. I., Hietanen, J. K., Oram, M. W., & Benson, P. J. (1992). Organization and functions of cells responsive to faces in the temporal cortex. *Philosophical transactions of the royal society of London. Series B: Biological sciences*, *335*(1273), 23-30.

Pitcher, D., Charles, L., Devlin, J. T., Walsh, V., & Duchaine, B. (2009). Triple Dissociation of Faces, Bodies, and Objects in Extrastriate Cortex. *Current Biology*, *19*(4), 319–324.

Pitcher, D., Walsh, V., Yovel, G., & Duchaine, B. (2007). TMS evidence for the involvement of the right occipital face area in early face processing. *Current Biology*, *17*(18), 1568–1573.

Qian, X., Castellanos, F. X., Uddin, L. Q., Loo, B. R. Y., Liu, S., Koh, H. L., Poh, X. W. W., Fung, D., Guan, C., Lee, T. S., Lim, C. G., & Zhou, J. (2019). Large-scale brain functional network topology disruptions underlie symptom heterogeneity in children with attention-deficit/hyperactivity disorder. *NeuroImage: Clinical*, *21*(101600).

Ramasubbu, R., Konduru, N., Cortese, F., Bray, S., Gaxiola-Valdez, I., & Goodyear, B. (2014). Reduced intrinsic connectivity of amygdala in adults with major depressive disorder. *Frontiers in Psychiatry*, *5*(17).

Ramot, M., Walsh, C., & Martin, A. (2019). Multifaceted integration: Memory for faces is subserved by widespread connections between visual, memory, auditory, and social networks. *Journal of Neuroscience*, *39*(25), 4976–4985.

Renzi De, E., Faglioni, P., Grossi, D., & Nichelli, P. (1991). Apperceptive and associative forms of prosopagnosia. *Cortex*, *27*(2), 213–221.

Rhodes, G., Brake, S., Taylor, K., & Tan, S. (1989). Expertise and configural coding in face recognition. *British Journal of Psychology*, *80*(3), 313–331.

Rice, G. E., Watson, D. M., Hartley, T., & Andrews, T. J. (2014). Low-level image properties of visual objects predict patterns of neural response across category-selective regions of the ventral visual pathway. *Journal of Neuroscience*, *34*(26), 8837–8844.

Ritchey, M., Wing, E. A., LaBar, K. S., & Cabeza, R. (2013). Neural similarity between encoding and retrieval is related to memory via hippocampal interactions. *Cerebral Cortex*, *23*(12), 2818–2828.

Rivolta, D., Woolgar, A., Palermo, R., Butko, M., Schmalzl, L., & Williams, M. A. (2014). Multi-voxel pattern analysis (MVPA) reveals abnormal fMRI activity in both the "core" and "extended" face network in congenital prosopagnosia. *Frontiers in Human Neuroscience*, *8*(November).

Robertson, D. J., Black, J., Chamberlain, B., Megreya, A. M., & Davis, J. P. (2020). Super-Recognisers show an advantage for other race face identification. *Applied Cognitive Psychology*, *34*(1), 205–216.

Rosenblueth, A., & Wiener, N. (1945). The role of models in science. *Philosophy of Science*, *12*(4), 316–321.

Rosenthal, G., & Avidan, G. (2018). A possible neuronal account for the behavioural heterogeneity in congenital prosopagnosia. *Cognitive Neuropsychology*, *35*(1–2), 74–77.

Rosenthal, G., Tanzer, M., Simony, E., Hasson, U., Behrmann, M., & Avidan, G. (2017). Altered topology of neural circuits in congenital prosopagnosia. *Elife*, *6*, e25069.

Rubinov, M., & Sporns, O. (2010). Complex network measures of brain connectivity: Uses and interpretations. *NeuroImage*, *52*(3), 1059–1069.

Scott, L. S., & Fava, E. (2013). The own-species face bias: A review of developmental and comparative data. *Visual Cognition*, *21*(9–10), 1364–1391.

Seo, E. H., Lee, D. Y., Lee, J. M., Park, J. S., Sohn, B. K., Lee, D. S., Choe, Y. M., & Woo, J. I. (2013). Whole-brain functional networks in cognitively normal, mild cognitive impairment, and Alzheimer's disease. *PLoS ONE*, *8*(1), e53922.

Shah, P., Gaule, A., Gaigg, S. B., Bird, G., & Cook, R. (2015). Probing short-term face memory in developmental prosopagnosia. *Cortex*, *64*, 115–122.

Shah, P., Gaule, A., Sowden, S., Bird, G., & Cook, R. (2015). The 20-item prosopagnosia index (PI20): a self-report instrument for identifying developmental prosopagnosia. *Royal Society Open Science*, *2*(6), 140343.

Shu, N., Wang, X., Bi, Q., Zhao, T., & Han, Y. (2018). Disrupted topologic efficiency of white matter structural connectome in individuals with subjective cognitive decline. Radiology, 286(1), 229-238.

Smith, S. M. (2002). Fast robust automated brain extraction. *Human Brain Mapping*, *17*(3), 143–155.

Sommer, V. R., & Sander, M. C. (2022). Contributions of representational distinctiveness and stability to memory performance and age differences. In *Aging, Neuropsychology, and Cognition* (Vol. 29, Issue 3, pp. 443–462). Routledge.

Song, S., Garrido, L., Nagy, Z., Mohammadi, S., Steel, A., Driver, J., Dolan, R. J., Duchaine, B., & Furl, N. (2015). Local but not long-range microstructural differences of the ventral temporal cortex in developmental prosopagnosia. *Neuropsychologia*, *78*, 195–206.

Song, Y., Zhu, Q., Li, J., Wang, X., & Liu, J. (2015). Typical and atypical development of functional connectivity in the face network. *Journal of Neuroscience*, *35*(43), 14624–14635.

Sormaz, M., Watson, D. M., Smith, W. A. P., Young, A. W., & Andrews, T. J. (2016). Modelling the perceptual similarity of facial expressions from image statistics and neural responses. *NeuroImage*, *129*, 64–71.

Stollhoff, R., Jost, J., Elze, T., & Kennerknecht, I. (2011). Deficits in long-term recognition memory reveal dissociated subtypes in congenital prosopagnosia. *PLoS One*, *6*(1).

Suárez, L. E., Markello, R. D., Betzel, R. F., & Misic, B. (2020). Linking structure and function in macroscale brain networks. *Trends in Cognitive Sciences*, *24*(4), 302–315.

Sugiura, M., Kawashima, R., Nakamura, K., Sato, N., Nakamura, A., Kato, T., Hatano, K., Schormann, T., Zilles, K., Sato, K., Ito, K., & Fukuda, H. (2001). Activation reduction in anterior temporal cortices during repeated recognition of faces of personal acquaintances. *NeuroImage*, *13*(5), 877–890.

Susilo, T., & Duchaine, B. (2013). Advances in developmental prosopagnosia research. *Current Opinion in Neurobiology*, *23*(3), 423–429.

Susilo, T., & Duchaine, B. (2013). Dissociations between faces and words: comment on Behrmann and Plaut. *Trends in Cognitive Sciences*, *17*(11), 545.

Svart, N., & Starrfelt, R. (2022). Is It Just Face Blindness? Exploring Developmental Comorbidity in Individuals with Self-Reported Developmental Prosopagnosia. *Brain Sciences*, *12*(2), 230.

Taubert, J., Wardle, S. G., & Ungerleider, L. G. (2020). What does a "face cell" want?'. *Progress in Neurobiology*, 101880.

Thomas, C., Avidan, G., Humphreys, K., Jung, K. J., Gao, F., & Behrmann, M. (2009). Reduced structural connectivity in ventral visual cortex in congenital prosopagnosia. *Nature Neuroscience*, *12*(1), 29–31.

Toftness, A. R. (2019). *The non-specificity of prosopagnosia: Can prosopagnosics distinguish sheep?* https://lib.dr.iastate.edu/etd/17109

Tong, F., Nakayama, K., Moscovitch, M., Weinrib, O., & Kanwisher, N. (2000). Response properties of the human fusiform face area. *Cognitive Neuropsychology*, *17*, 257–279.

Torralba, A., & Oliva, A. (2001). Modeling the shape of the scene: A holistic representation of the spatial envelope. *International Journal of Computer Vision*, *42*(3), 145–175.

Tsantani, M., Vestner, T., & Cook, R. (2021). The Twenty Item Prosopagnosia Index (PI20) provides meaningful evidence of face recognition impairment. *Royal Society Open Science*, *8*(11), 202062.

Ulrich, P. I. N., Wilkinson, D. T., Ferguson, H. J., Smith, L. J., Bindemann, M., Johnston, R. A., & Schmalzl, L. (2017). Perceptual and memorial contributions to developmental prosopagnosia. *Quarterly Journal of Experimental Psychology*, *70*(2), 298–315.

Valentine, T. (1991). A unified account of the effects of distinctiveness, inversion, and race in face recognition. *The Quarterly Journal of Experimental Psychology Section A*, *43*(2), 161–204.

Walker, P. M., & Tanaka, J. W. (2003). An encoding advantage for own-race versus other-race faces. *Perception*, *32*(9), 1117–1125.

Wang, A., Laming, C., & Andrews, T. J. (2022). Covariation in the recognition of own-race and other-race faces argues against the role of group bias in the other race effect. *Scientific Reports*, *12*(1), 13088.

Wang, L., Zhu, C., He, Y., Zang, Y., Cao, Q., Zhang, H., Zhong, Q., & Wang, Y. (2009). Altered small-world brain functional networks in children with attention-deficit/hyperactivity disorder. *Human Brain Mapping*, *30*(2), 638–649.

Wang, Y., Metoki, A., Smith, D. v., Medaglia, J. D., Zang, Y., Benear, S., Popal, H., Lin, Y., & Olson, I. R. (2020). Multimodal mapping of the face connectome. *Nature Human Behaviour*, *4*(4), 397–411.

Ward, E. J., Chun, M. M., & Kuhl, B. A. (2013). Repetition suppression and multi-Voxel pattern similarity differentially track implicit and explicit visual memory. *Journal of Neuroscience*, *33*(37), 14749–14757.

Wardle, S. G., Paranjape, S., Taubert, J., & Baker, C. I. (2022). Illusory faces are more likely to be perceived as male than female. *Proceedings of the National Academy of Sciences*, *119*(5), e2117413119.

Wardle, S. G., Taubert, J., Teichmann, L., & Baker, C. I. (2020). Rapid and dynamic processing of face pareidolia in the human brain. *Nature Communications*, *11*(1), 1–14.

Watson, D. M., Hartley, T., & Andrews, T. J. (2014). Patterns of response to visual scenes are linked to the low-level properties of the image. *NeuroImage*, *99*, 402–410.

Watson, D. M., Hartley, T., & Andrews, T. J. (2017). Patterns of response to scrambled scenes reveal the importance of visual properties in the organization of scene-selective cortex. *Cortex*, *92*, 162–174.

Wen, H., Shi, J., Chen, W., & Liu, Z. (2018). Deep Residual Network Predicts Cortical Representation and Organization of Visual Features for Rapid Categorization. *Scientific Reports*, *8*(1), 1–17.

White, D., Rivolta, D., Burton, A. M., Al-Janabi, S., & Palermo, R. (2017). Face matching impairment in developmental prosopagnosia. *Quarterly Journal of Experimental Psychology*, *70*(2), 287–297.

Whitfield-Gabrieli, S., & Nieto-Castanon, A. (2012). Conn: A Functional Connectivity Toolbox for Correlated and Anticorrelated Brain Networks. *Brain Connectivity*, *2*(3), 125–141.

Wilkinson, F., James, T. W., Wilson, H. R., Gati, J. S., Menon, R. S., & Goodale, M. A. (2000). An fMRI study of the selective activation of human extrastriate form vision areas by radial and concentric gratings. *Current Biology*, *10*(22), 1455–1458.

Wing, E. A., Geib, B. R., Wang, W. C., Monge, Z., Davis, X. S. W., & Cabeza, R. (2020). Cortical overlap and cortical-hippocampal interactions predict subsequent true and false memory. *Journal of Neuroscience*, *40*(9), 1920–1930.

Wing, E. A., Ritchey, M., & Cabeza, R. (2015). Reinstatement of individual past events revealed by the similarity of distributed activation patterns during encoding and retrieval. *Journal of Cognitive Neuroscience*, *27*(4), 679–691.

Xiao, J., Hays, J., Ehinger, K. A., Oliva, A., & Torralba, A. (2010). SUN database: Large-scale scene recognition from abbey to zoo. *Proceedings of the IEEE Computer Society Conference on Computer Vision and Pattern Recognition*, 3485–3492.

Xu, X., Dai, J., Chen, Y., Liu, C., Xin, F., Zhou, X., Zhou, F., Stamatakis, E. A., Yao, S., Luo, L., Huang, Y., Wang, J., Zou, Z., Vatansever, D., Kendrick, K. M., Zhou, B., & Becker, B. (2021).

Intrinsic connectivity of the prefrontal cortex and striato-limbic system respectively differentiate major depressive from generalized anxiety disorder. *Neuropsychopharmacology*, *46*(4), 791–798.

Xue, G., Qi Dong, Chuansheng, C., Zhonglin, L., Jeanette A. Mumford, & Russell A. Poldrack. (2010). Greater neural pattern similarity across repetitions is associated with better memory. *Science*, *330*(6000), 94–97.

Xue, T., Wang, R., Zhao, Y., Zhen, Z., Songia, Y., & Liu, J. (2020). Multi-Item Discriminability Pattern to Faces in Developmental Prosopagnosia Reveals Distinct Mechanisms of Face Processing. *Cerebral Cortex*, *30*(5), 2986–2996.

Yang, H., Susilo, T., & Duchaine, B. (2016). The anterior temporal face area contains invariant representations of face identity that can persist despite the loss of right FFA and OFA. *Cerebral Cortex*, *26*(3), 1096–1107.

Yardley, L., McDermott, L., Pisarski, S., Duchaine, B., & Nakayama, K. (2008). Psychosocial consequences of developmental prosopagnosia: A problem of recognition. *Journal of Psychosomatic Research*, *65*(5), 445–451.

Yarkoni, T., Poldrack, R. A., Nichols, T. E., Van Essen, D. C., & Wager, T. D. (2011). Large-scale automated synthesis of human functional neuroimaging data. *Nature Methods*, *8*(8), 665–670.

Yeager, B. E., Bruss, J., Duffau, H., Herbet, G., Hwang, K., Tranel, D., & Boes, A. D. (2022). Central precuneus lesions are associated with impaired executive function. *Brain Structure and Function*, *227*(9), 3099–3108.

Yeh, F.-C. (2020). Shape analysis of the human association pathways. *NeuroImage*, *223*(117329).

Yeh, F.-C., Verstynen, T. D., Wang, Y., Fernández-Miranda, J. C., & Tseng, W.-Y. I. (2013). Deterministic diffusion fiber tracking improved by quantitative anisotropy. *PLoS ONE*, *8*(11), e80713.

Yeh, F.-C., Wedeen, V. J., & Tseng, W.-Y. I. (2010). Generalized q-sampling imaging. *IEEE Transactions on Medical Imaging*, *29*(9), 1626–1635.

Zdorovtsova, N., Jones, J., Akarca, D., Benhamou, E., CALM Team, & Astle, D. E. (2022). Exploring Neural Heterogeneity in Inattention and Hyperactivity. *BioRxiv*.

Zhang, J., & Mueller, S. T. (2005). A note on ROC analysis and non-parametric estimate of sensitivity. *Psychometrika*, *70*(1), 203–212.

Zhao, Y., Li, J., Liu, X., Song, Y., Wang, R., Yang, Z., & Liu, J. (2016). Altered spontaneous neural activity in the occipital face area reflects behavioral deficits in developmental prosopagnosia. *Neuropsychologia*, *89*, 344–355.